1

MATHEMATICAL BACKGROUND AND ANALYSIS TECHNIQUES

1.1 INTRODUCTION

This introductory chapter focuses on various mathematical techniques and solutions to practical problems encountered in many of the following chapters. The discussions are divided into three distinct topics: deterministic signal analysis involving linear systems and channels; statistical analysis involving probabilities, random variables, and random processes; miscellaneous topics involving windowing functions, mathematical solutions to commonly encountered problems, and tables of commonly used mathematical functions. It is desired that this introductory material will provide the foundation for modeling and finding practical design solutions to communication system performance specifications. Although this chapter contains a wealth of information regarding a variety of topics, the contents may be viewed as reference material for specific topics as they are encountered in the subsequent chapters.

This introductory section describes the commonly used waveform modulations characterized as amplitude modulation (AM), phase modulation (PM), and frequency modulation (FM) waveforms. These modulations result in the transmission of the carrier- and data-modulated subcarriers that are accompanied by negative frequency images. These techniques are compared to the more efficient suppressed carrier modulation that possesses attributes of the AM, PM, and FM modulations. This introduction concludes with a discussion of *real* and *analytic* signals, the Hilbert transform, and demodulator heterodyning, or frequency mixing, to baseband.

Sections 1.2–1.4, *deterministic signal analysis*, transform in the context of a uniformly weighted pulse *f(t)* and its spectrum *F(f)* and the duality between ideal time and frequency sampling that forms the basis of Shannon's sampling theorem [1]. This section also discusses the discrete Fourier transform (DFT), the fast Fourier transform (FFT), the pipeline implementation of the FFT, and applications involving waveform detection, interpolation, and power spectrum estimation. The concept of paired echoes is discussed and used to analyze the signal distortion resulting from a deterministic band-limited channel with amplitude and phase distortion. These sections conclude on the subject of autocorrelation and cross-correlation of real and complex deterministic functions; the corresponding covariance functions are also examined.

Sections 1.5–1.10, *statistical analysis*, introduce the concept of *random variables* and various probability density functions (*pdf*) and cumulative distribution functions (*cdf*) for continuous and discrete random variables. *Stochastic* processes are then defined and the properties of *ergodic* and *stationary* random processes are examined. The characteristic function is defined and examples, based on the summation of several underlying random variables, exhibit the trend in the limiting behavior of the *pdf* and *cdf* functions toward the normal distribution; thereby demonstrating the central limit theorem. Statistical analysis using distribution-free or nonparametric techniques is introduced with a focus on *order statistics*. The random process involving narrowband white Gaussian noise is characterized in terms of the noise spectral density at the input and output of an optimum detection filter. This is followed by the derivation of the *matched filter* and the

equivalence between the matched filter and a correlation detector is also established. The next subject discussed involves the *likelihood ratio* and *log-likelihood ratio* as they pertain to optimum signal detection. These topics are generalized and expanded in Chapter 3 and form the basis for the optimum detection of the modulated waveforms discussed in Chapters 4–9. Section 1.9 introduces the subject of parameter estimation which is revisited in Chapters 11 and 12 in the context of waveform acquisition and adaptive systems. The final topic in this section involves a discussion of modem configurations and the important topic of automatic repeat request (ARQ) to improve the reliability of message reception.

Sections 1.11–1.14, *miscellaneous topics*, include a characterization of several *window functions* that are used to improve the performance the FFT, decimation filtering, and signal parameter estimation. Section 1.12 provides an introductory discussion of matrix and vector operations. In Section 1.13 several mathematical procedures and formulas are discussed that are useful in system analysis and simulation programming. These formulas involve *prime factorization* of an integer and determination of the *greatest common factor* (GCF) and *least common multiple* (LCM) of two integers, *Newton's approximation* method for finding the roots of a transcendental function, and the definition of the *standard deviation* of a sampled population. This chapter concludes with a list of frequently used mathematical formulas involving *infinite* and *finite summations*, *the binomial expansion theorem*, *trigonometric identities*, *differentiation and integration rules*, *inequalities*, and other *miscellaneous relationships*.

Many of the examples and case studies in the following chapters involve systems operating in a specific frequency band that is dictated by a number of factors, including, the system objectives and requirements, the communication range equation, the channel characteristics, and the resulting link budget. The system objectives and requirements often dictate the frequency band that, in turn, identifies the channel characteristics. Table 1.1 identifies the frequency

TABLE 1.1 Frequency Band Designations

Designation	Frequency	Letter Designation	Frequency (GHz)
ELF	3–30 Hz	*L*	1–2
SLF	30–300 Hz	*S*	2–4
ULF	0.3–3 kHz	*C*	4–8
VLF	3–30 kHz	*X*	8–12
LF	30–300 kHz	*Ku*	12–18
MF	0.3–3 MHz	*K*	18–27
HF	3–30 MHz	*Ka*	27–40
VHF	30–300 MHz	*V*	40–75
UHF	0.3–3 GHz	*W*	75–110
SHF	3–30 GHz	*mm (millimeter)*	110–300
EHF	30–300 GHz		

band designations with the corresponding range of frequencies. The designations low frequency (LF), medium frequency (MF), and high frequency (HF) refer to low, medium, and high frequencies and the prefixes E, V, U, and S correspond to *e*xtremely, *v*ary, *u*ltra, and *s*uper.

1.1.1 Waveform Modulation Descriptions

This section characterizes signal waveforms comprised of baseband information modulated on an arbitrary carrier frequency, denoted as f_c Hz. The baseband information is characterized as having a lowpass bandwidth of B Hz and, in typical applications, $f_c \gg B$. In many communication system applications, the carrier frequency facilitates the transmission between the transmitter and receiver terminals and can be removed without effecting the information. When the carrier frequency is removed from the received signal the signal processing sampling requirements are dependent only on the bandwidth B.

The signal modulations described in Sections 1.1.1.1 through 1.1.1.4 are amplitude, phase, frequency, and suppressed carrier modulations. The amplitude, phase, and frequency modulations are often applied to the transmission of analog information; however, they are also used in various applications involving digital data transmission. For example, these modulations, to varying degrees, are the underlying waveforms used in the U.S. Air Force Satellite Control Network (AFSCN) involving satellite uplink and downlink control, status, and ranging.

In describing the demodulator processing of the received waveforms, the information, following removal of the carrier frequency, is associated with in-phase and quadphase (I/Q) baseband channels or rails. Although these I/Q channels are described as containing quadrature real signals, they are characterized as *complex* signals with *real* and *imaginary* parts. This complex signal description is referred to as complex envelope or analytic signal representations and is discussed in Section 1.1.1.5. Suppressed carrier modulation and the analytic signal representation emphasize quadrature data modulation that leads to a discussion of the Hilbert transform in Section 1.1.1.6. Section 1.1.1.7 discusses conventional heterodyning of the received signal to baseband followed by data demodulation.

1.1.1.1 Amplitude Modulation Conventional amplitude modulation (AM) is characterized as

$$s(t) = A(1 + m_I m(t)\sin(\omega_m t))\sin(\omega_c t) \qquad (1.1)$$

where A is the peak carrier voltage, $m_I > 0$ is the modulation index, $m(t)$ is the information modulation function, ω_m is the modulation angular frequency, and ω_c is the AM carrier angular frequency. Upon multiplying (1.1) through by sin

($\omega_c t$) and applying elementary trigonometric identities, the AM-modulated signal is expressed as

$$s(t) = A\sin(\omega_c t) + \frac{Am_I}{2}m(t)\cos((\omega_c - \omega_m)t)$$
$$- \frac{Am_I}{2}m(t)\cos((\omega_c + \omega_m)t)$$

(1.2)

Therefore, $s(t)$ represents the conventional double sideband (DSB) AM waveform with the upper and lower sidebands at $\omega_c \pm \omega_m$ equally spaced about the carrier at ω_c. With the information modulation function $m(t)$ normalized to unit power, the power in each sideband is $m_I P_S/4$ where P_S is the power in the carrier frequency f_c.

1.1.1.2   Phase Modulation   Conventional phase modulation (PM) is characterized as

$$s(t) = A\sin(\omega_c t + \varphi(t))$$

(1.3)

where A is the peak carrier voltage, ω_c is the carrier angular frequency, and $\varphi(t)$ is an arbitrary phase modulation function containing the information. The commonly used phase function is expressed as

$$\varphi(t) = \phi\sin(\omega_m t)$$

(1.4)

where ϕ is the peak phase deviation. Substituting (1.4) into (1.3), the phase-modulated signal is expressed as

$$s(t) = A\left(\sin(\omega_c t + \phi\sin(\omega_m t))\right)$$

(1.5)

and, upon applying elementary trigonometric identities, (1.5) yields

$$s(t) = A\sin(\omega_c t)\cos(\phi\sin(\omega_m t)) + A\cos(\omega_c t)\sin(\phi\sin(\omega_m t))$$

(1.6)

The trigonometric functions involving sinusoidal arguments can be expanded in terms of Bessel functions [2] and (1.6) simplifies to

$$s(t) = AJ_0(\phi)\sin(\omega_c t) + A\sum_{n=1}^{\infty}[J_n(\phi)\sin((\omega_c + n\omega_m)t)$$
$$+ (-1)^n J_n(\phi)\sin((\omega_c - n\omega_m)t)]$$

(1.7)

Equation (1.7) is characterized by the carrier frequency with peak amplitude $AJ_0(\phi)$ and upper and lower sideband pairs at $\omega_c \pm n\omega_m$ with peak amplitudes $AJ_n(\phi)$. For small arguments the Bessel functions reduce to the approximations $J_0(\phi) \cong 1, J_1(\phi) \cong \phi/2$ with $J_n(\phi) \cong 0 : n > 1$ and (1.7) reduces to

$$s(t) \cong A\sin(\omega_c t) + \frac{A\phi}{2}\sin((\omega_c + \omega_m)t) - \frac{A\phi}{2}\sin((\omega_c - \omega_m)t)$$
$$: \text{small } \phi$$

(1.8)

Under these small argument approximations, the similarities between (1.8) and (1.2) are apparent.

1.1.1.3   Frequency Modulation   The frequency-modulated (FM) waveform is described as

$$s(t) = A\sin\left(\omega_c t + \frac{\Delta f}{f_m}\sin(\omega_m t)\right)$$

(1.9)

where A is the peak carrier voltage, ω_c is the carrier angular frequency, Δf is the peak frequency deviation of the modulation frequency f_m, and ω_m is the modulation angular frequency. The ratio $\Delta f/f_m$ is the frequency modulation index. Noting the similarities between (1.9) and (1.5), the expression for the frequency-modulated waveform is expressed, in terms of the Bessel functions, as

$$s(t) = AJ_0\left(\frac{\Delta f}{f_m}\right)\sin(\omega_c t) + A\sum_{n=1}^{\infty}\left[J_n\left(\frac{\Delta f}{f_m}\right)\sin((\omega_c + n\omega_m)t)\right.$$
$$\left. + (-1)^n J_n\left(\frac{\Delta f}{f_m}\right)\sin((\omega_c - n\omega_m)t)\right]$$

(1.10)

with the corresponding small argument approximation for the Bessel function expressed as

$$s(t) \cong A\sin(\omega_c t) + \frac{A\Delta f}{2f_m}\sin((\omega_c + \omega_m)t) - \frac{A\Delta f}{2f_m}\sin((\omega_c - \omega_m)t)$$
$$: \text{small } \frac{\Delta f}{f_m}$$

(1.11)

The similarities between (1.11), (1.8), and (1.2) are apparent.

1.1.1.4   Suppressed Carrier Modulation   A commonly used form of modulation is suppressed carrier modulation expressed as

$$s(t) = Am(t)\sin(\omega_c t + \varphi(t))$$

(1.12)

In this case, when the carrier is mixed to baseband, information modulation function $m(t)$ does not have a direct current (DC) spectral component involving $\delta(\omega)$. So, upon multiplication by the carrier, there is no residual carrier component ω_c in the received baseband signal. Because the carrier is suppressed it is not available at the receiver/demodulator to provide a coherent reference, so special considerations must be given

to the carrier recovery and subsequent data demodulation. Suppressed carrier-modulated waveforms are efficient, in that, all of the transmitted power is devoted to the information. Suppressed carrier modulation and the various methods of carrier recovery are the central focus of the digital communication waveforms discussed in the following chapters.

1.1.1.5   Real and Analytic Signals   The earlier modulation waveforms are described mathematically as *real* waveforms that can be transmitted over real or physical channels. The general description of the suppressed carrier waveform, described in (1.12), can be expressed in terms of in-phase and quadrature modulation functions $m_c(t)$ and $m_s(t)$ as

$$s(t) = m_c(t)\cos(\omega_c t) - m_s(t)\sin(\omega_c t) \qquad (1.13)$$

The quadrature modulation functions are expressed as

$$m_c(t) = Ad_c m(t)\cos(\varphi(t)) \qquad (1.14)$$

and

$$m_s(t) = Ad_s m(t)\sin(\varphi(t)) \qquad (1.15)$$

With PM the data $\{d_c, d_s\}$ may be contained in a phase function $\varphi_d(t)$, $m(t)$ is a unit energy symbol shaping function that provides for spectral control relative to the commonly used *rect*(t/T) function, and A represents the peak carrier voltage on each rail. With quadrature modulations, unique symbol shaping functions, $m_c(t)$ and $m_s(t)$, may be applied to each rail; for example, unbalanced quadrature modulations involve different data rates on each quadrature rail. With quadrature amplitude modulation (QAM) the data is described in terms of the multilevel quadrature amplitudes $\{\alpha_c, \alpha_s\}$ that are used in place of $\{d_c, d_s\}$ in (1.14) and (1.15).

Equation (1.13) can also be expressed in terms of the *real* part of a *complex* function as

$$s(t) = \text{Re}\{\tilde{s}(t)e^{j\omega_c t}\} \qquad (1.16)$$

where

$$\tilde{s}(t) = m_c(t) + jm_s(t) \qquad (1.17)$$

The function $\tilde{s}(t)$ is referred to as the complex envelope or analytic representation of the baseband signal and plays a fundamental role in the data demodulation, in that, it contains all of the information necessary to optimally recover the transmitted information. Equation (1.17) applies to receivers that use linear frequency translation to baseband. Linear frequency translation is typical of heterodyne receivers using intermediate frequency (IF) stages. This is a significant result because the system performance can be evaluated using the

analytic signal without regard to the carrier frequency [3]; this is particularly important in computer performance simulations.

Evaluation of the *real* part of the signal expressed in (1.16) is performed using the complex identity No. 4 in Section 1.14.6 with the result

$$s(t) = \frac{1}{2}\{\tilde{s}(t)e^{j\omega_c t} + \tilde{s}(t)*e^{-j\omega_c t}\} \qquad (1.18)$$

A note of caution is in order, in that, the received signal power based on the analytic signal is twice that of the power in the carrier. This results because the analytic signal does not account for the factor of 1/2 when mixing or heterodyning with a locally generated carrier frequency and is directly related the factor of 1/2 in (1.18). The signal descriptions expressed in (1.12) through (1.18) are used to describe the narrowband signal characteristics used throughout much of this book.

1.1.1.6   Hilbert Transform and Analytic Signals   The Hilbert transform of the real $s(t)$ is defined as

$$\breve{s}(t) \triangleq \frac{1}{\pi}\int\limits_{-\infty}^{\infty}\frac{s(\tau)}{t-\tau}d\tau = s(t)*\frac{1}{\pi t} \qquad (1.19)$$

The second expression in (1.19) represents the convolution of $s(t)$ with a filter with impulse response $h(t) = 1/\pi t$ where $h(t)$ represents the response to a Hilbert filter with frequency response $H(\omega)$ characterized as

$$h(t) \Leftrightarrow H(\omega)$$
$$= \begin{cases} -jsign(\omega) & : |\omega| > 0 \\ \\ 0 & : o.w. \end{cases} \qquad (1.20)$$

The Hilbert transform of $s(t)$ results in a spectrum that is zero for all negative frequencies with positive frequencies representing a complex spectrum associated with the real and imaginary parts of an analytic function. Applying (1.20) to the signal spectrum $S(\omega) \Leftrightarrow s(t)$ results in the spectrum of the Hilbert transformed signal

$$\breve{S}(\omega) = \begin{cases} jS(\omega) & : \omega < 0 \\ 0 & : \omega = 0 \\ -jS(\omega) & : \omega > 0 \end{cases} \qquad (1.21)$$

Applying (1.21) to the spectrum $S(\omega)$ of (1.12) or (1.13), the bandwidth B of $m(t)$ must satisfy the condition $B << f_c$. In this case, the inverse Fourier transform of the spectrum $\breve{S}(\omega)$ yields the Hilbert filter output $\breve{s}(t)$ given by
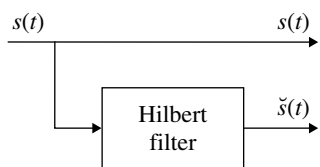
FIGURE 1.1   Hilbert transform of carrier-modulated signal $s(t)$ $(B/f_c \ll 1)$.
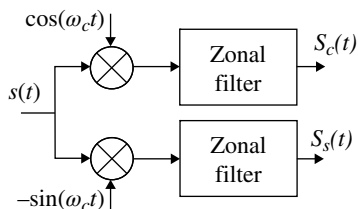

FIGURE 1.2   Heterodyning of carrier-modulated signal $s(t)$ $(B/f_c \ll 1)$.

$$\check{s}(t) = T_H[Am(t)\sin(\omega_c t + \phi(t))] = Am(t)\sin(\omega_c t + \phi(t) - \pi/2)$$

$$= -Am(t)\cos(\omega_c t + \phi(t))$$

$$(1.22)$$

where $T_H[s(t)]$ represents the Hilbert transform of $s(t)$.

The function $\check{s}(t)$ expressed by (1.22) is orthogonal to $s(t)$ and, if the carrier frequency were removed following the Hilbert transform, the result would be identical to the imaginary part of the analytic signal expressed by (1.17). The processing is depicted in Figure 1.1.

1.1.1.7   Conventional and Complex Heterodyning   Conventional heterodyning is depicted in Figure 1.2. The zonal filters are ideal low-pass filters with frequency response given by

$$H(f) = rect\left(f - \frac{f_c}{2}\right)   : \text{zonal lowpass filter}$$

$$(1.23)$$

These filters remove the $2\omega_c$ term that results from the mixing operation and, for $s(t)$ as expressed by (1.13), the quadrature outputs are given by

$$s_c(t) = \frac{A}{2}[m_c(t)\cos(\phi(t)) - m_s(t)\sin(\phi(t))]   (1.24)$$

and

$$s_s(t) = \frac{A}{2}[m_c(t)\sin(\phi(t)) + m_s(t)\cos(\phi(t))]   (1.25)$$

With ideal phase tracking the phase term $\phi(t)$ is zero resulting in the quadrature modulation functions $m_c(t)$ and $m_s(t)$ in the respective low-pass channels.

1.2   THE FOURIER TRANSFORM AND FOURIER SERIES

The Fourier transform is so ubiquitous in the technical literature [4–6], and its application are so widely used that it seems unnecessary to dwell at any length on the subject. However, a brief description is in order to aid in the understanding of the parameters used in the applications discussed in the following chapters.

The Fourier transform $F(f)$ of $f(t)$ is defined over the interval $|t| \leq \infty$ and, if $f(t)$ is absolutely integrable, that is, if

$$\int_{-\infty}^{\infty} |f(t)| dt < \infty$$

$$(1.26)$$

then $F(f)$ exists, furthermore, the inverse Fourier transform of $F(f)$ results in $f(t)$. In most applications[*] of practical interest, $f(t)$ satisfies (1.26) leading to the Fourier transform pair $f(t) \Leftrightarrow F(f)$ defined as

$$F(f) = \int_{-\infty}^{\infty} f(t)e^{-j2\pi ft} dt \Leftrightarrow f(t) = \int_{-\infty}^{\infty} F(f)e^{j2\pi ft} df   (1.27)$$

In general, $f(t)$ is real and the Fourier transform $F(f)$ is complex and Parseval's theorem relates the signal energy in the time and frequency domains as

$$\int_{-\infty}^{\infty} f(t)^2 dt = \int_{-\infty}^{\infty} |F(f)|^2 df$$

$$(1.28)$$

The Fourier series representation of a periodic function is closely related to the Fourier transform; however, it is based on orthogonal expansions of sinusoidal functions at discrete frequencies. For example, if the function of interest is periodic, such that, $f(t) = f(t - iT_o)$ with period T_o and is finite and single valued over the period, then $f(t)$ can be represented by the Fourier series

$$f(t) = \sum_{n=-\infty}^{\infty} C_n e^{jn\omega_o t}$$

$$(1.29)$$

where $\omega_o = 2\pi/T_o$ and C_n is the n-th Fourier coefficient given by

[*]For special cases refer to Papoulis (Reference 7, Chapter 2).

$$C_n = \frac{1}{T_o} \int_{-T_o/2}^{T_o/2} f(t)e^{-jn\omega_o t} dt \qquad (1.30)$$

Equation (1.29) is an interesting relationship, in that, $f(t)$ can be described over the time interval T_o by an infinite set of frequency-domain coefficient C_n; however, because $f(t)$ is contiguously replicated over all time, that is, it is periodic, the spectrum of $f(t)$ is completely defined by the coefficients C_n. Unlike the Fourier transform, the spectrum of (1.29) is not continuous in frequency but is zero except at discrete frequencies occurring at multiples of $n\omega_o$. This is seen by taking the Fourier transform of (1.29) and, using (1.27), the result is expressed as

$$F(f) = \sum_{n=-\infty}^{\infty} C_n \int_{-\infty}^{\infty} e^{-j2\pi(f-nf_o)t} dt$$
$$= \sum_{n=-\infty}^{\infty} C_n \delta(f-nf_o) \qquad (1.31)$$

where $\delta(f-nf_o)$ is the Fourier Transform[*] of $e^{jn\omega_o T}$. Equation (1.31) is applied in Chapter 2 in the discussion of sampling theory and in Chapter 11 in the context of signal acquisition.

Alternate forms of (1.29) that emphasize the series expansion in terms of harmonics of trigonometric functions are given in (1.32) and (1.33) when $f(t)$ is a real-valued function. This is important because when $f(t)$ is *real* the complex coefficients C_n and C_{-n} form a complex conjugate pair such that $C_{-n} = C_n^*$ which simplifies the evaluation of $f(t)$. For example, using the complex notations $C_n = \alpha_n + j\beta_n$ and $C_n^* = \alpha_n - j\beta_n$, the function $f(t)$ is evaluated as

$$f(t) = C_o + 2\sum_{n=1}^{\infty} [\alpha_n \cos(n\omega_o t) - \beta_n \sin(n\omega_o t)] \qquad (1.32)$$

this simplifies to

$$f(t) = C_o + 2\sum_{n=1}^{\infty} |C_n| \cos(n\omega_o t + \phi_n) \qquad (1.33)$$

where $|C_n| = \sqrt{\alpha^2 + \beta^2}$ and $\phi_n = \arctan(\beta/\alpha)$.

An important consideration in spectrum analysis is the determination of signal spectrums involving random data sequences, referred to as stochastic processes [8]. A stochastic process does not have a unique spectrum; however, the power spectral density (PSD) is defined as the Fourier transform of the autocorrelation response. Oppenheim and

Schafer [9] discuss methods of estimating the PSD of a real finite-length (N) sampled sequence by averaging periodograms, defined as

$$I_N(\omega) = \frac{1}{N}|F(\omega)|^2 \qquad (1.34)$$

where $F(\omega)$ is the Fourier transform of the sampled sequence. This method is accredited to Bartlett [10] and is used in the evaluation of the PSD in the following chapters. For a fixed length (L) of random data, the number of periodograms (K) that can be averaged is $K = L/N$. As K increases the variance of the spectral estimate approaches zero and as N increases the resolution of the spectrum increases, so there is a trade-off between the selection of K and N. To resolve narrowband spectral features that occur, for example, with nonlinear frequency shift keying (FSK)-modulated waveforms, it is important to use large values of N. Fortunately, many of the spectrum analyses presented in the following chapters are not constrained by L so K and N are chosen to provide a low estimation bias, that is, low variance, and high spectral resolution. Windowing[†] the periodograms will also reduce the estimation bias at the expense of decreasing the spectral resolution.

1.2.1   The Transform Pair *rect*(t/T) ⟺ *Tsinc*(fT)

The transform relationship $rect(t/T) \Leftrightarrow Tsinc(fT)$ occurs so often that it deserves special consideration. For example, consider the following function:

$$s(t) = A\cos(\omega_c(t-\tau)-\phi)rect\left(\frac{(t-\tau)}{T}\right) \qquad (1.35)$$

where ω_c, τ, and ϕ represent arbitrary angular frequency, delay, and phase parameters. The signal $s(t)$ is depicted in Figure 1.3.

The Fourier transform of $s(t)$ is evaluated as

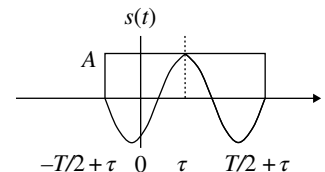$$S(f) = A \int_{-T/2+\tau}^{T/2+\tau} \cos(\omega_c(t-\tau)-\phi)e^{-j2\pi ft} dt \qquad (1.36)$$

FIGURE 1.3   Pulse-modulated carrier.

Expressing the cosine function in terms of complex exponential functions and performing some simplifications results in the expression

$$S(f) = \frac{A}{2}\left\{ e^{-j(2\pi f\tau + \phi)} \left[\int_{\tau - T/2}^{\tau + T/2} e^{-j2\pi(f - f_c)t} dt \right] \right.$$
$$\left. + e^{-j(2\pi f\tau - \phi)} \left[\int_{\tau - T/2}^{\tau + T/2} e^{-j2\pi(f + f_c)t} dt \right] \right\} \qquad (1.37)$$

Evaluation of the integrals in (1.37) appears so often that it is useful to generalize the solutions as follows:

Consider the integral

$$I(y) = \int_{x_1}^{x_2} e^{-j(y \pm \bar{y})x} dx$$
$$= \frac{e^{-j(y \pm \bar{y})x_2} - e^{-j(y \pm \bar{y})x_1}}{-j(y \pm \bar{y})} \qquad (1.38)$$

The general solution involves multiplying the last equality in (1.38) by the factors $e^{-j(y \pm \bar{y})(x_2 + x_1)/2}$ and $e^{j(y \pm \bar{y})(x_2 + x_1)/2}$, having a product of one, where $(x_2 + x_1)/2$ is the average of the integration limits. Distributing the second factor over the numerator of (1.38) and then simplifying yields the result

$$I(y) = (x_2 - x_1)e^{-j(y \pm \bar{y})(x_2 + x_1)/2} \frac{\sin((y \pm \bar{y})(x_2 - x_1)/2)}{(y \pm \bar{y})(x_2 - x_1)/2} \qquad (1.39)$$

Applying (1.39) to (1.37) and simplifying gives the desired result

$$S(f) = \frac{AT}{2}\left\{ e^{-j(2\pi f\tau + \phi)} sinc((f - f_c)T) + e^{-j(2\pi f\tau - \phi)} sinc((f + f_c)T) \right\} \qquad (1.40)$$

When $f_c \gg 1/T$, the positive and negative frequency spectrums do not influence one another and, in this case, the positive frequency spectrum is defined as

$$S^+(f) = \frac{AT}{2} sinc((f - f_c)T) \quad :f_c \gg \frac{1}{T} \qquad (1.41)$$

On the other hand, when the carrier frequency and phase are zero, (1.40) simplifies to the baseband spectrum, evaluated as

$$S_{bb}(f) = ATe^{-j2\pi f\tau} sinc(fT) \quad :f_c = 0, \ \phi = 0 \qquad (1.42)$$

Using (1.42), the baseband Fourier transform pair, corresponding to of (1.35) with $f_c = 0$, is established as

$$rect\left(\frac{(t - \tau)}{T}\right) \Leftrightarrow Te^{-j2\pi f\tau} sinc(fT) \quad :|t - \tau| \le \frac{T}{2} \qquad (1.43)$$

and, with $\tau = 0$,

$$rect\left(\frac{t}{T}\right) \Leftrightarrow Tsinc(fT) \quad :|t| \le \frac{T}{2} \qquad (1.44)$$

1.2.2   The $sinc(x)$ Function

The $sinc(x)$ function is defined as

$$sinc(x) = \frac{\sin(\pi x)}{\pi x} \qquad (1.45)$$

and is depicted in Figure 1.4. When x is expressed as the normalized frequency variable $x = fT$ then (1.45), when scaled by T, is the frequency spectrum of the unit amplitude pulse *rect* (t/T) of duration T seconds such that $t \le |T/2|$. This function is symmetrical in x and the maximum value of the first sidelobe occurs at $x = 1.431$ with a level of $10\log(sinc^2(x)) = -13.26$ dB; the peak sidelobe levels decrease in proportion to $1/|x|$. The noise bandwidth of a filter function $H(f)$ is defined as

$$B_n \triangleq \frac{\int_{-\infty}^{\infty} |H(f)|^2 df}{|H(f_o)|^2} \qquad (1.46)$$

where f_o is the filter frequency corresponding to the maximum response. When a receiver filter is described as $H(f) = sinc(fT)$ the receiver low-pass noise bandwidth is evaluated as $B_n = 1/T$ where T is the duration of the filter impulse response.

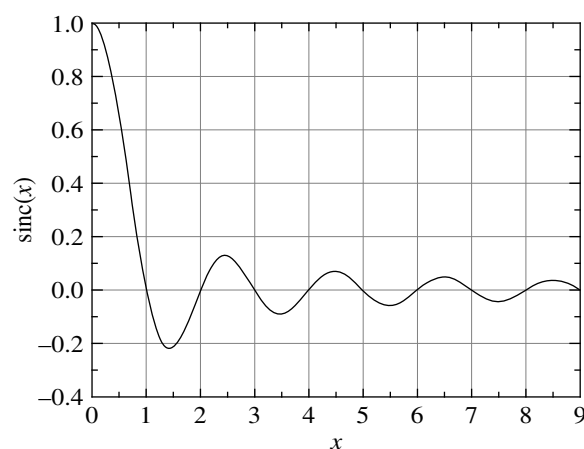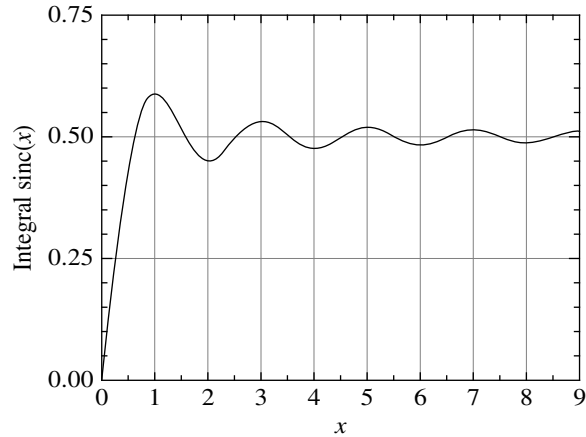**FIGURE 1.4**   The $sinc(x)$ function.

FIGURE 1.5 Integral of $sinc(x)$.

FIGURE 1.6 Integral of $sinc^2(x)$ function.

It is sometimes useful to evaluate the area of the $sinc(x)$ function and, while there is no closed form solutions, the solution can be evaluated in terms of the *sine-integral* $S_i(x)^*$ as

$$\int_0^z sinc(x)\,dx = \int_0^z \frac{\sin(\pi x)}{\pi x}dx = \frac{1}{\pi}\int_0^{\pi z}\frac{\sin(\lambda)}{\lambda}d\lambda$$
$$= \frac{1}{\pi}S_i(\pi z) \tag{1.47}$$

where the *sine-integral* is defined as the integral of $\sin(\lambda)/\lambda$. Equation (1.47) is shown in Figure 1.5. The limit of $S_i(\pi z)$ as $|z| \to \infty$ is[†] $\pi\, sign(1,z)/2$ so the corresponding limit of (1.47) is $0.5 sgn(z)$.

A useful parameter, often used as a benchmark for comparing spectral efficiencies, is the area under $sinc^2(x)$ as a function of x. The area is evaluated in terms of the *sine-integral* as
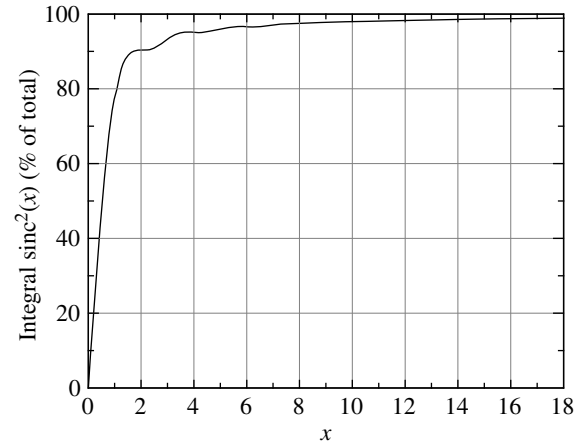
$$\int_0^z sinc^2(x)\,dx = \int_0^z \frac{\sin^2(\pi x)}{(\pi x)^2}dx$$
$$= \frac{1}{\pi}\left[S_i(2\pi z) - \frac{\sin^2(2\pi z)}{(2\pi z)}\right] \tag{1.48}$$

Equation (1.48) is plotted in Figure 1.6 as a percent of the total area and it is seen that the spectral containment of 99% is in excess of 18 spectral sidelobes, that is, $x = fT = 18$. In the following chapters, spectral efficient waveforms are examined with 99% containment within 2 or 3 sidelobes, so the $sinc(x)$ function does not represent a spectrally efficient waveform modulation.

---

[*]The arguments x and z may be complex; however, the following analysis uses only real arguments.
[†]The $sign(a, x)$ function is defined in Section 1.14.7.

1.2.3 The Fourier Transform Pair
$$\sum_n \delta(t - nT) \Leftrightarrow \omega_o \sum_n \delta(\omega - n\omega_o)$$

The evaluation of this Fourier transform pair is fundamental to Nyquist sampling theory and is demonstrated in Section 2.3 in the evaluation of discrete-time sampling. In this case, the function $f(t)$ is an infinite repetition of equally spaced delta functions $\delta(t)$ with intervals T seconds as expressed by

$$f(t) = \sum_{n=-\infty}^{\infty} \delta(t - nT) \tag{1.49}$$

The challenge is to show that the Fourier transform of (1.49) is equal to an infinite repetition of equally spaced and weighted frequency domain delta functions expressed as

$$F(\omega) = \omega_o \sum_{n=-\infty}^{\infty} \delta(\omega - n\omega_o) \tag{1.50}$$

with weighting ω_o and frequency intervals $\omega_o = 2\pi/T$. Direct application of the Fourier transform to (1.49) leads to the spectrum $\sum_n e^{-jn\omega T}$ but this does not demonstrate the equality in (1.50). Similarly, evaluation of the inverse Fourier transform of (1.50) results in the time-domain expression

$$g(t) = \frac{1}{T}\sum_{n=-\infty}^{\infty} e^{jn\omega_o t} \tag{1.51}$$

So, by showing that $g(t) = f(t)$, the transform pair between (1.49) and (1.50) will be established. Consider $g_N(t)$ to be a finite summation of terms in (1.51) given by

$$g_N(t) = \frac{1}{T}\sum_{n=-N}^{N} e^{jn\omega_o t}$$
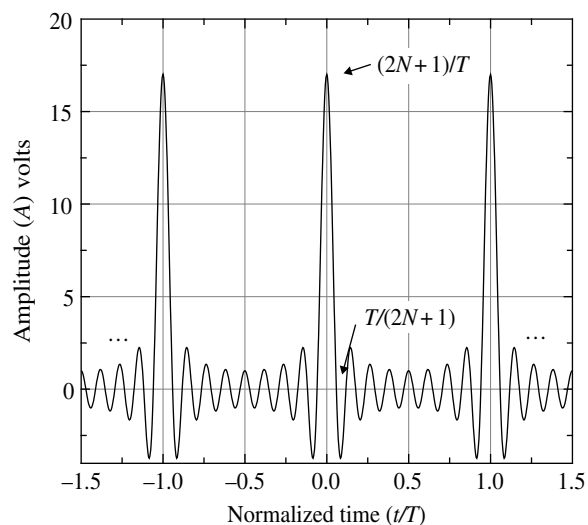$$= \frac{\sin((2N+1)\omega_o t/2)}{T\sin(\omega_o t/2)} \tag{1.52}$$

FIGURE 1.7   The Fourier-series kernel $g_N(t)$ ($N = 8$).

The second equality in (1.52) can be shown using the finite series identity No. 12, Section 1.14.1. Equation (1.52) is referred to by Papoulis [7] as the *Fourier-series kernel* and appears in a number of applications involving the Fourier transform.

The function $g_N(t)$ is plotted in Figure 1.7 for $N = 8$. The abscissa is time normalized by the pulse repetition interval $T = 1/f_o$ such that, $g_N(t) = g_N(t - nT)$, and there are a total of $2N + 1$ peaks of which three are shown in the figure. Furthermore, there are eight time sidelobes between $t/T = 0$ and 0.5 with the first nulls from the peak value at $t/T = 0$ occurring at $\pm T/(2N+1)$; the peak values are $(2N + 1)/T = 17/T$ in this example.

The maximum values of $2N + 1$, occurring at $t/T = n$, are determined by applying L'Hospital's rule to (1.52), which is rewritten as

$$g_N(t) = (2N+1)\frac{\sin((2N+1)\omega_o t/2)}{T(2N+1)\sin(\omega_o t/2)}$$
$$\cong (2N+1)\frac{\sin((2N+1)\omega_o t/2)}{T(2N+1)\omega_o t/2} \tag{1.53}$$

The approximation in (1.53) is obtained by noting that as N increases the rate of the sinusoidal variations in the numerator term increases with a frequency of $(2N+1)f_o$ Hz while the rate of sinusoidal variation in the denominator remains unchanged. Therefore, in the vicinity of $t/T = n$, $\sin(\omega_o t/2) \cong \omega_o t/2$ and (1.53) reduces to a $\sin(x)/x$ function with $x = (2N+1)\omega_o t/2$ and a peak amplitude $(2N + 1)$. The proof of the transform pair is completed by showing that $f(t) = g(t)$. Referring to (1.51) $g(t)$ is expressed as

$$g(t) = \lim_{N \to \infty} g_N(t) \tag{1.54}$$

From (1.53) as N approaches infinity the $\sin(x)/x$ sidelobe nulls converge to $t/T = n$, the peak values become infinite, and the corresponding area over the interval $|t/T| = n \pm 1/2$ approaches unity. Therefore, $g(t)$ resembles a periodic series of delta functions resulting in the equality

$$g(t) = \lim_{N \to \infty} g_N(t) = \sum_{n=-\infty}^{\infty} \delta(t - nT)$$
$$= f(t) \tag{1.55}$$

thus completing the proof that (1.49) and (1.50) correspond to a Fourier transform pair. Papoulis (Reference 7, pp. 50–52) provides a more eloquent proof that the limiting form of $g_N(t)$ is indeed an infinite sequence of delta functions.

1.2.4   The Discrete Fourier Transform

The DFT pair relating the discrete-time function $f(m\Delta t) \equiv f(m)$ and discrete-frequency function $F(n\Delta f) \equiv F(n)$ is denoted as $f(m) \Leftrightarrow F(n)$ where

$$F(n) = \Delta t \sum_{m=0}^{M-1} f(m)e^{-j2\pi n\Delta f m\Delta t} \Leftrightarrow f(m) = \Delta f \sum_{n=0}^{N-1} F(n)e^{j2\pi n\Delta f m\Delta t}$$

$$: \text{DFT}$$
$$\tag{1.56}$$

With the DFT the number of time and frequency samples can be chosen independently. This is advantageous when preparing presentation material or examining fine spectral or temporal details, as might be useful when debugging simulation programs, by the independent selection of the integers m and n.

1.2.5   The Fast Fourier Transform

As discussed in the preceding section, the DFT pair, relating the discrete-time function $f(m\Delta t) \equiv f(m)$ and the discrete-frequency function $F(n\Delta f) \equiv F(n)$, is denoted as $f(m) \Leftrightarrow F(n)$ where $f(m)$ and $F(n)$ are characterized by the expressions for the DFT. The FFT [11–17], is a special case corresponding to m and n being equal to N as described in the remainder of this section. In these relationships N is the number of time samples and is defined as the power of a fixed radix-r FFT or as the powers of a mixed radix-r_j FFT.[*] The fixed radix-2 FFT, with $r = 2$ and $N = 2^i$, results in the most processing efficient implementation.

[*]Mixed radix FFTs provide an efficient method of computing the Fourier transform when the number of samples is not a power of r. In general, $N = r_1^{i_1} r_2^{i_2} \ldots$ and the radices of the FFT are determined as the prime factors of N. For example, $N = 31 = 1*31$ requires a single radix = 31 FFT, $N = 32 = 2*2*2*2*2$ requires a radix-2 FFT, and $N = 33 = 3*11$ requires a radix-3 and a radix-11 FFT.

Defining the time window of the FFT as T_w results in an implicit periodicity of $f(t)$ such that $f(t) = f(t \pm kT_w)$ and $\Delta t = T_w/N$. The sampling frequency is defined as $f_s = 1/\Delta t = N/T_w$ and, based on Shannon's sampling theorem, the periodicity does not pose a practical problem as long as the signal bandwidth is completely contained in the interval $|B| \le f_s/2 = N/(2T_w)$. Since the FFT results in an equal number of time and frequency domain samples, that is, $\Delta f = f_s/N$ and $\Delta t = T_w/N$, it follows that $\Delta f \Delta t = f_s T_w/N^2 = 1/N$. Normalizing the expression of the time function, $f(m)$, in (1.56), that is, multiplying the inverse DFT (IDFT) by Δt requires dividing the expression for $F(n)$ by Δt. Upon substituting these results into (1.56), the FFT transform pairs become

$$F(n) = \sum_{m=0}^{N-1} f(m)e^{-j2\pi nm/N} \Leftrightarrow f(m) = \frac{1}{N}\sum_{n=0}^{N-1} F(n)e^{j2\pi nm/N}$$
$$: \text{FFT}$$
(1.57)

The time and frequency domain sampling characteristics of the FFT are shown in Figure 1.8. This depiction focuses on a communication system example, in that, the time samples over the FFT window interval T_w are subdivided into N_{sym} symbol intervals of duration T seconds with N_s samples/symbol.

Typically the bandwidth of the modulated waveform is taken to be the reciprocal of the symbol duration, that is, $1/T$ Hz; however, the receiver bandwidth required for low symbol distortion is typically several times greater than $1/T$ depending upon the type of modulation. Referring to Figure 1.8 the sampling frequency is $f_s = 1/\Delta t$, the sampling interval is $\Delta t = T/N_s$, the size of the FFT is $N_{fft} = N_s N_{sym}$, and the frequency sampling increment is $\Delta f = f_s/N_{fft}$. Upon using these relationships, the frequency resolution, or frequency samples per symbol bandwidth $B = 1/T$, is found to be

$$\frac{B}{\Delta f} = N_{sym} \quad : \text{determines frequency resolution} \quad (1.58)$$

and the number of spectral sidelobes[*] or symbol bandwidths over the sampling frequency range is

$$\frac{f_s}{B} = N_s \quad : \text{determines spectral sidelobes} \quad (1.59)$$

Therefore, to increase the resolution of the sampled signal spectrum, the number of symbols must be increased and this

---

[*]These results are based on the underlying *rect*(*t*/*T*) window and the *sinc*(*fT*) frequency function that includes the principal lobe and the positive and negative spectral side lobes.

(a)

$f(m\Delta t)$

$$\begin{cases} N_s : \text{samples / symbol}\,(T) \\ N_{sym} : \text{symbols / window}\,(T_w) \end{cases}$$

Time sampled waveform
$(t = m\Delta t)$

(b)

$F(n\Delta f)$

$$\begin{cases} N_{sym} : \text{samples / bandwidth}\,(B) \\ N_s : \text{bandwidths / frequency}\,(f_s) \end{cases}$$
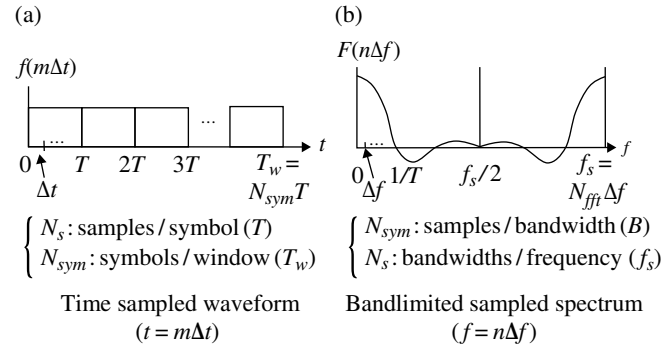
Bandlimited sampled spectrum
$(f = n\Delta f)$

FIGURE 1.8 FFT time and frequency domain sampling.

is comparable to increasing T_w. On the other hand, to increase the number of signal sidelobes contained in the frequency spectrum the number of samples per symbol must be increased and this is comparable to decreasing Δt. Both of these conditions require increasing the size (N) of the FFT. However, for a given size, the FFT does not allow independent selection of the frequency and time resolution as determined, respectively, by (1.58) and (1.59). This can be accomplished by using the DFT as discussed in Section 1.2.4. Since the spectrum samples in the range $0 \le f < f_s/2$ represent the positive frequency signal spectrum and those over the range $f_s/2 \le f < f_s$ represent the negative frequency signal spectrum, the range of signal sidelobes of interest is $\pm f_s/(2B) = \pm N_s/2$. As a practical matter, if the signal carrier frequency is not zero then the sampling frequency must be increased to maintain the signal sidelobes aliasing criterion. The sampling frequency selection is discussed in Chapter 11 in the context of signal acquisition when the received signal frequency is estimated based on locally known conditions.

The following implementation of the FFT is based on the Cooley and Tukey [18] decimation-in-time algorithm as described by Brigham and Morrow [19] and Brigham [20]. Although (1.57) characterizes the FFT transform pairs, the real innovation leading to the *fast* transformation is realized by the efficient algorithms used to execute the transformation. Considering the radix-2 FFT with $N = 2^n$, this involves defining the constant

$$W \triangleq e^{-j2\pi/N} \quad (1.60)$$

and recognizing that

$$F(n) = \Delta t \sum_{m=0}^{N-1} f(m)W^{nm} \quad (1.61)$$

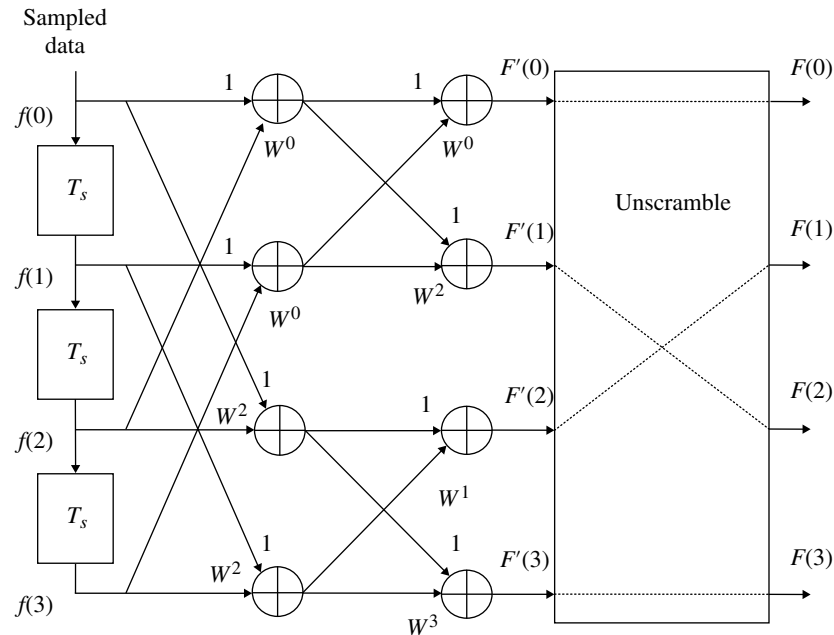Equation (1.61) can be expressed in matrix form, using $N = 4$ for simplicity, as

FIGURE 1.9   Radix-2, $N = 4$-point FFT implementation tree diagram.

$$\begin{bmatrix} F(0) \\ F(1) \\ F(2) \\ F(3) \end{bmatrix} = \Delta t \begin{bmatrix} W^0 & W^0 & W^0 & W^0 \\ W^0 & W^1 & W^2 & W^3 \\ W^0 & W^2 & W^4 & W^6 \\ W^0 & W^3 & W^6 & W^9 \end{bmatrix} \begin{bmatrix} f(0) \\ f(1) \\ f(2) \\ f(3) \end{bmatrix} \quad (1.62)$$

Recognizing that $W^0 = 1$ and the exponent nm is modulo (N), upon factoring the matrix in (1.62) into the product of two submatrices (in general the product of $\log_2 N$ submatrices) leads to the implementation involving the minimum number of computations expressed as

$$\begin{bmatrix} F(0) \\ F(2) \\ F(1) \\ F(3) \end{bmatrix} = \Delta t \begin{bmatrix} 1 & W^0 & 0 & 0 \\ 1 & W^2 & 0 & 0 \\ 0 & 0 & 1 & W^1 \\ 0 & 0 & 1 & W^3 \end{bmatrix} \begin{bmatrix} 1 & 0 & W^0 & 0 \\ 0 & 1 & 0 & W^2 \\ 1 & 0 & W^2 & 0 \\ 0 & 1 & 0 & W^2 \end{bmatrix} \begin{bmatrix} f(0) \\ f(1) \\ f(2) \\ f(3) \end{bmatrix}$$
$$(1.63)$$

The simplifications result in the outputs $F(2)$ and $F(1)$ being scrambled and the unscrambling to the natural-number ordering simply involves reversing the binary number equivalents, that is, with $F'(1) = F(2)$ and $F'(2) = F(1)$; therefore, the unscrambling is accomplished as $F(1) = F(01) = F'(2) = F'(10)$ and $F(2) = F(10) = F'(1) = F'(01)$. The radix-2 with $N = 4$ FFT, described by (1.63), is implemented as shown in the diagram of Figure 1.9.

The inverse FFT (IFFT) is implemented by changing the sign of the exponent of W in (1.60), interchanging the roles of $F(n)$ and $f(m)$, as described earlier, and replacing Δt by Δf.

Recognizing that $\Delta t \Delta f = 1/N$, it is a common practice not to weight the FFT but to weight the IFFT by $1/N$ as indicated in (1.57). The number of complex multiplication is determined from (1.63) by recognizing that $W^2 = -W^0$ and not counting previous products like $W^0 f(2)$ from row 1 and $W^2 f(2) = -W^0 f(0)$ from row 3 in the first matrix multiplication on the *rhs* of (1.63). For the commonly used radix-2 FFT, the number of complex multiplications is $(N/2)\log_2(N)$ and the number of complex additions is $N\log_2(N)$. By comparison, the number of complex multiplications and additions in the direct Fourier transform are N^2 and $N(N-1)$, respectively. These computational advantages are enormous for even modest transform sizes.

1.2.5.1   *The Pipeline FFT*   The FFT algorithm discussed in the preceding section involves decimation-in-time processing and requires collecting an entire block of time-sampled data prior to performing the Fourier transform. In contrast, the pipeline FFT [21] processes the sampled data sequentially and outputs a complete Fourier transform of the stored data at each sample. The implementation of a radix-2, $N = 8$-point pipeline FFT is shown in Figure 1.10. The pipeline FFT inherently scrambles the outputs $F'(n)$ and the unscrambled outputs are not shown in the figure; the unscrambling is accomplished by simply reversing the order of the binary representation of the output locations, n, as described in the preceding section.

In general, the number of complex multiplications for a complete transform is $(N/2)(N-1)$. In Chapter 11 the pipeline FFT is applied in the acquisition of a waveform where a
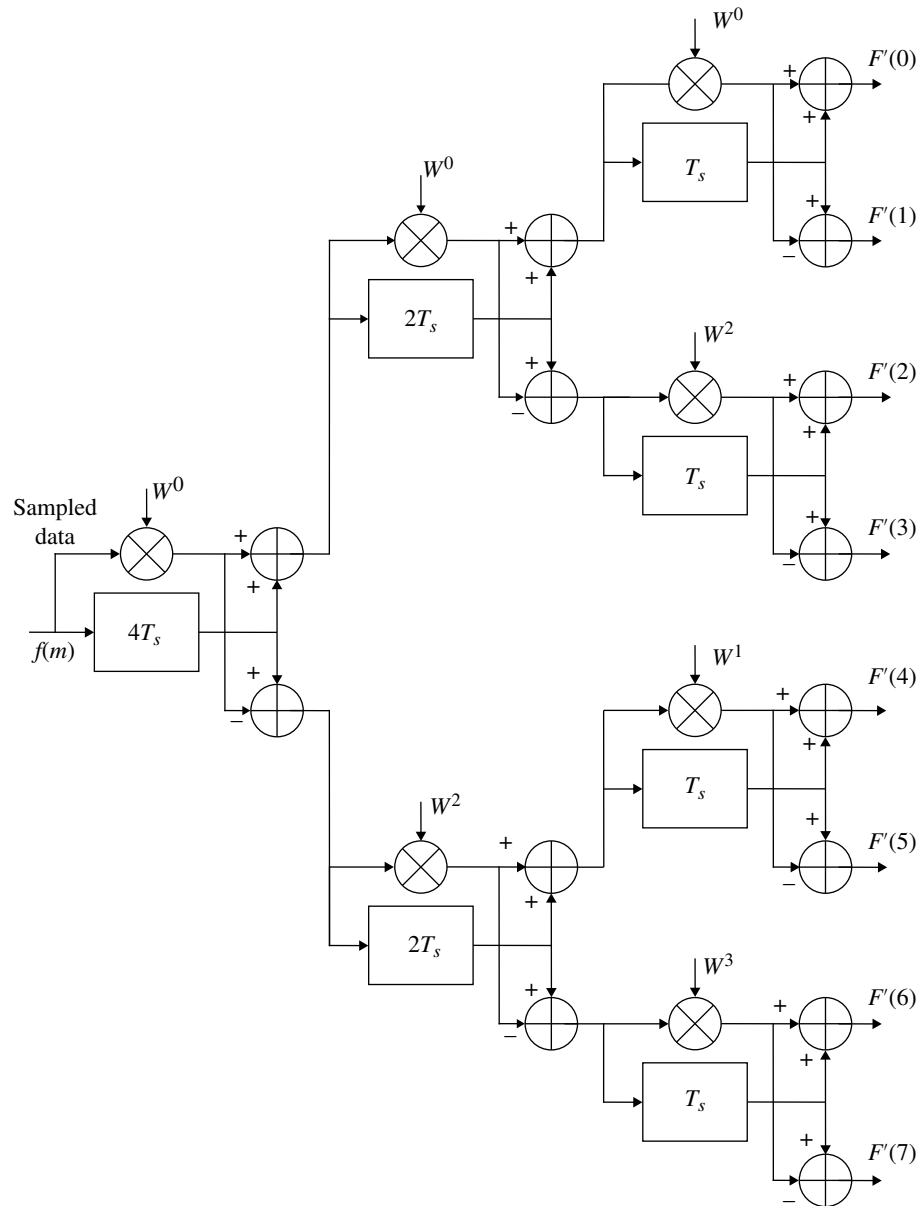
FIGURE 1.10   Radix-2, $N = 8$-point pipeline FFT implementation tree diagram.

complete N-point FFT output is not required at every sample. For example, if the complete N-point FFT is only required at sample intervals of $N_s T_s$, the number of complex multiplications can be significantly reduced (see Problem 10). The pipeline FFT can be used to interpolate between the fundamental frequency cells by appending zeros to the data samples and appropriately increasing the size of the FFT; it can also be used with data samples requiring mixed radix processing. The pipeline FFT is applicable to radar and sonar signal detection processing [21] using a variety of spectral shaping windows; however, the intrinsic $rect(t/T)$ FFT window is nearly matched for the detection of orthogonally spaced M-ary FSK modulated frequency tones.

1.2.6   The FFT as a Detection Filter

The pipeline Fourier transform is made up of a cascade of transversal filter building blocks shown in Figure 1.10. The transfer function of this building block is

$$T_i(s) = \frac{e_o(s)}{e_i(s)}$$

$$= W_i + e^{-sk_i T_s} \tag{1.64}$$

The overall transfer function from the input to a particular output is evaluated as

$$T_\ell(s) = \frac{e_\ell(s)}{e_i(s)}$$

$$= \prod_{i=1}^{k}\left(W_{\ell,i} + e^{-sk_iT_s}\right) \tag{1.65}$$

where $k = \log_2(N)$ and $k_i = 2i - 1$, $i = 1, \ldots, k$. The complex weights are given by

$$W_{\ell,i} = e^{-j\phi_{\ell,i}} \tag{1.66}$$

where

$$\phi_{\ell,i} = \frac{2\pi\ell i}{N} \tag{1.67}$$

Substitution of $W_{\ell,i}$ into (1.65) results in

$$T_\ell(s) = e^{-j\Phi_\ell}\sum_{k=0}^{N-1} e^{-k(sT_s - j\phi_\ell)} \tag{1.68}$$

where

$$\Phi_\ell = \sum_{i=1}^{k}\phi_{\ell,i} \tag{1.69}$$

This transfer function is expressed in terms of a magnitude and phase functions in ω by substituting $s = j\omega$ with the result

$$T_\ell(\omega) = \frac{\sin\left(N(\omega T_s - \phi_{\ell,k})/2\right)}{\sin\left((\omega T_s - \phi_{\ell,k})/2\right)}e^{-j\Phi'_\ell}\,e^{-j(N-1)\omega T_s/2} \tag{1.70}$$

where

$$\Phi'_\ell = \Phi_\ell - (N-1)\phi_{\ell,k}/2 \tag{1.71}$$

Therefore, the FFT forms N filters, $\ell = 0, \ldots, N-1$ each having a maximum response $|T_\ell(\omega)|_{max} = N$ that occurs at the frequencies $\omega = \phi_{\ell,k}/T_s$. As N increases these transfer functions result in the response

$$T_\ell(\omega) = N\frac{\sin\left(N(\omega T_s - \phi_{\ell,k})/2\right)}{N(\omega T_s - \phi_{\ell,k})/2}e^{-j\Phi'_\ell}\,e^{-j(N-1)\omega T_s/2}\ :N \to \infty \tag{1.72}$$

The magnitude of (1.72) is the *sinc(x)* function associated with the uniformly weighted envelope modulation function and, therefore, the FFT filter functions as a matched detection filter for these forms of modulations. Examples of these modulated waveforms are binary phase shift keying (BPSK), quadrature phase shift keying (QPSK), offset quadrature phase shift keying (OQPSK), and *M*-ary FSK.

The FFT detection filter loss relative to the ideal matched filter is examined as N increases. The input signal is expressed as

$$s(t) = \sqrt{2P}\cos(\omega_c t - \phi)rect\left(\frac{t}{T}\right) \tag{1.73}$$

and the corresponding signal spectrum for positive frequencies with $\omega_c \gg 2\pi/T$ is

$$S(\omega) = \frac{T}{2}\frac{\sin((\omega - \omega_c)T/2)}{(\omega - \omega_c)T/2}e^{-j\phi} \tag{1.74}$$

The matched filter for the optimum detection of $s(t)$ in additive white noise with spectral density N_o is defined as

$$H(\omega) = KS^*(\omega)e^{-j\omega T_o} \tag{1.75}$$

where K is an arbitrary scale factor and T_o is an arbitrary delay influencing the causality of the filter. By letting $K = 2N\sqrt{2P}/T$, $\phi = -\Phi'_\ell$, $T_o = (N - 1)T_s/2$, and $\omega_c = \phi_{\ell,n}/T_s$ it is seen that the FFT approaches a matched filter as N increases.

The question of how closely the FFT approximates a matched filter detector is examined in terms of the loss in signal-to-noise ratio. The filter loss is expressed in dB as

$$\rho = 10\log_{10}\left(\frac{\text{SNR}_o}{(\text{SNR}_o)_{opt}}\right) \tag{1.76}$$

where $(\text{SNR}_o)_{opt} = 2E/N_o$ is the signal-to-noise ratio out of the matched filter and E is the signal energy. The signal-to-noise ratio out of the FFT filter is expressed in terms of the peak signal output of the detection filter and the output noise power as

$$\text{SNR}_o = \frac{|g_\ell(t)\text{max}|^2}{N_o B_n} \tag{1.77}$$

where B_n is the detection filter noise bandwidth. For convenience the zero-frequency FFT filter output is considered, that is, for $\ell = 0$, and letting the signal phase $\phi = 0$, the response of interest is

$$T_o(\omega) = \frac{\sin(N\omega T_s/2)}{\sin(\omega T_s/2)} \tag{1.78}$$

and, from (1.74),

$$S(\omega) = \frac{T}{2}\frac{\sin(\omega T/2)}{\omega T/2} \tag{1.79}$$

TABLE 1.2 N-ary FSK Waveform Detection Loss Using an N-Point FFT Detection Filter

N	ρ (dB)
2	0.452
3	0.236
8	0.116
16	0.053

To evaluate SNR_o at the output of the FFT filter, $g_o(t)_{max}$ and B_n are computed as

$$
\begin{aligned}
g_o(t)_{max} &= \frac{1}{2\pi N} \int_{-\infty}^{\infty} T_o(\omega)S(\omega)d\omega \\
&= \frac{1}{2\pi N} \int_{0}^{\pi/T_s} \frac{\sin(\omega T/2)\sin(N\omega T_s/2)}{(\omega T/2)\sin(\omega T_s/2)}d\omega
\end{aligned}
\tag{1.80}
$$

and

$$
\begin{aligned}
B_n &= \frac{1}{2\pi} \frac{\int_{-\infty}^{\infty} |T_o(\omega)|^2 d\omega}{|T_o(0)|^2} \\
&= \frac{1}{\pi N} \int_{0}^{\pi/T_s} \frac{\sin^2(N\omega T_o/2)}{\sin^2(\omega T_o/2)}d\omega \\
&= \frac{1}{2NT_s}
\end{aligned}
\tag{1.81}
$$

Substituting these results into (1.77) and using (1.76), the parameter ρ is evaluated as

$$
\rho = 20\log\left(\frac{2}{N\pi} \int_{0}^{\pi/2} \frac{\sin^2(Nx)}{x\sin(x)}dx \right) \quad : \text{dB}
\tag{1.82}
$$

Equation (1.82) is evaluated numerically for several values of N and the results are tabulated in Table 1.2. These results indicate, for example, that detecting an 8-ary FSK-modulated waveform with orthogonal tone spacing using an $N = 8$-point FFT results in a performance loss of 0.116 dB relative to an ideal matched filter.

1.2.7   Interpolation Using the FFT

When an FFT is performed on a uniformly weighted set of N data samples a set of N $sinc(fT_w)$ orthogonal filters is generated where $T_w = NT_s$ is the sampled data window and T_s is the sampling interval. The N filters span the frequency range $f_s = 1/T_s$ and provide N frequency estimates that are separated by $\Delta f = f_s/N$ Hz. Frequency interpolation is achieved if the FFT window is padded by adding nN zero-samples, thereby increasing the window by nNT_s seconds. In this case, a set of $(n + 1)N$ $sinc(fT_w)$ filters spanning the frequency f_s is generated that provides n-point interpolation between each of the original N filters.

The FFT can also be used to interpolate between time samples. For example, consider a sampled time function characterized by N samples over the interval $T_w = NT_s$ where T_s is the sampling interval. The corresponding N-point FFT has N filters separated by $\Delta f = f_s/N$ where $f_s = 1/T_s$. If nN zero-frequency samples are inserted between frequency samples $N/2$ and $N/2 + 1$ and the IFFT is taken on the resulting $(n + 1)N$ samples, the resulting time function contains n interpolation samples between each of the original N time samples. These interpolations methods increase the size of the FFT or IFFT and thereby the computational complexity.

1.2.8   Spectral Estimation Using the FFT

Many applications involve the characterization of the PSD of a finite sequence of random data. A random data sequence represents a stochastic process, for which, the PSD is defined as the Fourier transform of the autocorrelation function of the sequence. If the random process is such that the statistical averages formed among independent stochastic process are equal to the time averages of the sequences, then the Fourier transform will converge in some sense[*] to the true PSD, $S^2(\omega)$; however, this typically requires very long sequences that are seldom available. Furthermore, the classical approach, using the Fourier transform of the autocorrelation function, is processing intense and time consuming, requiring long data sequences to yield an accurate representation to the PSD. A much simpler approach, analyzed by Oppenheim and Schafer [22], is to recognize that the Fourier transform of a relatively short data sequence $x(n)$ of N samples is

$$
X\left(e^{j\omega}\right) = \sum_{n=0}^{N-1} x(n)e^{-j\omega n}
\tag{1.83}
$$

and, defining the Fourier transform of the autocorrelation function $C_{xx}(m)$ of $x(n)$ as the periodogram

$$
\begin{aligned}
I_N(\omega) &= \sum_{m=-(N-1)}^{N-1} C_{xx}(m)e^{-j\omega m} \\
&= \frac{1}{N}\left|X\left(e^{j\omega}\right)\right|^2
\end{aligned}
\tag{1.84}
$$

---

[*]These are referred to as ergodic process and, under some circumstances, converge to the mean of the stochastic process.

However, the periodogram is not a consistent estimate[*] of the true PSD, having a large variance about the true values resulting in *wild* fluctuations. Oppenheim and Schafer then show that Bartlett's procedure [10, 23] of averaging periodograms of independent data sequences results in a consistent estimate and, if K periodograms are averaged, the resulting variance is decreased by K. In this case, the PSD estimate is evaluated as

$$\hat{S}_{xx}^2 = \frac{1}{K}\sum_{i=1}^{K} I_N^{(i)}(\omega) \qquad (1.85)$$

Oppenheim and Schafer also discuss the application of windows to the periodograms and Welch [17] describes a procedure involving the averaging of modified periodograms.

1.2.9　Fourier Transform Properties

The following Fourier transform properties are based on the transform pairs $x(t) \Leftrightarrow S(f)$ and $y(t) \Leftrightarrow Y(f)$ where $x(t)$ and $y(t)$ may be real or complex.

1.2.9.1　*Linearity*

$$ax(t) + by(t) \Leftrightarrow aX(f) + bY(f) \qquad (1.86)$$

1.2.9.2　*Translation*

$$x(t-\tau) \Leftrightarrow X(f)e^{-j2\pi f\tau} \qquad (1.87)$$

and

$$X(f-f_o) \Leftrightarrow x(t)e^{-j2\pi f_o t} \qquad (1.88)$$

1.2.9.3　*Conjugation*

$$x^*(t) \Leftrightarrow X^*(-f) \qquad (1.89)$$

and

$$X^*(f) \Leftrightarrow x^*(-t) \qquad (1.90)$$

1.2.9.4　*Differentiation*　With $z(t) \triangleq d^n x(t)/dt^n$ and $Z(f) \triangleq d^n X(f)/df^n$ then

$$z(t) \Leftrightarrow (j2\pi f)^n X(f) \qquad (1.91)$$

[*]A consistent estimate is one in which the variance about the true value and the bias approaches zero as N increases.

and

$$Z(f) \Leftrightarrow (-j2\pi t)^n x(t) \qquad (1.92)$$

1.2.9.5　*Integration*　Defining $z(t) \triangleq \int_{-\infty}^{t} \cdots \int_{-\infty}^{\tau_1} x(\tau)$ $d\tau \ldots d\tau_n$ and $Z(f) \triangleq \int_{-\infty}^{f} \cdots \int_{-\infty}^{f_1} Z(f)df \ldots df_n$ then

$$z(t) \Leftrightarrow X(f)\left(\frac{\delta(t)}{2} + \frac{1}{(j2\pi f)^n}\right) \qquad (1.93)$$

and

$$Z(f) \Leftrightarrow x(t)\left(\frac{\delta(t)}{2} + \frac{1}{(-j2\pi t)^n}\right) \qquad (1.94)$$

1.2.10　Fourier Transform Relationships

The following Fourier transform relationships are based on the transform pairs $x(t) \Leftrightarrow X(f)$ and $y(t) \Leftrightarrow Y(f)$ where $x(t)$ and $y(t)$ may be real or complex.

1.2.10.1　*Convolution*　Defining the Fourier transforms $z(t) \Leftrightarrow X(f)Y^*(f)$ and $Z(f) \Leftrightarrow x(t)y^*(t)$ then

$$z(t) = \int_{-\infty}^{\infty} x(t-\tau)y^*(\tau)d\tau = \int_{-\infty}^{\infty} x(\tau)y^*(t-\tau)d\tau \qquad (1.95)$$

and

$$Z(f) = \int_{-\infty}^{\infty} X(f-\bar{f})y^*(\bar{f})d\bar{f} = \int_{-\infty}^{\infty} X(\bar{f})Y^*(f-\bar{f})d\bar{f} \qquad (1.96)$$

1.2.10.2　*Integral of Product (Parseval's Theorem)*

$$\int_{-\infty}^{\infty} x(t)y^*(t)dt = \int_{-\infty}^{\infty} X(f)Y^*(f)df \qquad (1.97)$$

Letting $y(t) = x(t)$ results in Parseval's Theorem that equates the signal energy in the time and frequency domains as

$$\int_{-\infty}^{\infty} |x(t)|^2 dt = \int_{-\infty}^{\infty} |X(f)|^2 df \quad : \text{Parseval's theorem}$$
$$(1.98)$$

TABLE 1.3 **Fourier Transforms for** $f(t) \Leftrightarrow F(f)$

Waveform $f(t)$	Spectrum $F(f)$
1	$\delta(f)$
$f(t - \tau)$	$F(f)\exp(-j2\pi f\tau)$
$f(t)e^{j2\pi f_o t}$	$f(f - f_o)$
$\delta(t)$	$\dfrac{1}{2\pi}\displaystyle\int e^{j\omega t}dt = 1$
$\delta(t - \tau)$	$\exp(-j2\pi f\tau)$
$f(at)$	$(1/a)F(f/a)$
$e^{j2\pi f_o t}$	$\delta(f - f_o)$
$\cos(2\pi f_o t)$	$\left(\dfrac{1}{2}\right)(\delta(f + f_o) + \delta(f - f_o))$
$\sin(2\pi f_o t)$	$\left(\dfrac{j}{2}\right)(\delta(f + f_o) - \delta(f - f_o))$
$\displaystyle\sum_{n=-\infty}^{\infty} \delta(t - n\tau)$	$\dfrac{1}{\tau}\displaystyle\sum_{n=-\infty}^{\infty} e^{-j2\pi nf\tau} = \dfrac{1}{\tau}\displaystyle\sum_{n=-\infty}^{\infty} \delta\left(f - \dfrac{n}{\tau}\right)$
$\dfrac{d^n f(t)}{dt^n}$	$(j2\pi f)^n F(f)$
$(-j2\pi t)^n f(t)$	$\dfrac{d^n F(f)}{df^n}$
$\displaystyle\int_{-\infty}^{t} f(\xi)d\xi$	$(1/2)(\delta(f) + 1/(j\pi f))F(f)$
$(1/2)(\delta(t) - 1/(j\pi t))s(t)$	$\displaystyle\int_{-\infty}^{f} F(\lambda)d\lambda$
$e^{-(t/a)^2/2}$	$\sqrt{2\pi}ae^{-(2\pi fa)^2/2}$
$f(t) = x(t)\, y(t)$	$X(f)*Y(f) = \displaystyle\int X(f - \lambda)Y(\lambda)d\lambda$
$f(t) = x(t)*y(t)$	$F(f) = X(f)\, Y(f)$
$u(t) = \begin{cases} 1 & : t \geq 0 \\ 0 & : o.w. \end{cases}$	$U(f) = \dfrac{1}{2}\left(\delta(f) + \dfrac{1}{j\pi f}\right)$
$u(t-\tau) = \begin{cases} 1 & : t - \tau \geq 0 \\ 0 & : o.w. \end{cases}$	$U(f)\exp(-j2\pi f\tau)$
$sgn(t) = 2u(t) - 1$	$sgn(f) = \dfrac{1}{j\pi f}$
$\quad = \begin{cases} 1 & : t > 0 \ ^a \\ -1 & : t < 0 \end{cases}$	
$sgn(t) = \dfrac{1}{j\pi t}$	$sgn(f) = 2u(f) - 1$
$rect\left(\dfrac{t}{T}\right) = 1 \quad : |t| < \dfrac{T}{2}$	$Tsinc(fT)^b$
$\quad\quad = 0 \quad : o.w.$	
$sinc(2t/T)$	$\left(\dfrac{T}{2}\right)rect\left(\dfrac{fT}{2}\right) = 1 \quad : |f| < \dfrac{1}{T}$
	$\quad\quad = 0 \quad : o.w.$

*Denotes convolution.
[a]The *signum* function $sgn(x)$ is also denoted as *signum*(x).
[b]Woodward [24].

1.2.11 Summary of Some Fourier Transform Pairs

Some often used transform relationships are listed in Table 1.3.

1.3 PULSE DISTORTION WITH IDEAL FILTER MODELS

In this section the distortion is examined for an isolated baseband pulse after passing through an ideal filter with uniquely prescribed amplitude and phase responses. In radar applications isolated pulse response leads to a loss in range resolution; however, in communication application, where the pulse is representative of a contiguous sequence of information-modulated symbols, the pulse distortion leads to inter-symbol interference (ISI) that degrades the information exchange. The following two examples use the baseband pulse, or symbol, as characterized in the time and frequency domains by the familiar functions

$$s(t) = rect\left(\frac{t}{T}\right) \quad \Leftrightarrow \quad S(f) = Tsinc(fT) \qquad (1.99)$$

1.3.1 Ideal Amplitude and Zero Phase Filter

In this example, the filter is characterized in the frequency domain as having a constant unit amplitude over the bandwidth $f \leq |B|$ with zero amplitude otherwise and a zero phase function. Using the previous notation the filter is characterized in the frequency and time domains as

$$H(f) = rect\left(\frac{f}{2B}\right) \quad \Leftrightarrow \quad h(t) = 2Bsinc(2Bt) \qquad (1.100)$$

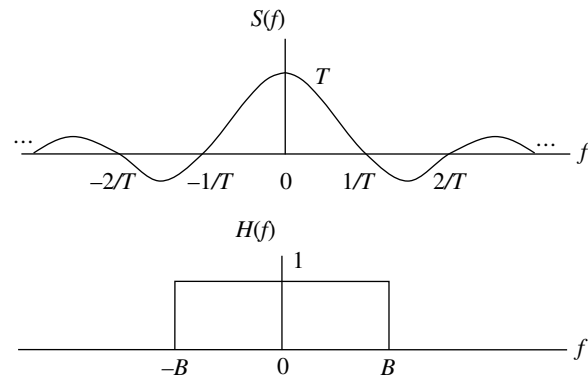The frequency characteristics of the signal and filter are shown in Figure 1.11.

FIGURE 1.11 Ideal signal and filter spectrums.

The easiest way to evaluate the filter response to a pulse input signal is by convolving the functions as

$$g(t) = \int_{-\infty}^{\infty} h(\tau)s(\tau - t)d\tau$$
$$= 2B\int_{-\infty}^{\infty} sinc(2B\tau)rect\left(\frac{\tau - t}{T}\right)d\tau \tag{1.101}$$

The $rect(\bullet)$ function determines the integration limits with the upper and lower limits evaluated for τ when the argument equals ±½, respectively. This evaluation leads to the integration

$$g(t) = 2B\int_{t-T/2}^{t+T/2} \frac{\sin(2\pi B\tau)}{2\pi B\tau}d\tau \tag{1.102}$$

Equation (1.102) is evaluated in terms of the *sine integral* [25]

$$S_i(y) = \int_0^y \frac{\sin(x)}{x}dx \tag{1.103}$$

resulting in the filter output $g(t)$ expressed as

$$g(t) = \frac{1}{\pi}S_i(2\pi B(t + T/2)) - \frac{1}{\pi}S_i(2\pi B(t - T/2)) \tag{1.104}$$

Defining the normalized variable $y = t/T$ and the parameter $\rho = BT$, Equation (1.104) is expressed as

$$g(y) = \frac{1}{\pi}S_i(2\pi\rho(y + 1/2)) - \frac{1}{\pi}S_i(2\pi\rho(y - 1/2)) \tag{1.105}$$

Equation (1.105) is plotted in Figure 1.12 for several values of the time-bandwidth (BT) parameter. Range resolution is proportional to bandwidth and the increased rise time
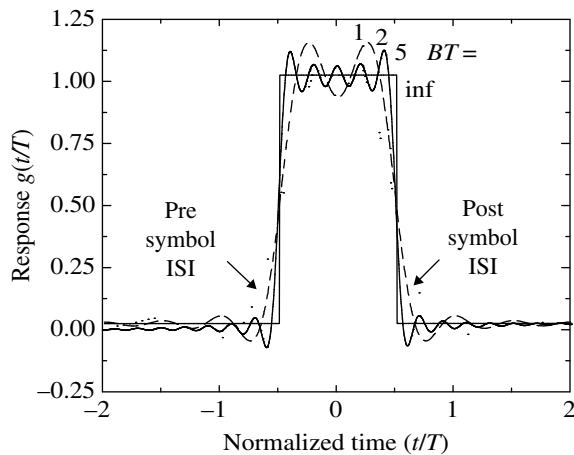

FIGURE 1.12 Ideal band-limited pulse response (constant-amplitude, zero-phase filter).

or *smearing* of the pulse edges with decreasing bandwidth is evident. The ISI that degrades the performance of a communication system results from the symbol energy that occurs in adjacent symbols due to the filtering.

This analysis considers only the pulse distortion caused by constant amplitude filter response and, as will be seen in the following section, filter amplitude ripple and nonlinear phase functions also result in additional signal distortion. If the filter were to exhibit a linear phase function $\phi(f) = -2\pi f T_o$ where T_o represents a constant time delay, then, referring to Table 1.3, the output is simply delayed by T_o without any additional distortion. If T_o is sufficiently large, the filter can be viewed as a causal filter, that is, no output is produced before the input signal is applied.

1.3.2 Nonideal Amplitude and Phase Filters: Paired Echo Analysis

In this section the pulse distortion caused by a filter with prescribed amplitude and phase functions is examined using the analysis technique of paired echoes [26]. A practical application of paired echo analysis occurred when a modem production line was stopped at considerable expense due to noncompliance of the bit-error test involving a few tenths of a decibel. The required confidence level of the bit-error performance under various IF filter conditions precluded the use of Monte Carlo simulations; however, much to the pleasure of management, the paired echo analysis was successfully applied to identify the cause of the subtle filter distortion losses.

Consider a filter with amplitude and phase functions expressed as

$$H(f) = A(f)e^{-j\phi(f)}rect\left(\frac{f}{2B}\right) \tag{1.106}$$

where the amplitude and phase fluctuations with frequency are expressed as

$$A(f) = 1 + a\sin(2\pi f \tau_a) \tag{1.107}$$

and

$$\phi(f) = 2\pi f T_o + b\sin(2\pi f \tau_b) \tag{1.108}$$

The parameters a and τ_a represent the amplitude and period of the amplitude ripple and b and τ_b represent the amplitude and period of the phase ripple. Using these functions in (1.106) and separating the constant delay term involving T_o, results in the filter function

$$H(f) = (1 + a\cos(2\pi f \tau_a))e^{-jb\sin(2\pi f \tau_b)}rect\left(\frac{f}{2B}\right)e^{-j2\pi f T_o} \tag{1.109}$$

Equation (1.109) is simplified by using the trigonometric identity

$$\cos(2\pi f \tau_a) = \frac{1}{2}\left(e^{-j2\pi f \tau_a} + e^{j2\pi f \tau_a}\right) \qquad (1.110)$$

and the Bessel function identity [27]

$$e^{-jb\sin(2\pi f \tau_b)} = \sum_{n=-\infty}^{\infty} J_n(-b)e^{j2\pi n f \tau_b}$$

$$= J_o(b) + J_1(b)\left(e^{-j2\pi f \tau_b} - e^{j2\pi f \tau_b}\right) + O_2(\pm n) \qquad (1.111)^*$$

In arriving at the last expression in (1.111), the following identities were used

$$J_n(-b) = J_{-n}(-b) = (-1)^n J_n(b) \qquad (1.112)$$

Upon substituting (1.110) and (1.111) into (1.109), and performing the multiplications to obtain additive terms representing unique delays results in the filter frequency response

$$H(f) = \left\{ J_0(b)e^{-j2\pi f T_o} + \frac{a}{2}J_0(b)e^{-j2\pi f(T_o + \tau_a)} \right.$$

$$+ \frac{a}{2}J_0(b)e^{-j2\pi f(T_o - \tau_a)} + J_1(b)e^{-j2\pi f(T_o + \tau_b)}$$

$$+ \frac{a}{2}J_1(b)e^{-j2\pi f(T_o + \tau_a + \tau_b)} + \frac{a}{2}J_1(b)e^{-j2\pi f(T_o - \tau_a + \tau_b)}$$

$$- J_1(b)e^{-j2\pi f(T_o - \tau_b)} - \frac{a}{2}J_1(b)e^{-j2\pi f(T_o + \tau_a - \tau_b)}$$

$$\left. - \frac{a}{2}J_1(b)e^{-j2\pi f(T_o - \tau_a - \tau_b)} \right\}$$

$$rect\left(\frac{f}{2B}\right) + \text{higher order filter terms involving } J_n(b)$$

$$(1.113)$$

Upon performing the inverse Fourier transform of each term in (1.113), the filter impulse response, $h(t)$, becomes a summation of weighted and delayed $sinc(x)$ functions of the form $2BKsinc(2B(t - T_d))$ where K and T_d are the amplitude and delay associated with each of the terms. Performing the convolution indicated by the first equality in (1.101), that is, for an arbitrary signal $s(t)$, the ideally filtered response $g(t)$ is expressed as

$$g(t) = 2B\int_{-\infty}^{\infty} sinc(2B\tau)s(\tau - t)d\tau \qquad (1.114)$$

---

*The notation $O_2(\pm n)$ refers to higher order terms involving $|n| \geq 2$. These terms can be neglected for small values of b, that is, $b < 0.2$.

When $g(t)$ is passed through the filter $H(f)$ with amplitude and phase described, respectively, by (1.107) and (1.108), the distorted output $g_o(t)$ is evaluated as

$$g_o(t) = J_0(b)g(t - T_o) + \frac{a}{2}J_0(b)g(t - T_o - \tau_a)$$

$$+ \frac{a}{2}J_0(b)g(t - T_o + \tau_a) + J_1(b)g(t - T_o - \tau_b)$$

$$+ \frac{a}{2}J_1(b)g(t - T_o - \tau_a - \tau_b) + \frac{a}{2}J_1(b)g(t - T_o + \tau_a - \tau_b)$$

$$- J_1(b)g(t - T_o + \tau_b) - \frac{a}{2}J_1(b)g(t - T_o - \tau_a + \tau_b)$$

$$- \frac{a}{2}J_1(b)g(t - T_o + \tau_a + \tau_b)$$

$$(1.115)$$

If the input signal is described by the $rect(t/T)$ function, then $g(t)$ is the response expressed by (1.104) and depicted in Figure 1.12. The distortion terms appear as paired echoes of the filtered input signal and Figure 1.13 shows the relative delay and amplitude of each *echo* of the filtered output $g(t)$. For $b << 1$ the approximations $J_0(b) = 1.0$ and $J_1(b) = b/2$ apply and when $a = b = 0$ the filter response is simply the
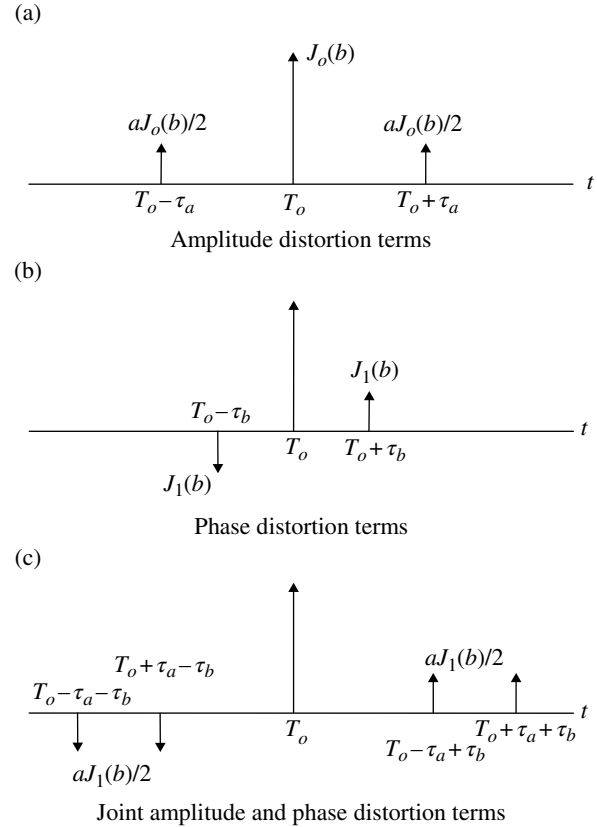
(a)

Amplitude distortion terms

(b)

Phase distortion terms

(c)

Joint amplitude and phase distortion terms

FIGURE 1.13 Location of amplitude and phase distortion paired echoes relative to delay T_o.

delayed but undistorted replica of the input signal, that is, $g_o(t) = g(t - T_o)$. More complex filter amplitude and phase distortion functions can be synthesized by applying Fourier series expansions that yield paired echoes that can be viewed as noisy interference terms that degrade the system performance; however, the analysis soon becomes unwieldy so computer simulation of the echo amplitudes and delays must be undertaken.

1.3.3 Example of Delay Distortion Loss Using Paired Echoes

The evaluation of the signal-to-interference ratio resulting from the delay distortion of a filter is examined using paired echo analysis. The objective is to examine the distortion resulting from a specification of the filters peak phase error and group delay within the filter bandwidth. The filter phase response is characterized as

$$\phi(f) = 2\pi f T_o - \phi_o \sin(2\pi f \tau) \qquad (1.116)$$

where T_o is the filter delay resulting from the linear phase term, ϕ_o is the peak phase deviation from linearity over the filter bandwidth, and τ is the period of the sinusoidal phase distortion function. The linear phase term introduces the filter delay T_o that does not result in signal distortion; however, the sinusoidal phase term does cause signal distortion. In this example, the phase deviation over the filter bandwidth is specified parametrically as $\phi_o(\text{deg}) = 3$ and $7°$. The parameter τ is chosen to satisfy the peak delay distortion defined as

$$\begin{aligned} T_d(f) &= -\frac{\partial\phi(f)}{2\pi\partial f} \\ &= \tau\phi_o\cos(2\pi f\tau) \end{aligned} \qquad (1.117)$$

where ϕ_o is in radians. The peak delay, evaluated for $f\tau = 0$, is specified as $T_d = 34$ and 100 ns and, using (1.117), the period of the sinusoidal phase function, $\tau = T_d/\phi_o$, is tabulated in Table 1.4 for the corresponding peak phase errors and peak delay specification. Practical maximum limits of the group delay normalized by the symbol rate, R_s, are also specified.

Considering an ideal unit gain filter with amplitude response of $A(\omega) = 1$, the filter transfer function is expressed as

$$\begin{aligned} H(f) &= e^{-j\phi(f)} \\ &= e^{-j2\pi fT_o}e^{j\phi_o\sin(2\pi f\tau)} \\ &= e^{-j2\pi fT_o}\sum_{n=-\infty}^{\infty}J_n(\phi_o)e^{jn\pi f\tau} \end{aligned} \qquad (1.118)$$

TABLE 1.4   Values of τ for the Phase and Delay Specifications

$\phi_o(\text{deg})$	$T_d(ns)$	$\tau(ns)$	$T_g/R_s{}^a$
3	34	649	±0.15
7	100	818	

^{a}Normalized group delay over filter bandwidth.

Upon taking the inverse Fourier transform of (1.118), the filter impulse response is evaluated as

$$\begin{aligned} g(t) = &J_o(\phi_o)\delta(t-T_o) \\ &+ \sum_{n=1}^{\infty}J_n(\phi_o)[\delta(t-T_o+n\tau/2)-\delta(t-T_o-n\tau/2)] \end{aligned}$$
$$(1.119)$$

The parameter τ determines the delay spread of all the interfering terms; however, for small arguments the interference is dominated by the $J_1(\phi_o)$ term and the signal-to-interference ratio is defined as

$$\gamma_i = 20\log\left(\frac{J_1(\phi_o)}{J_o(\phi_o)}\right) \qquad (1.120)$$

For $\phi_o(\text{deg}) = 3$ and $7°$, the respective signal-to-interference ratios are 32 and 24.3 dB and under these conditions, a 10 dB filter input signal-to-noise ratio results in the output signal-to-noise ratio degraded by 0.02 and 0.17 dB, respectively.

1.4 CORRELATION PROCESSING

Signal correlation is an important aspect of signal processing that is used to characterize various channel temporal and spectral properties, for example, multipath delay and frequency dispersion profiles. The correlation can be performed as a time-averaged autocorrelation or a time-averaged cross-correlation between two different signals. Frequency domain, autocorrelation, and cross-correlation are performed using frequency offsets rather than time delays. The Doppler and multipath profiles are characteristics of the channel that are typically based on correlations involving statistical expectations as opposed to time-averaged correlations that are applied to deterministic signal waveforms and linear time-invariant channels. The following discussion focuses on the correlation of deterministic waveforms and linear time-invariant channels.

The autocorrelation of the complex signal $\tilde{x}(t)$ is defined as[*]

$$R_{\tilde{x}\tilde{x}}(\tau) \triangleq \int_{-\infty}^{\infty}\tilde{x}(t)\tilde{x}^*(t-\tau)dt = \int_{-\infty}^{\infty}\tilde{x}(t+\tau)\tilde{x}^*(t)dt \quad (1.121)$$

[*]The asterisk denotes complex conjugation. The double subscripts on $R_{xx}(\tau)$ are not always included for the autocorrelation notation; however, they are important when describing the cross-correlation response.

TABLE 1.5   Properties of Correlation Functions

Property	Comments
$R_{\tilde{x}\tilde{x}}(-\tau) = R_{\tilde{x}\tilde{x}}^*(\tau)$	
$C_{\tilde{x}\tilde{x}}(-\tau) = R_{\tilde{x}\tilde{x}}(\tau) - \|\tilde{m}_x\|^2$	
$R_{xx}(-\tau) = R_{xx}(\tau)$	x : real
$C_{xx}(-\tau) = R_{xx}(\tau) - m_x^2$	x : real
$R_{\tilde{x}\tilde{y}}(-\tau) = R_{\tilde{y}\tilde{x}}^*(\tau)$	
$C_{\tilde{x}\tilde{y}}(\tau) = R_{\tilde{x}\tilde{y}}(\tau) - \tilde{m}_x \tilde{m}_y^*$	
$C_{xy}(\tau) = R_{xy}(\tau) - m_x m_y$	x,y : real
$R_{\tilde{z}\tilde{z}}(\tau) = R_{\tilde{x}\tilde{x}}(\tau) + R_{\tilde{y}\tilde{y}}(\tau) + R_{\tilde{x}\tilde{y}}(\tau) + R_{\tilde{y}\tilde{x}}(\tau)$	$\tilde{z} = \tilde{x} + \tilde{y}$

The autocorrelation function implicitly contains the mean value of the signal and the autocovariance is evaluated, by removing the mean value, as

$$C_{\tilde{x}\tilde{x}}(\tau) = \int_{-\infty}^{\infty} [\tilde{x}(t) - \tilde{m}_x][\tilde{x}(t-\tau) - \tilde{m}_x]^* dt$$
$$= R_{\tilde{x}\tilde{x}}(\tau) - |\tilde{m}_x|^2 \tag{1.122}$$

where $\tilde{m}_x = m_{xc} + j m_{xs}$ is the complex mean of the signal $\tilde{x}(t)$. The cross-correlation of the complex signals $\tilde{x}(t)$ and $\tilde{y}(t)$ is defined as

$$R_{\tilde{x}\tilde{y}}(\tau) \triangleq \int_{-\infty}^{\infty} \tilde{x}(t)\tilde{y}^*(t-\tau) dt = \int_{-\infty}^{\infty} \tilde{x}(t+\tau)\tilde{y}^*(t) dt \tag{1.123}$$

Similarly, the corresponding cross-covariance is evaluated as

$$C_{\tilde{x}\tilde{y}}(\tau) = \int_{-\infty}^{\infty} [\tilde{x}(t) - \tilde{m}_x][\tilde{y}(t-\tau) - \tilde{m}_y]^* dt$$
$$= R_{\tilde{x}\tilde{y}}(\tau) - \tilde{m}_x \tilde{m}_y^* \tag{1.124}$$

The properties of various correlation functions applied to complex and real valued functions are summarized in Table 1.5. The properties of correlation functions are also discussed in Section 1.5.9 in the context of stochastic processes.

1.5   RANDOM VARIABLES AND PROBABILITY

This section contains a brief introduction to random variables and probability [6, 8, 28–30]. A random variable is described in the context of Figure 1.14 in which an event χ in the space S is mapped to the real number x characterized as $X(\chi) = x$ or $f(x)$: $x_a \le x \le x_b$. The function $X(\chi)$ is defined as a random variable

which assigns the real number x or $f(x)$ to each event $\chi \in S$.[*] The limits $[x_a, x_b]$ of the mapping are dependent upon the physical nature or definition of the event space. The second depiction shown in Figure 1.14 comprises disjoint, or nonintersecting, subspaces, such that, for $i \ne j$ the intersection $S_i \cap S_j = \emptyset$ is the null space. Each subspace possesses a unique mapping $x|S_j$ conditioned on the subspace $S_j : j = 1, \ldots, J$. The union of subspaces is denoted as $S_i \cup S_j$. This is an important distinction since each subspace can be analyzed in a manner similar to the mapping of $\chi \in S$. The three basic forms of the random variable X are continuous, discrete, and a mixture of continuous and discrete random variables as distinguished in the following sections.

1.5.1   Probability and Cumulative Distribution and Probability Density Functions

The mathematical description [6, 8, 24, 28, 30–32] of the random variable X resulting from the mapping $X(\chi)$ given the random event $\chi \in S$ is based on the statistical properties of the random event characterized by the probability $P(\{X \le x\})$ where $\{X \le x\}$ denotes all of the events $X(\chi)$ in S. For continuous random variables $P(X = x) = 0$. The probability function $P(X_i \in S_i)$ satisfies the following axioms:

A1. $P(X(\chi) \in S) \ge 0$
A2. $P(\{X(\chi) \in S\}) = 1$
A3. If $P(S_i \cap S_j) = \emptyset \ \forall i \ne j$ then $P(S_1 \cup, \ldots, S_J) = \sum_{j=1}^{J} P(S_j)$

Axiom A3 applies for infinite event spaces by letting $J = \infty$. Several corollaries resulting from these axioms are as follows:

C1. $P(\chi^c) = 1 - P(\chi)$ where χ^c is the complement of χ such that $\chi^c \cap \chi = \emptyset$
C2. $P(\chi) \le 1$
C3. $P(\chi_i \cup \chi_j) = P(\chi_i) + P(\chi_j) - P(\chi_i \cap \chi_j)$
C4. If $P(\emptyset) = 0$

The *cumulative distribution function* (*cdf*) of the variable X is defined in terms of the value of x on the real line as

$$F_X(x) \triangleq P(X \le x) \quad : -\infty < x < \infty, \text{ cumulative distribution function} \tag{1.125}$$

[*]A particular outcome $x' = f(x)$ is a random variable resulting from the mapping $X(\chi)$ onto the real line; however, $X(\chi)$ is also referred to as a random variable. Wozencraft and Jacobs (Reference 30, p. 39) point out that this nomenclature stems from practical applications and is somewhat misleading.
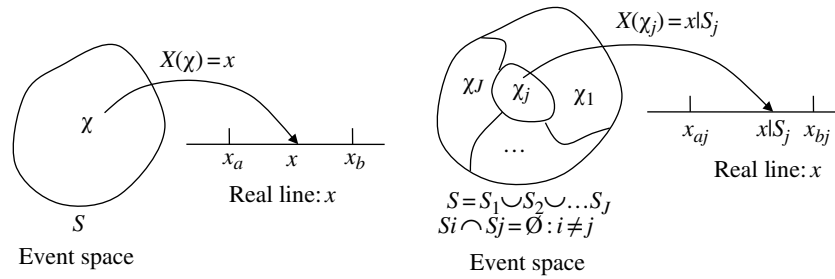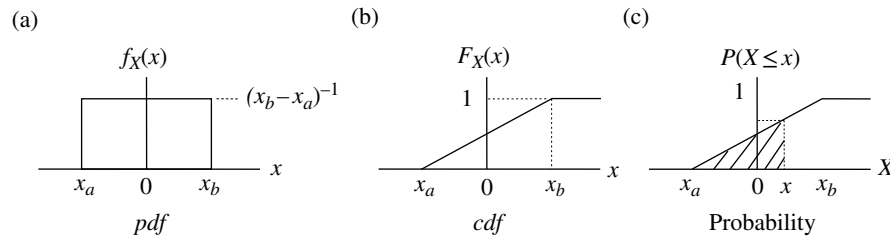
FIGURE 1.14   Mapping of random variable $X(\chi)$ on the real line x.

FIGURE 1.15   Uniformly distributed continuous random variable.

where $F_X(x)$ has the following properties:

P1. $0 \le F_X(x) \le 1$

P2. In the limit as x approaches ∞, $F_X(x) = 1$

P3. In the limit as x approaches $-\infty$, $F_X(x) = 0$

P4. $F_X(x)$ is a nondecreasing function of x

P5. In the limit as ε approaches 0, $F_X(x_i) = F_X(x_i + \varepsilon)$

P6. The probability in the interval $x_i < x \le x_j$ is: $P(x_i < x \le x_j) = F_X(x_j) - F_X(x_i)$

P7. In the limit as ε approaches 0, the probability of the event x_i is $P(x_i - \varepsilon < x \le x_i) = F_X(x_i) - F_X(x_i - \varepsilon)$.

Property P5 is referred to as being *continuous from the right* and is particularly important with discrete random variables, in that, $F_X(x_i)$ includes a discrete random variable at x_i. Property P7, for a continuous random variable, states that $P(x_i) = 0$; however, for a discrete random variable, $P(x_i) = p_X(x_i)$ where $p_X(x_i)$ is the *probability mass function* (*pmf*) defined in Section 1.5.1.2.

The *probability density function*[*] (*pdf*) of X is defined as

$$f_X(x) \triangleq \frac{dF_X(x)}{dx} \quad : \text{probability density function} \quad (1.126)$$

The *pdf* is frequency used to characterize a random variable because, compared to the *cdf*, it is easier to describe and visualize the characteristics of the random variable.

---

[*]The *pdf* is formally denoted $f_X(x)$ and in the notation $f(x)$ the random variable X is understood by the usage; the notation $p(x)$ is also used to denote the *pdf*; however, these notations are sometimes justified by notational simplicity.

1.5.1.1   Continuous Random Variables   A random variable is continuous if the *cdf* is continuous so that $F_X(x)$ can be expressed by the integral of the *pdf*. The mapping in Figure 1.14 results in the continuous real variable x. From (1.125) and (1.126) it follows that

$$P(X \le x) = F_X(x) = \int_{-\infty}^{x} f_X(x') dx' \quad (1.127)$$

A frequently encountered and simple example of a continuous random variable is characterized by the uniformly distributed *pdf* shown in Figure 1.15 with the corresponding *cdf* and probability function.

From property P7, the probability of $X = x_i$ is evaluated as

$$P(X = x_i) = \lim_{\varepsilon \to 0} \left(F_X(x_i - \varepsilon) \right) - F_X(x_i) \quad (1.128)$$

However, for continuous random variables, the limit in (1.128) is equal to $F_X(x_i)$ so $P(X = x_i) = 0$; this event is handled as described in Section 1.5.2.

1.5.1.2   Discrete Random Variables   The *probability mass function* [8, 28, 29] (*pmf*) of the discrete random variable X is defined in terms of the discrete probabilities on the real line as

$$p_X(x_i) \triangleq P(X = x_i) \quad (1.129)$$

The corresponding *cdf* is expressed as

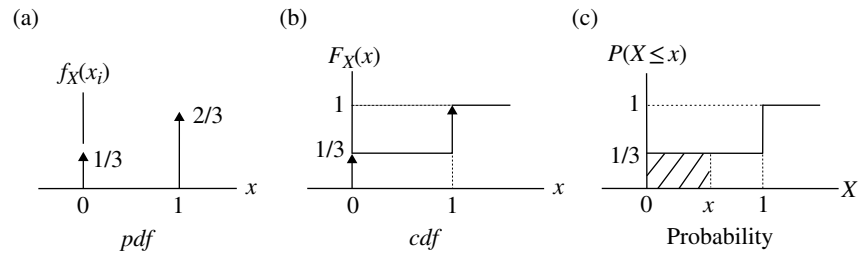$$F_X(x) = \sum_i p_X(x_i) u(x - x_i) \quad (1.130)$$

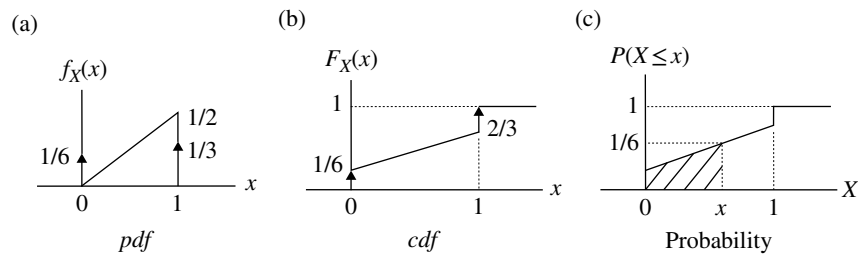**FIGURE 1.16**   Discrete binary random variables.

FIGURE 1.17   Mixed random variables.

where $u(x - x_i)$ is the *unit-step function* occurring at $x = x_i$ and is defined as

$$u(x - x_i) \triangleq \begin{cases} 0 & : u < x_i \\ 1 & : u \geq x_i \end{cases} \qquad (1.131)$$

Using (1.126), and recognizing that the derivative of $u(x - x_i)$ is the delta function $\delta(x - x_i)$, the *pdf* of the discrete random variable is expressed as

$$f_X(x) = \sum_i p_X(x_i)\delta(x - x_i) \qquad (1.132)$$

The *pmf* $p_X(x_i)$ results in a weighted delta function and, from (1.130), (1.131), and property P2, the summation must satisfy the condition $\sum_{\forall i} p_X(x_i) = 1$.

The *pdf*, *cdf*, and the corresponding probability for the discrete random variable corresponding to binary data {0,1} with *pmf* functions $p_X(0) = 1/3$ and $p_X(1) = 2/3$ are shown in Figure 1.16. The importance of property P5 is evident in Figure 1.16, in that, the delta function at $x = 1$ is included in the *cdf* resulting in $P(X \leq 1) = 1$. Regarding property P7, the limit in (1.128) approaches $X = x_i$ from the left, corresponding to the *base* of the discontinuity, so that $P(X = x_i) = p_X(x_i)$.

1.5.1.3   *Mixed Random Variables*   Mixed random variables are composed of continuous and discrete random variables and the following example is a combination of the continuous and discrete random variables in the examples of Sections 1.5.1.1 and 1.5.1.2. The major consideration in this case is the determination of the event *pmf* for the continuous (C) and discrete (D) random variables to satisfy property P2. Considering equal *pmfs*, such that, $p_X(S = C) = p_X(S = D) = 1/2$, the *pdf*, *cdf*, and probability are depicted in Figure 1.17.

1.5.2   Definitions and Fundamental Relationships for Continuous Random Variables

For the continuous random variables X, such that the events $X(\chi_j) \in S_i$, the joint *cdf* is determined by integrating the joint *pdf* expressed as

$$F_{X_1,\ldots,X_N}(x_1,\ldots,x_N) = \int_{-\infty}^{x_1} \cdots \int_{-\infty}^{x_N} f_{X_1,\ldots,X_N}(x_1'),\ldots,x_N')dx_1',\ldots,dx_N' \qquad (1.133)$$

and, provided that $F_{X_1,\ldots,X_N}(x_1,\ldots,x_N)$ is continuous and exists, it follows that

$$f_{X_1,\ldots,X_N}(x_1,\ldots,x_N) = \frac{\partial^N F_{X_1,\ldots,X_N}(x_1,\ldots,x_N)}{\partial x_1 \ldots \partial x_N} \qquad (1.134)$$

The probability function is then evaluated by integrating x_i over the appropriate regions $x_{i1} < r_i \leq x_{i2}$: $i = 1, \ldots, N$ with the result

$$P(X_{r1},\ldots,X_{r_N}) = \int_{r_1} \cdots \int_{r_N} f_{X_1,\ldots,X_N}(x_1',\ldots,x_N')dx_1'\ldots dx_N' \qquad (1.135)$$

1.5.2.1 *Marginal pdf* of Continuous Random Variables
The marginal *pdf* is determined by integrating over the entire region of all the random variables except for the desired marginal *pdf*. For example, the marginal *pdf* for x_1 is evaluated as (see Problem 17)

$$M_{X_1}(x_1) = \frac{d}{dx_1}\int_{-\infty}^{x_1}\int_{-\infty}^{\infty}\cdots\int_{-\infty}^{\infty} f_{X_1\cdots X_N}\left(x'_1,\ldots,x'_N\right)dx'_1,\ldots,dx'_N$$

$$= f_{X_1}(x_1)\int_{-\infty}^{\infty}\cdots\int_{-\infty}^{\infty} f_{X_2\cdots X_N}\left(x'_2,\ldots,x'_N\right)dx'_2,\ldots,dx'_N$$

$$= f_{X_1}(x_1)$$

$$(1.136)$$

The random variables X_i are independent *iff* the joint *cdf* can be expressed as product of the each *cdf*, that is

$$F_{X_1,\ldots,X_N}(x_1,\ldots,x_N) = F_{X_1}(x_1)F_{X_2}(x_2)\cdots F_{X_N}(x_N) \quad (1.137)$$

In addition, if $X_i \,\forall\, i$ are jointly continuous, the random variables are independent if the joint *pdf* can be expressed as the product of each *pdf* as

$$f_{X_1,\ldots,X_N}(x_1,\ldots,x_N) = f_{X_1}(x_1)f_{X_2}(x_2)\cdots f_{X_N}(x_N) \qquad (1.138)$$

Therefore, the joint *pdf* of independent random variables is the same as the product of each marginal *pdf* computed sequentially as in (1.136).

The joint *cdf* of two continuous random variables is defined as

$$F_{X,Y}(x,y) \triangleq P(X \le x, Y \le y) \qquad (1.139)$$

with the following properties,

$$\left.\begin{array}{l} F_{X,Y}(x,\infty) = F_X(x), \ F_{X,Y}(\infty,y) = F_Y(y), \ F_{X,Y}(\infty,\infty) = 1 \\ F_{X,Y}(x,-\infty) = 0, \ \ F_{X,Y}(-\infty,y) = 0 \end{array}\right\}$$

$$(1.140)$$

and the joint *pdf* is defined as

$$f(X,Y) = \frac{\partial^2}{\partial x \partial y}F_{X,Y}(x,y) \qquad (1.141)$$

with the following properties,

$$\left.\begin{array}{l} \int_{-\infty}^{\infty}\int_{-\infty}^{\infty} f_{X,Y}(x,y)dxdy = 1, \ \dfrac{\partial F_{X,Y}(x,y)}{\partial x} = \int_{-\infty}^{y} f_{X,Y}(x,y')dy', \\ \dfrac{\partial F_{X,Y}(x,y)}{\partial y} = \int_{-\infty}^{x} f_{X,Y}(x',y)dx' \end{array}\right\}$$

$$(1.142)$$

1.5.2.2 *Conditional pdf* and *cdf* of Continuous Random Variables   The conditional *pdf* is expressed as

$$f_{X_1\ldots X_i}(x_1,\ldots,x_i|x_{i+1},\ldots,x_n) = \frac{f_{X_1\ldots X_n}(x_1,\ldots,x_n)}{f_{X_{i+1}\ldots X_n}(x_{i+1},\ldots,x_n)} \quad (1.143)$$

and the conditional *cdf* is evaluated as

$$F_{X_1\ldots X_i}(x_1,\ldots,x_i|x_{i+1},\ldots,x_n)$$

$$= \frac{\displaystyle\int_{-\infty}^{x_1}\cdots\int_{-\infty}^{x_i} f_{X_1\ldots X_n}\left(x'_1,\ldots,x'_i,x_{i+1},\ldots,x_n\right)d\,x'_1,\ldots,d\,x'_i}{f_{X_{i+1}\ldots X_n}(x_{i+1},\ldots,x_n)}$$

$$(1.144)$$

A *basic rule* for removing random variables from the *left and right* side of the conditional symbol (|) is given by Papoulis [33]. To remove random variables from the *left side* simply integrate each variable x_j from $-\infty$ to ∞: $j \le i$. To remove random variables from the *right side*, for example, x_j and x_k: $i + 1 \le j, k \le n$, multiply by the conditional *pdfs* of x_j and x_k with respect to the remaining variables and integrate x_j and x_k from $-\infty$ to ∞. For example, referring to (1.143) and considering $f_{X_1}(x_1|x_2,x_3,x_4)$, eliminating the random variables x_3 and x_4 from the *right side* is evaluated as

$$f_{X_1}(x_1|x_2) = \int_{-\infty}^{\infty}\int_{-\infty}^{\infty} f_{X_1}(x_1|x_2,x_3,x_4)f(x_3,x_4|x_2)dx_3dx_4$$

$$(1.145)$$

The conditional probability of $Y \in S_1$ given $X(\chi) = x$ is expressed as

$$P(Y \in S_1|X=x) = \frac{P(Y \in S_1, X=x)}{P(X=x)} \qquad (1.146)$$

Since $P(X = x) = 0$ for the continuous random variable X, (1.146) is undefined; however, if X and Y are jointly continuous with continuous joint *cdfs*, as defined in (1.139), then the conditional *cdf* of Y, given X, is defined as

$$F_Y(y|X \le x) \triangleq \frac{P(X \le x, Y \le y)}{P(X \le x)} = \frac{F_{X,Y}(x,y)}{F_X(x)} \qquad (1.147)$$

and differentiating (1.147) with respect to y results in

$$f_Y(y|X \le x) = \frac{\partial y F_{X,Y}(x,y)/dy}{F_X(x)} = \frac{\displaystyle\int_{-\infty}^{x} f_{X,Y}(x',y)dx'}{\displaystyle\int_{-\infty}^{\infty}\int_{-\infty}^{x} f_X(x',y)dx'dy}$$

$$= \frac{f_{X,Y}(x,y)}{f_X(x)}$$

$$(1.148)$$

If $f_X(x) \neq 0$, the conditional *cdf* of y, given $X = x$, is expressed as [34]

$$F_Y(y|X=x) = \frac{\int_{-\infty}^{y} f_{X,Y}(x,y')dy'}{f_X(x)} \qquad (1.149)$$

and the corresponding conditional *pdf* is evaluated by differentiating (1.149) with respect to y and is expressed as

$$f_Y(y|X=x) = \frac{f_{X,Y}(x,y)}{f_X(x)} = \frac{f_{X,Y}(x,y)}{\int\limits_{-\infty}^{\infty} f_{X,Y}(x,y)dy} \qquad (1.150)$$

If X and Y are independent random variables then $f_{Y,X}(y,x) = f_Y(y)f_X(x)$ and (1.147) and (1.150) become $F_Y(y|x) = F_Y(y)$ and $f_Y(y|x) = f_Y(y)$.

Upon rearranging (1.150), the joint *pdf* of X and Y is expressed as

$$f_{Y,X}(y,x) = f_Y(y|x)f_X(x) \qquad (1.151)$$

Considering the probability space $S_1 = S_{Y|X} \cap S_X$, such that $S_X^c \neq \emptyset$, the probability $P(Y \in S_X)$ is determined by the *total probability law* defined as

$$P(Y \in S_X) = \int_{S_X} \left[\int_{S_{Y|X}} f_Y(y'|x)dy' \right] f_X(x)dx$$
$$= \int_{S_X} P(Y \in S_Y|x)f_X(x)dx \qquad (1.152)$$

In this case, the subspace S_X can be examined as if it were a total probability space obeying the axioms, corollaries, and properties stated earlier.

1.5.2.3   Expectations of Continuous Random Variables

In general, the k-th moment of the random variable X is defined as the expectation

$$E\left[X^k\right] \triangleq \int_{-\infty}^{\infty} x^k f_X(x)dx \qquad (1.153)$$

and the k-th central moments are defined as the expectation

$$E\left[(X-m_x)^k\right] \triangleq \int_{-\infty}^{\infty} (x-m_x)^k f_X(x)dx \qquad (1.154)$$

The mean value m_x of X is defined as the expectation

$$m_x \triangleq E[X] = \int_{-\infty}^{\infty} x f_X(x)dx \qquad (1.155)$$

The second central moment of X is evaluated as

$$E\left[(X-m_x)^2\right] \triangleq \int_{-\infty}^{\infty} (x-m_x)^2 f_X(x)dx$$
$$= E\left[x^2\right] - m_x^2 \qquad (1.156)$$
$$= Var[x]$$

where $Var[x]$ is the variance of x. An efficient approach in evaluating the k-th moments of a random variable, without performing the integration in (1.153) or (1.155), is based on the *moment theorem* as expressed by the *moment generation function* (1.241) in Section 1.5.6.

The expectation of the function $g(x)$ is evaluated as

$$E[g(X)] = \int_{-\infty}^{\infty} g(x)f_X(x)dx \qquad (1.157)$$

and the expectation of the function $g(X,Y)$ of two continuous random variables is

$$E[g(X,Y)] = \int_{-\infty}^{\infty}\int_{-\infty}^{\infty} g(x,y)f_{X,Y}(x,y)dxdy \qquad (1.158)$$

The expectation is distributive over summation so that

$$E[X+Y] = E[X] + E[Y] \qquad (1.159)$$

and

$$E\left[(X+Y)^2\right] = E\left[X^2\right] + 2E[XY] + E\left[Y^2\right] \qquad (1.160)$$

The following relationships between X and Y apply under the indicated conditions:

$$E[XY] = \begin{cases} E[X]E[Y] & : X \text{ and } Y \text{ are uncorrelated} \\ 0 & : X \text{ and } Y \text{ are orthogonal} \end{cases} \qquad (1.161)$$

From (1.160) and (1.161) it is seen that if X and Y are uncorrelated random variables they are also orthogonal random variables if the mean of either X or Y is zero. The following example demonstrates that if two jointly Gaussian distributed random variables are orthogonal they are also independent.

The conditional expectation of X given Y is defined as

$$E[X|Y] = \int_{-\infty}^{\infty} x f_X(x|y)dx \qquad (1.162)$$

However, if Y is a random variable the function $g_2(Y) = E(X|Y)$ is also a random variable and, using (1.157), the expectation (1.162) becomes

$$E[g_2(Y)] = E[E[X|Y]] = \int_{-\infty}^{\infty} E[x|y]f_Y(y)dy \qquad (1.163)$$

Papoulis [35] establishes the basic theorem for the conditional expectation of the function $g(X,Y)$ conditioned on $X = x$, expressed as the random variable $E[g(X,Y)|X = x]$. The theorem is:

$$E[E[g(X,Y)|X]] = E[g(X,Y)] \qquad (1.164)$$

with the corollary relationship

$$E[g_1(X)g_2(Y)] = E[E[g_1(X)g_2(Y)|X]] = E[g_1(X)E[g_2(Y)|X]] \qquad (1.165)$$

Papoulis refers to (1.165) as a *powerful formula*.

The Bivariate Distribution—An Example of Conditional Distributions   Consider that x_1 and x_2 are Gaussian random variables with means m_1, m_2 and variances σ_1, σ_2, respectively, with the joint *pdf* is expressed as [36]

$$f_{x_1,x_2}(x_1,x_2)$$

$$= \frac{\exp\left[-\dfrac{\sigma_2^2(x_1-m_1)^2 - 2\sigma_1\sigma_2\rho(x_1-m_1)(x_2-m_2) + \sigma_1^2(x_2-m_2)^2}{2\,\sigma_1^2\,\sigma_2^2(1-\rho^2)} \right]}{2\pi\sigma_1\sigma_2\sqrt{1-\rho^2}}$$

$$(1.166)$$

where ρ is the correlation coefficient, such that, $|\rho| \leq 1$, expressed as

$$\rho = \frac{E[(x_1-m_1)(x_2-m_2)]}{\sigma_1\sigma_2} = \frac{E[x_1 x_2] - m_1 m_2}{\sigma_1\sigma_2} \qquad (1.167)$$

Using (1.150), the distribution of x_1 conditioned on x_2 is expressed as

$$f_{x_1|x_2}(x_1|x_2) = \frac{f_{x_1,x_2}(x_1,x_2)}{f_{x_2}(x_2)}$$

$$= \frac{1}{\sqrt{2\pi(1-\rho^2)}\sigma_1}\exp\left[-\frac{((x_1-m_1)-\rho(\sigma_1/\sigma_2)(x_2-m_2))^2}{2\,\sigma_1^2(1-\rho^2)} \right]$$

$$= \frac{1}{\sqrt{2\pi(1-\rho^2)}\sigma_1}\exp\left[-\frac{((x_1-m_1)-\rho(x_2-m_2))^2}{2\,\sigma_1^2(1-\rho^2)} \right] \; : \sigma_2 = \sigma_1$$

$$(1.168)$$

If x_1 and x_2 are uncorrelated random variables then $E[x_1 x_2] = E[x_1]E[x_2]$ and, from (1.167), the correlation coefficient is zero and (1.168) reduces to the Gaussian distribution of x_1 with $f_{x_1|x_2}(x_1|x_2) = f_{x_1}(x_1) \; : \rho = 0$. Therefore, two jointly Gaussian distributed random variables are orthogonal and independent if they are uncorrelated.

Referring to (1.165), the first and second conditional moments of the second equality in (1.168) are evaluated

using as $E[g_1(X_1)g_2(X_2)]$ and $E[g_1^2(X_1)g_2^2(X_2)]$, respectively, with $g_1(X_1) = X_1$ and $g_2(X_2) = X_2$ In the evaluation, the conditional mean of the Gaussian distribution is established from (1.168) by observation as

$$E[X_1|X_2 = x_2] = \rho\frac{\sigma_1}{\sigma_2}x_2 - \rho\frac{\sigma_1}{\sigma_2}m_2 + m_1 \qquad (1.169)$$

and the desired result is evaluated as

$$E[X_2 E[X_1|X_2 = x_2]] = E\left[x_2\left\{ \rho\left(\frac{\sigma_1}{\sigma_2}\right)x_2 - \rho\left(\frac{\sigma_1}{\sigma_2}\right)m_2 + m_1 \right\} \right]$$

$$= \rho\left(\frac{\sigma_1}{\sigma_2}\right)E[x_2^2] - \left(\rho\left(\frac{\sigma_1}{\sigma_2}\right)m_2 - m_1 \right)E[x_2]$$

$$= \rho\sigma_1\sigma_2 + m_1 m_2$$

$$(1.170)$$

where $E[x_2^2] = \sigma_2^2 + m_2^2$ and $E[x_2] = m_2$. The evaluation of $E[g_1^2(X_1)g_2^2(X_2)]$ is left as an exercise in Problem 12. The evaluation of (1.169) could have been performed using the integration in (1.155); however, it is significantly easier and less prone to error to simply associate the required parameters with the known form of the conditional Gaussian distribution as indicated in (1.168).

With zero-mean random variables X_1 and X_2, that is, when $m_1 = m_2 = 0$, the second equality in (1.168) results in (see Papoulis [37])

$$E[X_1 X_2] = \rho\sigma_1\sigma_2 \;\; : \text{zero-mean Gaussain conditional pdf}$$

$$(1.171)$$

and

$$E[X_1^2 X_2^2] = E[X_1^2]E[X_2^2] + 2E^2[X_1 X_2] \qquad (1.172)$$

The time correlated zero-mean, equal-variance Gaussian random variables denoted as x_i and x_{i-1} taken at $t_i = t_{i-1} + \Delta t$ are characterized, using the last equality in (1.168), as

$$f_{X_i|X_{i-1}}(x_i|x_{i-1}) = \frac{1}{\sqrt{2\pi}\sigma_1(1-\rho^2)}\exp\left[-\frac{(x_i - \rho x_{i-1})^2}{2\,\sigma_1^2(1-\rho^2)} \right]$$

$$(1.173)$$

Equation (1.173) is used to model Gaussian fading channels with the fade duration dependent on Δt and ρ and the fade depth dependent on σ_1.

1.5.3   Definitions and Fundamental Relationships for Discrete Random Variables

In the following relationships, x_i, y_i, x, and y are considered to be discrete random variables corresponding to the event probabilities $P_X(x_i)$, $P_Y(y_i)$, $P_X(x)$, and $P_Y(y)$ with the

corresponding *pmfs* $p_Z(z) = P_Z(Z = z) : Z = \{X,Y\}$, $z = \{x_i, y_i, z, y\}$ corresponding to the amplitude of the discrete delta functions. In general, the characterization of discrete random variables is similar to that of continuous random variables with the integrations replaced by summations and the *pdf* replaced with the *pmf*.

1.5.3.1 Statistical Independence If $X(\chi_i) = x$ with $\chi_i \in S$ and the events χ_i are independent $\forall\, i$, then the joint probabilities are expressed as the product

$$P(X_1 = x_1, \ldots, X_N = x_N) = \prod_{i=1}^{N} P_i(X_i = x_i) \qquad (1.174)$$

or, in terms of the *pmf*, $p_X(x_i) = P(X = x_i)$

$$p_{X_1}, \ldots, p_{X_N}(x_1, \ldots, x_N) = \prod_{i=1}^{N} p_{X_i(x_i)} \qquad (1.175)$$

If $S = S_1 \cap S_2$ such that $X(\chi_i) = x_i$ with $\chi_i \in S_1$, $Y(\chi_j) = y_j$ with $\chi_j \in S_2$, and the individual *mdfs* satisfy (1.175), then

$$
\begin{aligned}
P[S] &= \sum_i \sum_j p_{X,Y}(x_i, y_j) = \sum_i \sum_j p_X(x_i) p_Y(y_j) \\
&= \sum_i p_X(x_i) \sum_j p_Y(y_j) \\
&= P(S_1) P(S_2)
\end{aligned} \qquad (1.176)
$$

Therefore, if the joint *pmfs* are independent, X and Y are also independent and, from the last equality in (1.176), S_1 and S_2 are also independent. Consequently, $\{X,Y\}$ are independent *iff* the *pmfs* of X and Y can be expressed in the product form as in (1.175).

The expectation of x is evaluated as

$$E[X] = \int_{-\infty}^{\infty} x \sum_i p_X(x)\delta(x - x_i) = \sum_i x_i p_X(x_i) = \sum_i x_i P(X = x_i)$$

$$(1.177)$$

For the discrete sampled function $g(X,Y)$, the expectation value is evaluated as

$$E[g(X,Y)] = \sum_{i,j} g(x_i, y_j) p_{XY}(X = x_i, Y = y_j) \qquad (1.178)$$

where the *pmf* is expressed as $p_{XY}(x_i, y_j) = P(X = x_i, Y = y_j)$.

1.5.3.2 Conditional Probability The conditional probability of X given $Y = y_j$ is expressed as

$$P(X = x_i | Y = y_j) = \frac{P(X = x_i, Y = y_j)}{P(Y = y_j)} \qquad (1.179)$$

and, in terms of the conditional *pmf*s, (1.179) becomes

$$p_X(x_i | y_j) = \frac{p_{X,Y}(x_i, y_j)}{p_Y(y_j)} \qquad (1.180)$$

The *pmf* behaves like the *pdf* of continuous random variables, in that, if the event $X(\chi_i) = x_i$ with $\chi_i \in S_1$, the probability of $X \in S_1$ given $Y = y_j$ is evaluated as

$$P(X \in S_1 | Y = y_j) = \sum_i p_X(x_i | y_j) \qquad (1.181)$$

If X and Y are independent (1.180) becomes

$$p_X(x_i | y_j) = \frac{p_X(x_i) p_Y(y_j)}{p_Y(y_j)} = p_X(x_i) \qquad (1.182)$$

1.5.3.3 Bayes Rule Bayes rule is expressed, in terms of the condition probability, as

$$P(X = x_i | Y = y_j) = \frac{P(Y = y_j | x_i) P(X = x_i)}{P(Y = y_j)} \qquad (1.183)$$

and, in terms of probabilities and *pmfs*, Bayes rule is expressed as

$$p_X(x_i | y_j) = \frac{p_Y(y_j | x_i) P(X = x_i)}{P(Y = y_j)} \qquad (1.184)$$

The probability state transition diagram is shown in Figure 1.18 for *N*-dimensional input and output states x_i and y_i, respectively. The outputs are completely defined by the *conditional*, or *transition, probabilities* $P(y_j|x_i)$ and the input *a priori probabilities* $P(x_i)$. Upon choosing the state y_j, that is, given y_j, the *a posteriori probability* $P(x_i|y_j)$ is
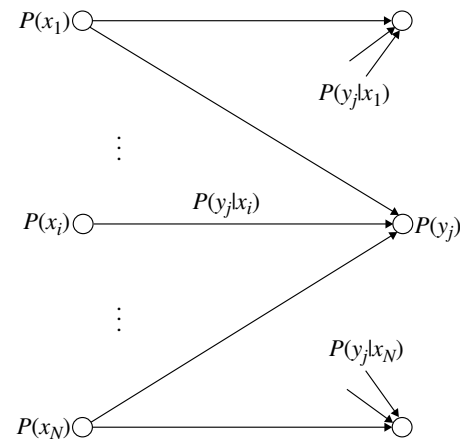

FIGURE 1.18 Probability state transition diagram.

the conditional probability that the input state was x_i. Wozencraft and Jacobs (Reference 30, p. 34) point out that, "The effect of the transmission [decision] is to alter the probability of each possible input from its a priori to its a posteriori value."

The conditional expectation of X given $Y = y$ is

$$E(X|Y) = \sum_{x_i} x_i p_X(x_i|y) \tag{1.185}$$

where the *pmf* $p_X(x_i|y) = P(X = x_i|y)$.

1.5.4   Functions of Random Variables

Applications involving random variables that are functions of random variables, that is, $z = g(x_1, \ldots, x_M)$, require that the density function $f_Z(z)$ be determined given $f_{X_m}(x_m)$: $n = 1$, $\ldots, M$. In the following subsections, the transformation from $f_{X_m}(x_m)$ to $f_Z(z)$ is discussed for the relatively easy case involving functions of one random variables, that is, $M = 1$. More complicated cases are also discussed involving functions of two random variables and M random variables of the form $Z = \sum_{m=1}^{M} X_m$. The following descriptions involve continuous random variables and cases involving discrete and mixed random variables are discussed in References 6, 8, 29.

1.5.4.1   Functions of One Random Variable   In the following description, the mapping of the random variable $X = x$ is continuous and $F_X(x)$ is differentiable at x as in (1.126), with finite values of $f_X(x)$. The transformation from X to Z can be based on the functional relationships $z = g(x)$ or $x = h(z)$ with the requirements that $P(X = \infty) = P(Z = \infty) = 1$ corresponding to unit areas under each transformation. These transformations correspond, respectively, to

$$f_Z(z) = \frac{f_X(x = h(z))}{|dg(x)/dx|_{x=h(z)}} \tag{1.186}$$

and

$$f_Z(z) = f_X(x = h(z)) \left| \frac{dh(z)}{dz} \right| \tag{1.187}$$

Equations (1.186) and (1.187) require the inverse relationship

$$\left| \frac{dh(z)}{dz} \right| = \left| \frac{dg(x)}{dx} \right|^{-1}_{x=h(z)} \tag{1.188}$$

The function $z = h(x)$ typically has a finite number of solutions x_n, corresponding to the roots $z = h(x_1)$, $h(x_2)$,…, $h(x_N)$ of the transformation and, under these conditions, the
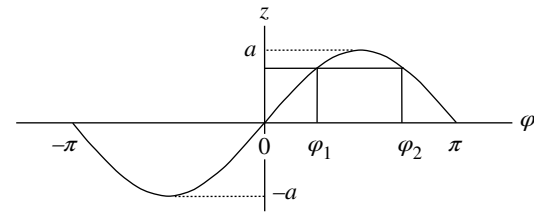

FIGURE 1.19   Random variable $x = a\sin(\varphi)$ ($f_\Phi(\varphi) = 1/(2\pi)$).

solution to $f_Z(z)$ given $f_X(x_n)$ is determined using the fundamental theorem [38, 39],

$$f_Z(z) = \sum_{n=1}^{N} f_X(x_n = h(z_n)) \left| \frac{dh(z_n)}{dz_n} \right| = \sum_{n=1}^{N} f_X(x_n = h(z_n)) |h'(z_n)| \tag{1.189}$$

where $h(z_n)$ corresponds to the transformation of x_n expressed in terms of z_n and $h'(z_n) = dh(z_n)/dz_n$.

As an example, consider a sinusoidal signal z, with constant amplitude a and random phase φ uniformly distributed between $\pm\pi$, expressed as

$$z = a\sin(\varphi) \tag{1.190}$$

Referring to Figure 1.19, and noting that $z = a\sin(\varphi_1) = a\sin(\varphi_2)$, the problem is to determine the *pdf* $f_Z(z)$ using the two roots of $\varphi_1 = h(z_1)$ and $\varphi_2 = h(z_2)$. Using (1.190), $\varphi = h(z)$ is evaluated as

$$\varphi = h(z) = \sin^{-1}\left(\frac{z}{a}\right) \quad : \varphi = \{\varphi_1, \varphi_2\} \tag{1.191}$$

and

$$h'(z) = \frac{dh(z)}{dz} = \frac{1}{\sqrt{a^2 - z^2}} \quad : \varphi = \{\varphi_1, \varphi_2\} \text{ and } |z| < a \tag{1.192}$$

Therefore, evaluating (1.189) with $f_\Phi(\varphi) = 1/(2\pi)$ results in

$$\begin{aligned} f_Z(z) &= f_\Phi(\varphi_1) |h'(z_1)| + f_\Phi(\varphi_2) |h'(z_2)| \\ &= \frac{1}{2\pi} \left(\frac{1}{\sqrt{a^2 - z^2}} + \frac{1}{\sqrt{a^2 - z^2}} \right) \\ &= \frac{1}{\pi} \frac{1}{\sqrt{a^2 - z^2}} \quad : |z| < a \end{aligned} \tag{1.193}$$

1.5.4.2   Functions of Two or More Random Variables
The concepts involving a function of one random variable can also be applied when the random variable Z is a function

of several random variables; for example, the dependence on two random variables, such that, $z = g(x,y)$ is discussed at length by Papoulis (Reference 8, Chapters 6 and 7) where the subjects involving marginal distributions, joint density functions, probability masses, conditional distributions and densities, and independence are introduced. According to (1.126), the probability density function $f_Z(z)$ is determined from the distribution function $F_Z(z)$ as

$$f_Z(z) = \frac{\partial F_Z(z)}{\partial z} \qquad (1.194)$$

and the joint *pfd* of X and Y is characterized for continuous distributions as

$$f_{XY}(x,y) = \frac{\partial^2 F_{XY}(x,y)}{\partial x \partial y} \qquad (1.195)$$

where the joint *cdf* is given by

$$F_{XY}(x,y) = \int_{-\infty}^{y} \int_{-\infty}^{x} f_{XY}(x',y')dx'dy' \qquad (1.196)$$

Based on the conditions for the equality of the probabilities, that is,

$$P_Z(Z \le z) = P_{XY}(x, y \in g(x,y) \le z)$$

the *pdfs* are equated as

$$F_Z(z) = F_{XY}(g(x,y) \le z) = \int_{g(x,y)\le z} \int f_{X,Y}(x,y)dxdy \quad (1.197)$$

Upon differentiating (1.197) with respect to z yields the desired result expressed as

$$f_Z(z) = \frac{\partial F_Z(z)}{\partial z} = \frac{\partial}{\partial z} \int_{g(x,y)\le z} \int f(x,y)dxdy \qquad (1.198)$$

As an example application consider the random variable $Z = X + Y$; Papoulis states that, "*This is the most important example of a function involving two random variables.*" Upon letting $y = z - x$ and using (1.198) the density function of Z is evaluated as

$$f_Z(z) = \frac{\partial}{\partial z} \int_{-\infty}^{\infty} \int_{-\infty}^{z-x} f(x,y)dxdy = \int_{-\infty}^{\infty} f_{XY}(x,z-x)dx$$
$$(1.199)$$

and, when X and Y are independent, (1.199) is simply the convolution of $f_X(x)$ with $f_Y(y)$. Several examples involving the use of (1.199) are given in Section 1.5.6.1.

Using the joint probability density function of two continuous random variables x and y, as expressed in (1.195), the marginal *pdfs* $f_X(x)$ and $f_Y(y)$ are obtained by integrating over y and x, respectively, resulting in

$$f_X(x) = \int_{-\infty}^{\infty} f_{XY}(x,y)dy \qquad (1.200)$$

and

$$f_Y(y) = \int_{-\infty}^{\infty} f_{XY}(x,y)dx \qquad (1.201)$$

These results can also be generalized to apply to the joint density function of any number of continuous random variables by integrating over each of the undesired variables.

1.5.5 Probability Density Functions

The following two subsections examine the probability density function [40] of the magnitude and phase of a sinusoidal signal with additive noise and the probability density function of the product of two zero-mean equal-variance Gaussian distributions. In these cases, the random variables of interest involve functions of two random variables. In Section 1.5.6, the characteristic function is defined and examined for several probability distribution functions demonstrating the central limit theorem with increasing summation of random variables. In Section 1.5.7, many of the probability distributions used in the following chapters are summarized and compared.

1.5.5.1 Distributions of Sinusoidal Signal Magnitude and Phase in Narrowband Additive White Gaussian Noise

This example involves the evaluation of the *pdf* of the magnitude and phase at the output of a narrowband filter when the input is a sinusoidal signal with uniformly distributed phase and zero-mean additive white Gaussian noise [41] (AWGN). In this case, the output of the narrowband filter is a narrowband random process. The evaluation involves three random variables: the input signal phase φ and the two independent-identically distributed (*iid*) zero-mean quadrature noise random variables with variance σ_n^2. The signal plus noise out of the filter is expressed as

$$s(t) = A\cos(\omega_c t + \varphi) + n(t)\cos(\omega_c t + \phi(t))$$
$$= A\cos(\varphi)\cos(\omega_c t) - A\sin(\varphi)\sin(\omega_c t)$$
$$+ n(t)\cos(\phi(t))\cos(\omega_c t) - n(t)\sin(\phi(t))\sin(\omega_c t)$$
$$= (A\cos(\varphi) + n_c(t))\cos(\omega_c t) - (A\sin(\varphi) + n_s(t))\sin(\omega_c t)$$
$$(1.202)$$

where the third equality in (1.202) emphasizes the in-phase and quadrature functions of the signal and noise terms and, when sampled at $t = iT_s$, represent the random variables
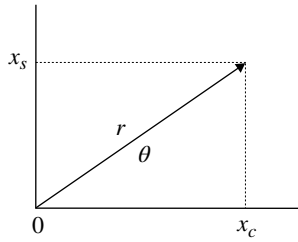
FIGURE 1.20 Relationship between transformation variables.

x_c, n_c, x_s, and n_s. The functional relationships are $x_c = A\cos(\varphi) + n_c$ and $x_s = A\sin(\varphi) + n_s$ with n_c and n_s representing zero-mean quadrature Gaussian random variables. The signal phase, φ, is uniformly distributed between 0 and 2π. Under these conditions, the quadrature signal and noise components x_c and x_s are independent random variables[*] and the *pdfs* of x_c and x_s are expressed as

$$f_{X_c}(x_c) = \frac{1}{\sqrt{2\pi}\sigma_n} e^{-(x_c - A\cos(\varphi))^2/2\sigma_n^2} \qquad (1.203)$$

and

$$f_{X_s}(x_s) = \frac{1}{\sqrt{2\pi}\sigma_n} e^{-(x_s - A\sin(\varphi))^2/2\sigma_n^2} \qquad (1.204)$$

The *pdf* of the phase is

$$f_{\Phi}(\varphi) = \frac{1}{2\pi} \quad : 0 \le \varphi \le 2\pi \qquad (1.205)$$

Using (1.203), (1.204), and (1.205) the joint *pdf* is expressed as

$$
\begin{aligned}
f_{X_c, X_s, \Phi}(x_c, x_s, \varphi) &= f_{X_c}(x_c) f_{X_s}(x_s) f_{\Phi}(\varphi) \\
&= \frac{1}{4\pi^2\sigma^2} e^{-\frac{(x_c - A\cos(\varphi))^2 + (x_s - A\sin(\varphi))^2}{2\sigma^2}}
\end{aligned}
$$
$$(1.206)$$

The evaluation of the joint *pdf* of the magnitude and phase of the sampled sine-wave plus noise involves the transformation of variables from (x_c, x_s) to (r, θ) as depicted in Figure 1.20. The magnitude is described as

$$r = |s(iT_s)| = \sqrt{x_c^2 + x_s^2} \qquad (1.207)$$

and the in-phase and quadrature components, x_c and x_s, are described in terms of the angle θ as

$$x_c = r\cos(\theta) \quad \text{and} \quad x_s = r\sin(\theta) \qquad (1.208)$$

[*]Orthogonal Gaussian random variables are also independent.

Right column:

and, using (1.208), the functions $h_1(r,\theta)$ and $h_2(r,\theta)$ are expressed as

$$h_1(r,\theta) = x_c|_{r\cos(\theta)} = r\cos(\theta) \tag{1.217}$$

and

$$h_2(r,\theta) = x_s|_{r\sin(\theta)} = r\sin(\theta) \tag{1.218}$$

Substituting (1.216), (1.217), and (1.218) into (1.212) and applying the independence of x_c, x_s, and φ, as in (1.206), the *pdf* of the transformed variables r and θ is expressed as

$$f_{R,\Theta,\Phi}(r,\theta,\varphi) = f_R(r)f_\Theta(\theta)f_\Phi(\varphi)$$

$$= \frac{r}{4\pi^2\sigma^2}e^{-\frac{(r\cos(\theta)-A\cos(\varphi))^2 + (r\sin(\theta)-A\sin(\varphi))^2}{2\sigma^2}}$$

$$= \frac{r}{4\pi^2\sigma^2}e^{-\frac{r^2 + A^2 - 2Ar\cos(\theta-\varphi)}{2\sigma^2}}$$

$$\tag{1.219}$$

where $r \geq 0$, otherwise the *pfd* is zero, and θ and φ are uniformly distributed over the range $0 \leq \theta, \varphi \leq 2\pi$. The *pdf* for the magnitude r is determined by computing the marginal distribution $M_R(r)$ by integrating over the ranges of θ and φ. Defining $\psi = \theta - \varphi$, the marginal is evaluated as

$$f_R(r) = \frac{r}{\sigma^2}e^{-\frac{r^2+A^2}{2\sigma^2}}\frac{1}{2\pi}\int_0^{2\pi}\left(\frac{1}{2\pi}\int_\varphi^{2\pi-\varphi}e^{Ar\cos(\psi)/\sigma^2}d\psi\right)d\varphi$$

$$\tag{1.220}$$

Davenport and Root [42] point out that the integrand of the bracketed integral is periodic in the uniformly distributed phase ψ and can be integrated over the interval 0 to 2π. With this integration range, the bracketed integral is identified as the zero-order modified Bessel function expressed as [43]

$$I_o\left(\frac{Ar}{\sigma^2}\right) = \frac{1}{2\pi}\int_0^{2\pi}e^{Ar\cos(\psi)/\sigma^2}d\psi \tag{1.221}$$

Therefore, upon using (1.221) and performing the integration over φ, the marginal distribution function $M_R(r)$ simplifies, at least in notation, to

$$f_R(r) = \frac{r}{\sigma^2}e^{-\frac{r^2+A^2}{2\sigma^2}}I_o\left(\frac{Ar}{\sigma^2}\right) \tag{1.222}$$

Equation (1.222) is the Rice distribution or, as referred to throughout this book, the Ricean distribution that, as developed in the forgoing analysis, characterizes the baseband magnitude distribution of a CW signal with narrowband additive white Gaussian noise. The Ricean distribution also characterizes the magnitude distribution of a received signal from a channel with multipath interference; this channel is referred to as a Ricean fading channel. The Ricean distribution becomes the Rayleigh distribution as $A \rightarrow 0$ and the Gaussian distribution as $A \rightarrow \infty$; the proof of these two limits is the subject of Problems 19 and 20. The Rayleigh distribution characterizes the amplitude distribution of narrowband noise or, in the case of multipath interference, the composite signal magnitude of many random scatter returns without a dominant specular return or signal component. The multipath interference is the subject of Chapter 18. Defining the signal-to-noise ratio as $\gamma = A^2/(2\sigma^2)$, (1.222) is expressed as

$$f_R(r) = \frac{r}{\sigma^2}e^{-(r^2/2\sigma^2+\gamma)}I_o\left(\frac{r\sqrt{2\gamma}}{\sigma}\right) \tag{1.223}$$

The *pdf* of the phase function is evaluated by computing the marginal distribution $M_{\Theta\Phi}(\theta,\varphi)$ by integrating over the range of the magnitude r. By forming or completing the square of the exponent in the last equality in (1.219) the integration is performed as

$$f_{\Theta\Phi}(\theta,\varphi) = \frac{1}{4\pi^2\sigma^2}e^{-A\sin^2(\theta-\varphi)/2\sigma^2}\int_0^\infty re^{-(r-A\cos(\theta-\varphi))^2/2\sigma^2}dr$$

$$\tag{1.224}$$

Davenport and Root [44] provide an approximate solution to (1.224), under the condition $A\cos(\theta-\varphi) \gg \sigma$. The approximation is expressed as

$$f_{\Theta\Phi}(\theta,\varphi) \cong \frac{A\cos(\theta-\varphi)}{(2\pi)^{3/2}\sigma}e^{-\gamma\sin^2(\theta-\varphi)} \quad : 0 \leq \theta, \varphi \leq 2\pi \tag{1.225}$$

where γ is the signal-to-noise ratio defined earlier. An alternate solution, without the earlier restriction, is expressed by Hancock [45], with $\psi = \theta - \varphi$, as

$$f_\Psi(\psi) = \frac{e^{-\gamma}}{2\pi}\left(1 + \sqrt{4\pi\gamma}\cos(\psi)e^{\gamma\cos^2(\psi)}P\left(\sqrt{2\gamma}\cos(\psi)\right)\right)$$

$$: -\pi \leq \psi \leq \pi$$

$$\tag{1.226}$$

where $P(z)$ is the probability integral defined in Section 3.5. Hancock's phase function is used in Section 4.2.1 to characterize the performance of phase-modulated waveforms.

As $\gamma \rightarrow 0$ in (1.226) the function $f_\Psi(\psi) \rightarrow 1/2\pi$ resulting in the uniform phase *pdf*. However, for γ greater than about 3, the probability integral is approximated as [26]

$$P(z) \cong 1 - \frac{e^{-z^2/2}}{\sqrt{2\pi}z} \quad : z > 3 \tag{1.227}$$

Using (1.227), the phase *pdf* is approximated as

$$f_{\Psi}(\psi) \cong \begin{cases} \sqrt{\gamma/\pi}\cos(\psi)e^{-\gamma\sin^2(\psi)} & : 1 > \cos(\psi) > 2.5/\sqrt{\gamma} \\ 0 & : -2.5/\sqrt{\gamma} > \cos(\psi) > -1 \end{cases}$$

(1.228)

With $|\psi| \cong 0$ such that $\sin^2(\psi) \cong \psi^2$ and defining $\gamma = 1/2\sigma_{\psi}^2$ (1.228) is approximated as

$$f_{\Psi}(\psi) \cong \frac{1}{\sqrt{2\pi}\sigma_{\psi}}e^{-\psi^2/2\sigma_{\psi}^2} \quad : |\psi| \cong 0 \text{ and } \gamma = 1/2\sigma_{\psi}^2 \quad (1.229)$$

Equation (1.229) describes a zero-mean Gaussian phase *pdf* with the phase variance $\sigma_{\psi}^2 = 1/2\gamma$. Hancock's phase function, expressed in (1.226), is plotted in Figure 4.3 for various signal-to-noise ratios.

1.5.5.2 Distribution of the Product of Two Independent Gaussian Random Variables In this section the *pdf* of the product $z = xy$ of two zero-mean equal-variance *iid* Gaussian random variables X and Y is determined. The solution involves defining an auxiliary random variable $w = h(x) = x$ with $z = g(x,y) = xy$ and evaluating $f_{Z,W}(w,z)$ characterized as

$$f_{W,Z}(w,z) = \frac{f_{X,Y}(w,z/w)}{|J_{X,Y}(x,y)|}$$

(1.230)

where $J_{X,Y}(x,y)$ is the Jacobian of the transformation evaluated as

$$J_{X,Y}(x,y) = \begin{vmatrix} \dfrac{\partial g(x,y)}{\partial x} & \dfrac{\partial g(x,y)}{\partial y} \\ \dfrac{\partial h(x,y)}{\partial x} & \dfrac{\partial h(x,y)}{\partial y} \end{vmatrix}_{\det} = -x$$

(1.231)

Using (1.231) and the joint Gaussian *pfd* of X and Y, expressed by (1.230), with $x = w$ and $y = z/w$, the marginal *pdf* of z is evaluated as

$$f_Z(z) = \int_{-\infty}^{\infty} \frac{1}{|w|} f_{X,Y}(w,z/w)dw$$

(1.232)

However, since X and Y are independent

$$f_{X,Y}(x,y) = f_X(x)f_Y(y) = \frac{1}{2\pi\sigma^2}e^{-\frac{(x^2+y^2)}{2\sigma^2}}$$

(1.233)

and, upon substituting $x = w$ and $y = z/w$ into (1.233), (1.232) is expressed as

$$f_Z(z) = \frac{1}{2\pi\sigma^2}\int_{-\infty}^{\infty}\frac{1}{|w|}e^{-\frac{w^2+(z/w)^2}{2\sigma^2}}dw$$

$$= \frac{1}{\pi\sigma^2}\int_0^{\infty}\frac{1}{w}e^{-\frac{w^2+(z/w)^2}{2\sigma^2}}dw$$

(1.234)

where the second equality recognizes that the first equality is symmetrical in w. Letting $\lambda = w^2/2\sigma^2$ (1.234) is expressed as

$$f_Z(z) = \frac{1}{2\pi\sigma^2}\int_0^{\infty}\frac{1}{\lambda}e^{-\left(\lambda+\frac{z^2}{4\sigma^4\lambda}\right)}d\lambda$$

(1.235)

The solution to the integral in (1.235) appears in the table of integrals by Gradshteyn and Ryzhik (Reference 46, p. 340, pair No. 12) as

$$\int_0^{\infty}\lambda^{v-1}e^{-\left(\lambda+\frac{u^2}{4\lambda}\right)}d\lambda = 2\left(\frac{u}{2}\right)^v K_{-v}(u)$$

(1.236)

where $K_v(u)$ is the modified Bessel function of the second kind of order v. With $v = 0$ and $u = z/\sigma^2$, (1.235) is evaluated as

$$f_Z(z) = \frac{1}{\pi\sigma^2}K_o\left(\frac{|z|}{\sigma^2}\right)$$

(1.237)

The magnitude of z in (1.237) is used because of the even symmetry of $f_Z(z)$ with respect to z. The symmetry of $f_Z(z)$ results in a zero-mean value so the variance is evaluated as

$$Var[z] = E[z^2] \quad : \text{zero-mean}$$

$$= \frac{2}{\pi\sigma^2}\int_0^{\infty}z^2 K_o\left(\frac{z}{\sigma^2}\right)dz$$

(1.238)

The solution to the integral in (1.238) is found in Gradshteyn and Ryzhik (Reference 46, p. 684, Integral No. 16) and the variance $f_Z(z)$ is evaluated as

$$Var[z] = \frac{4}{\pi}\Gamma^2\left(\frac{3}{2}\right)\sigma^4 = \sigma^4$$

(1.239)

where the second equality in (1.239) results from the value of the Gamma function $\Gamma(3/2) = \sqrt{\pi}/2$. In Example 4 of Section 1.5.6.1, the *pdf* of the summation of N *iid* random variables with *pdfs* expressed by (1.237) is examined.

1.5.6 The Characteristic Function

The characteristic function of the random variable X is defined as the average value of e^{jvx} and is expressed as

$$C_X(v) \triangleq E[e^{jvx}] = \int_{-\infty}^{\infty}f_X(x)e^{jvx}dx$$

(1.240)

With $v = -\omega$ and $x = t$ (1.240) is similar to the Fourier transform of a time-domain function. The characteristic function is also referred to as the moment-generating function, in that, the nth moment of the random variable X, defined as the expected value $E[x^n]$, is evaluated (see Problem 26) as

$$E[x^n] = (-j)^n \frac{d^n C_X(v)}{dv^n}\bigg|_{v=0} \qquad (1.241)$$

The Fourier transform relationship between time domain convolution and frequency domain multiplication also applies to the convolution of random variables and the multiplication of the corresponding characteristic functions. Therefore, based on the discussion in Section 1.5.6.1, the summation of N identically distributed (id) random variables corresponds to the product of their individual characteristic functions, that is,

$$C_Z(v) = \prod_{i=1}^{N} C_{X_i}(v) \quad : Z = \sum X_i, \quad i = 1, \ldots, N; \; X_i \in id \qquad (1.242)$$

This is a very useful result, in that, the distribution of the summation of N independent random variables is obtained as the inverse transform [47] of (1.242) expressed as

$$f_Z(z) = \int_{-\infty}^{\infty} C_Z(v) e^{-jvz} dz \qquad (1.243)$$

Campbell and Foster [47] provide an extensive listing of Fourier transform pairs defined as

$$G(g) = \int_{-\infty}^{\infty} F(f) e^{j2\pi fg} df \quad \text{and} \quad F(f) = \int_{-\infty}^{\infty} G(g) e^{-j2\pi fg} dg \qquad (1.244)$$

and, by defining $v = -2\pi f$, the Fourier transform pairs apply to the transform pairs between $f_X(x)$ and $C_X(v)$ as expressed in (1.240).

1.5.6.1 Summation of Independently Distributed Random Variables
If two random variables X and Y are independent then the probability density $f_Z(z)$ of their sum $Z = X + Y$ is determined from the convolution of $f_X(x)$ with $f_Y(y)$ so that[*]

$$f_Z(z) = \int_{-\infty}^{\infty} f_X(z-y) f_Y(y) dy = \int_{-\infty}^{\infty} f_X(x) f_Y(z-x) dx \quad (1.245)$$

For multiple summations of a random variable, the convolution is repeated for each random variable in the summation.

[*]For proof see Reference 8, p. 189.
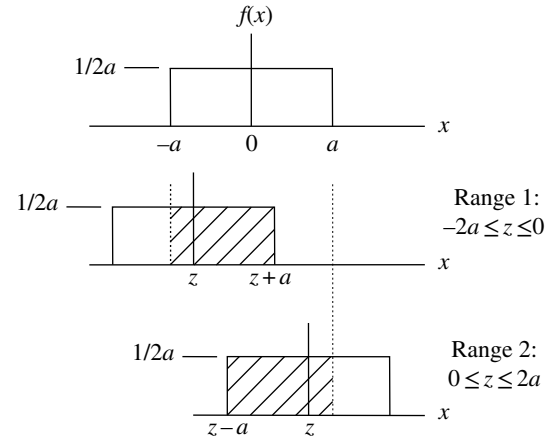
FIGURE 1.21 Convolution of two zero-mean uniform distributions.

Example 1 Consider the summation of N zero-mean uniformly distributed random variables X_i expressed as

$$Z = \sum_{i=1}^{N} X_i \qquad (1.246)$$

with

$$f_X(x) = \frac{1}{2a} \quad : -a \le x \le a \qquad (1.247)$$

For $N = 2$ the convolution involves two ranges of the variable z as shown in Figure 1.21 and the integrations are evaluated as

$$f_Z(z) = \frac{1}{4a^2} \int_{-a}^{z+a} dx \quad : -2a \le z \le 0 \qquad (1.248)$$

and

$$f_Z(z) = \frac{1}{4a^2} \int_{z-a}^{a} dx \quad : 0 \le z \le 2a \qquad (1.249)$$

Upon evaluation of (1.248) and (1.249) and recognizing the symmetry about z the density function is expressed as

$$f_Z(z) = \frac{1}{2a}\left(-\frac{|z|}{2a} + 1\right) \quad : |z| \le 2a \qquad (1.250)$$

Repeating the application of the convolution for $N = 3$ and 4 (see Problem 24) results in the probability density functions shown in Figure 1.22 with the corresponding *cdf* results shown in Figure 1.23. As $N \to \infty$ the probability density and characteristic functions will approach those of the Gaussian distributed random variable (see Problem 23).

FIGURE 1.22 *pdf* for sum of $N = 2$, 3 and 4 independent zero-mean uniform distributions ($a = 1$).
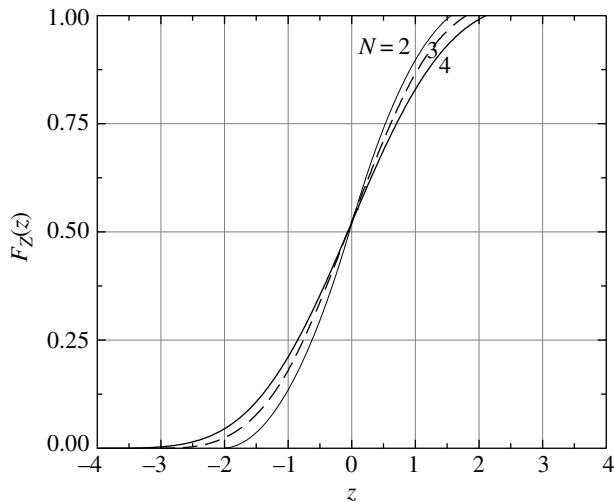
FIGURE 1.23 *cdf* for sum of $N = 2$, 3 and 4 independent zero-mean uniform distributions ($a = 1$).

The moments of the random variable X are evaluated using the characteristic function

$$C_X(v) = \frac{\sin(av)}{av} \qquad (1.251)$$

In regions where the characteristic function converges, the moments $E[x^n]$ completely define the characteristic function and the *pdf* of the random variable X, so, upon expanding (1.251) as the power series
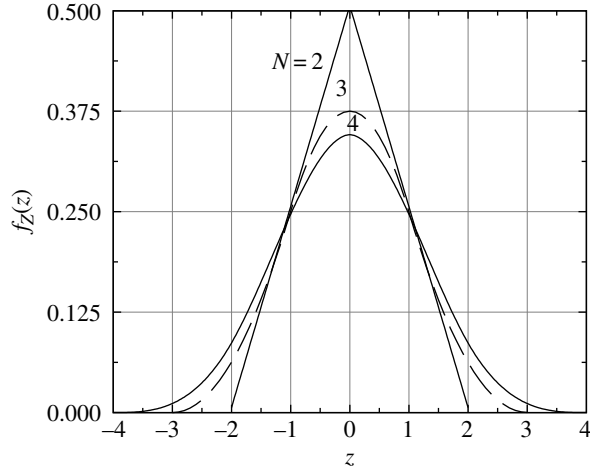
$$C_X(v) = 1 - \frac{(av)^2}{3!} + \frac{(av)^4}{5!} - \cdots \qquad (1.252)$$

TABLE 1.6 Moments of $f_Z(z_N)$ for $Z = \sum X_i \; : i = 1,\ldots,4$, X_i *iid* Zero-Mean Uniform Distributions

N	$E[z]$	$E[z^2]$
1	0	$a^2/3$
2	0	$2a^2/3$
3	0	a^2
4	0	$4a^2/3$

the moments are easily evaluated using (1.241). The moments for the random variable Z, formed as in (1.246), are determined using (1.242) and, with $X_i : i = 1, \ldots, N$ *iid* random variables, the characteristic function for Z is approximated as

$$C_Z(v) = C_X^N(v) \cong 1 - \frac{N(av)^2}{3!} \qquad (1.253)$$

The first and second moments for $N = 1, \ldots, 4$ are listed in Table 1.6. These results are also obtained by evaluating $f_Z(z)$ using (1.250) and then evaluating the moments (see Problem 25) as

$$E[z^n] = \int_{-Na}^{Na} z^n f_Z(z) dz \qquad (1.254)$$

However, it is much easier to use the characteristic function.

Example 2   As another example, consider the summation of N random variables X_i characterized as the sinusoidal function

$$X_i = A_i \sin(\Phi_i) \qquad (1.255)$$

with constant amplitudes A_i and zero-mean uniformly distributed phase, expressed as

$$f_\Phi(\varphi) = \frac{1}{2\phi} \quad : |\varphi| \le \phi \qquad (1.256)$$

The resulting *pdf* of the random variable X_i for $\phi = \pi$, is evaluated in (1.193) as

$$f_X(x_i) = \frac{1}{\pi \sqrt{A_i^2 - x_i^2}} \qquad (1.257)$$

and is plotted in Figure 1.24.

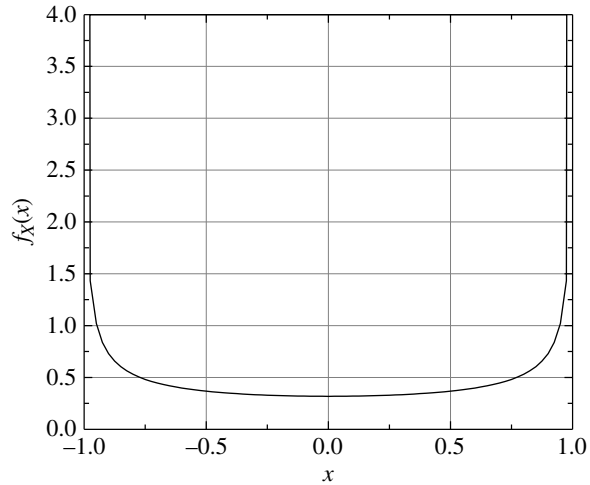**FIGURE 1.24**   *pdf* of $x = A\sin(\varphi)$ with zero-mean uniformly distributed phase, $A = 1$ and $\phi = \pi$.
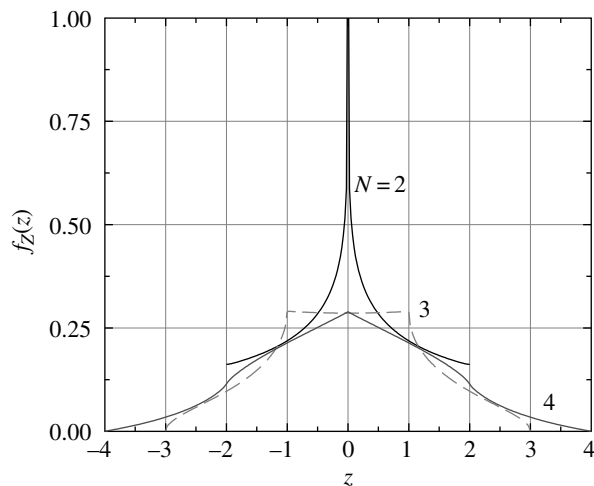

FIGURE 1.25   *pdf* of $N = 2$, 3, and 4 successive convolutions of $f_X(x)$.

The *pdf* of the random variable Z, expressed as in (1.246),[*] is evaluated by successive convolutions as in (1.245) and the results for $N = 2$, 3, and 4 are plotted in Figure 1.25 with the corresponding *cdf* functions shown in Figure 1.26. The results in Figures 1.25 and 1.26 for $N > 1$ are obtained by numerical evaluations of the convolutions using incremental values of $\Delta z = 2.5 \times 10^{-5}$; this is a reasonable compromise between simulation time and fidelity in dealing with the infinite value at $|x| = 1.0$.

In this case, the mean and variance of the random variable X are evaluated using the characteristic function of (1.257)

FIGURE 1.26   *cdf* of $N = 2$, 3, and 4 successive convolutions of $f_X(x)$.

TABLE 1.7   Moments of $f_Z(z_N)$ for $Z = \sum X_i : i = 1, \ldots, N$, X_i iid Random Variables Expressed by (1.255)

	Theoretical		Numerical[a] ($A = 1$)	
N	$E[z]$	$E[z^2]$	$E[z]$	$E[z^2]$
1	0	$A^2/2$	0	0.4999
2	0	A^2	0	1.0044
3	0	$3A^2/2$	0	1.5055
4	0	$2A^2$	0	2.0146

[a]Numerical values are sampled with $\Delta z = 2.5 \times 10^{-5}$.

found in (Reference 47, p. 123, Transform Pair 914.5); the result is

$$C_X(v) = I_o(-jAv) \qquad (1.258)$$

where $I_o(-)$ is the modified Bessel function of order zero. Expanding (1.258) for $Av < 1$ as a power series, (Reference 46, p. 375, Ascending Series 9.6.10), results in[†]

$$C_X(v) = 1 - \frac{(Av)^2}{4(1!)^2} + \frac{(Av)^4}{4^2(2!)^2} - \frac{(Av)^6}{4^3(3!)^2} \cdots \qquad (1.259)$$

and the moments are easily evaluated using (1.241). The first and second moments are listed as the theoretical values in Table 1.7. The moments for the random variable Z, formed as in (1.246) with X_i *iid* random variables for all i as expressed by the *pdf* in (1.255), are determined using the characteristic function expressed as

---

[*]By forming the average summation $Z = (1/N)\sum_{i=1}^{N} x_i$, the range of the *pdf* is limited to $\pm a$ with an associated decrease in the standard deviation.
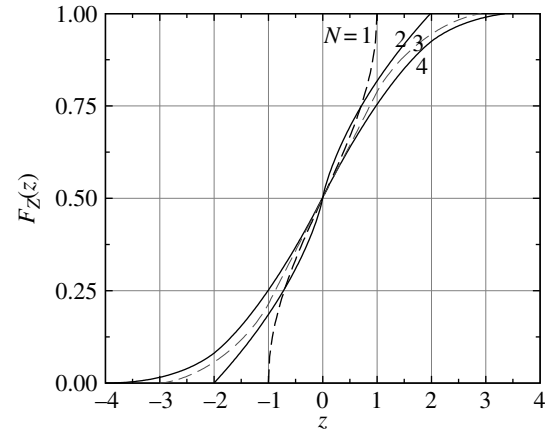
[†]By comparing the ascending series expansion of $I_o(z)$ with that of the Bessel function $J_o(z)$ it is found that $I_o(-jz) = J_o(z)$.

$$C_Z(v) = C_X^N(v) \cong 1 - \frac{N(Av)^2}{4(1!)^2} \qquad (1.260)$$

The corresponding first two moments of the random variable Z for $N = 2, 3$, and 4 are also listed in Table 1.7. The numerical results listed in Table 1.7 are based on computer evaluations of the various convolutions resulting in the *pdfs* shown in Figures 1.24 and 1.25.

A major observation in these two examples is that the probability distribution of the random variable Z approaches a Gaussian distribution as N increases (see Problem 27). This is evidence of the central limit theorem which states that (see Davenport and Root, Reference 6, p. 81) *the sample mean of the sum of N arbitrarily distributed statistically independent samples becomes normally distributed as N increases*. This is referred to the equal-components case of the central limit theorem. However, as pointed out by Papoulis (Reference 8, p. 266), a consequence of the central limit theorem is that *the distribution $f_Z(z)$ of the sum of N statistically independent distributions having arbitrary pdf's tends to a normal distribution as N increases*. This is a stronger statement and suggests that the probability $P(z) = f_Z(Z < z)$ can be considered a Gaussian distribution for all z as is frequency assumed to be the case in practice. Davenport and Root also point out that, even though N is seemingly large, the tails of the resulting distribution may result in a *poor* approximation to the Gaussian distribution.

Upon computing the mean and variance using the power series expansion of $C_Z(v)$ expressed by (1.252) with $av \ll 1$, the approximate expression for the corresponding Gaussian distribution is easily obtained. After summing N uniformly distributed amplitudes the expression for the *pdf* is

$$f_Z(z) = \frac{1}{\sqrt{2\pi N a^2/3}} e^{-z^2/(2Na^2/3)} \quad : z = \sum x_i, \ i = 1, \ldots, N,$$

$$p(x_i) = \frac{1}{2a}, \quad |x_i| \le a$$

$$(1.261)$$

Similarly, for the summation of N sinusoids with $Av \ll 1$, the *pdf* in Example 2 is expressed as

$$f_Z(z) = \frac{1}{\sqrt{2\pi N A^2/2}} e^{-z^2/(2NA^2/2)}$$

$$: z = \sum x_i, \ i = 1, \ldots, N, \ x_i = A\sin(\varphi_i) \qquad (1.262)$$

$$p(\varphi_i) = \frac{1}{2\pi}, \quad |\varphi_i| \le \pi$$

It is interesting to note that the second moments are $N\lambda^2$ for all values of N including those for which the *pdf* does not have the slightest resemblance to the Gaussian *pdf*.

In these cases, the important difference is that the corresponding probabilities $P(x) = F_X(X < x)$ are entirely different from those of the Gaussian distribution with the possible exception of the median value. Finally, it is noted that the limiting behavior for $\lambda v \ll 1$ and $N \to \infty$ applies to the summation of *independently distributed* distributions that may, or may not, be *identically distributed* distributions.

Example 3   This example involves the summation of random chips $\{\pm 1\}$ in a direct-sequence spread-spectrum (DSSS) waveform. In this case, the chips occur with equal probabilities according to the *pdf* expressed as

$$f_X(x) = \frac{1}{2}\delta(x-1) + \frac{1}{2}\delta(x+1) \qquad (1.263)$$

Using (1.240), the characteristic function is evaluated as

$$C_X(v) = \int_{-\infty}^{\infty} f_X(x)e^{jvx}dx$$

$$= \frac{1}{2}\left(\int_{-\infty}^{\infty} e^{jvx}\delta(x-1)dx + \int_{-\infty}^{\infty} e^{jvx}\delta(x+1)dx\right)$$

$$= \cos(v)$$

$$(1.264)$$

The DSSS waveform uses N chips per bit and the demodulator correlation sums the N chips to form the correlation output $y = \sum_{n=0}^{N-1} x_n$ with the corresponding characteristic function given by

$$C_Y(v) = C_X^N(x) = \cos^N(v)$$

$$= \left(1 - \frac{v^2}{2!} + \frac{v^4}{4!} - \frac{v^6}{6!} + \cdots\right)^N \qquad (1.265)$$

$$= 1 - \frac{Nv^2}{2!} + \cdots$$

To evaluate the first and second moments of y only the first two terms in the expansion of $\cos^N(v)$ are required and, upon using (1.241), these moments are evaluated as

$$E[x] = j\frac{2Nv}{2!}\bigg|_{v=0} = 0 \quad : \text{first moment (mean value, } \bar{x})$$

$$(1.266)$$

and

$$E[x^2] = (-1)\frac{-2N}{2!}\bigg|_{v=0} = N \quad : \text{second moment} \qquad (1.267)$$

The variance of y is defined as the second central moment $E\left[(x-\bar{x})^2\right]=E[x^2]-\bar{x}^2$ and with zero-mean the variance is $\sigma_y^2=E[x^2]=N$.

Example 4　The *pdf* $f_Z(z)$ of the product of two, zero-mean, equal-variance, *iid* Gaussian random variables, $z = xy$, is expressed in (1.237) as a function of the zero-order modified Bessel function $K_o(|z|/\sigma^2)$ where the magnitude of z provides for the range: $-\infty \le z \le \infty$. In this example, the *pdf* $f_{\bar{Z}}(\bar{z})$ is evaluated where $\bar{Z}=\sum_i Z_i : i = 1, ..., N$. The evaluation is based on the N-th power of the characteristic function $C_Z(v)$ and, from the work of Campbell and Foster (Reference 47, p. 60, pair No. 558), the characteristic function is evaluated as[*]

$$C_Z(v) = \frac{1/\sigma^2}{\sqrt{1/\sigma^4-p^2}} \qquad (1.268)$$

The characteristic function of $\bar{Z}$ is the N-th power of (1.268) expressed as

$$C_{\bar{Z}}^N(v) = \frac{1/\sigma^{2N}}{(1/\sigma^4-p^2)^{N/2}} \qquad (1.269)$$

and, using the transform pair of Campbell and Foster (Reference 47, p. 61, pair No. 569.0), the *pdf* of $\bar{Z}$ is evaluated as

$$f_{\bar{Z}}(\bar{z}) = \frac{1/\sigma^{2N}}{\sqrt{\pi}\,\Gamma(N/2)(2/\sigma^2)^{(N-1)/2}} \left\{ |\bar{z}|^{(N-1)/2} K_{(N-1)/2}\left(\frac{|\bar{z}|}{\sigma^2}\right) \right\} \qquad (1.270)$$

As in the case for $f_Z(z)$, the *pdf* $f_{\bar{Z}}(\bar{z})$ applies for $-\infty \le \bar{z} \le \infty$ and is symmetrical with respect to $\bar{z}$ resulting in a zero-mean value with the variance expressed as

$$Var[\bar{z}] = E\left[\bar{z}^2\right] \quad : \text{with zero-mean}$$

$$= \frac{2/\sigma^{2N}}{\sqrt{\pi}\,\Gamma(N/2)(2/\sigma^2)^{(N-1)/2}} \int_0^\infty \bar{z}^2 \bar{z}^{(N-1)/2} K_{(N-1)/2}\left(\frac{\bar{z}}{\sigma^2}\right) dz \qquad (1.271)$$

The solution to the integral in (1.271) is found in Gradshteyn and Ryzhik (Reference 46, p. 684, Integral No. 16) and the variance $f_Z(z)$ is evaluated using

$$\int_0^\infty \bar{z}^u K_v(a\bar{z}) d\bar{z} = \frac{2^{u-1}}{a^{u+1}} \Gamma\left(\frac{1+u+v}{2}\right) \Gamma\left(\frac{1+u-v}{2}\right) \qquad (1.272)$$

Substituting the solution to the integral in (1.272) into (1.271), with $u = (N + 3)/2$, $v = (N - 1)/2$, and $a = 1/\sigma^2$, the solution to variance simplifies to

$$Var[z] = N\sigma^4 \qquad (1.273)$$

In the earlier evaluation, the integer argument Gamma function is related to the factorial as $\Gamma(N) = (N-1)!$ and $\Gamma(3/2) = \sqrt{\pi}/2$. This result could also be evaluated using the movement generating function of (1.241), however, using the integral solution as in (1.272) it is sometimes easier to evaluate the moments. With a sufficiently large value of N the *pdf* $f_{\bar{Z}}(\bar{z})$ is approximated as the Gaussian *pfd* expressed as

$$f_{\bar{Z}}(\bar{z}) \underset{N\to\infty}{\sim} \frac{1}{\sqrt{2\pi N\sigma^4}} e^{-\bar{z}^2/(2N\sigma^4)} \quad : \text{zero-mean Gaussian pdf}$$

$$(1.274)$$

The probability density functions discussed earlier and others encountered in the following chapters are summarized in Table 1.8 with the corresponding mean values, variances, and characteristic functions.

1.5.7 Relationships between Distributions

In the following two subsections, the relationship between various probability density functions is examined by straightforward parameter transformations, allowing parameters to approach limits, or simply altering various parameter values. The most notable relationship is based on the central limit theorem in which a distribution approaches the Gaussian distribution by increasingly summing the operative random variable.

1.5.7.1 Relationship between Chi-Square, Gaussian, Rayleigh, and Ricean Distributions　A random variable has a chi-square (χ^2) distribution with N degrees of freedom if it has the same distribution as the sum of the squares of N-independent, normally distributed random variables, each with zero-mean and unit variance.[†]

Consider the zero-mean Gaussian or normal distributed random variable x with variance σ_x^2 and *pdf* expressed as

$$p_X(x) = \frac{1}{\sqrt{2\pi}\sigma_x} e^{-x^2/2\sigma_x^2} \qquad (1.275)$$

The *pdf* of a new random variable $y = x^2$, obtained by simply squaring x, is determined by considering the positive and negative regions of $x = \pm\sqrt{y}$ as shown in Figure 1.27.

---

[*]The tables of Campbell and Foster are Fourier transform pairs that correspond to characteristic function pairs with $p = -jv$.

[†]A normally distributed random variable x with mean value m_x and variance σ_x^2 can be transformed into a zero-mean, unit-variance normally distributed random variable y by substituting $y = (x - m_x)/\sigma_x$.

TABLE 1.8 Probability Distributions and Characteristic Functions

Name	$f_X(x)$	$E[x]$	$Var[x]$	$C_X(v)$	Conditions
Uniform	$\dfrac{1}{b-a}$	$\dfrac{a+b}{2}$	$\dfrac{(b-a)^2}{12}$	$\dfrac{\left(e^{jvb}-e^{jva}\right)}{jv(b-a)}$	$a \ge x \le b$
Bernoulli	$\begin{cases} p & : i=1 \\ 1-p & : i=2 \end{cases}$	p	$p(1-p)$	$(1-p)+pv$	Discrete binary variable $x = k_i : i = 1, 2$
Binomial	$\dbinom{n}{k}p^k(1-p)^{n-k}$	np	$np(1-p)$	$((1-p)+pv)^n$	Discrete variable $x=k=1,2,\ldots,n$
Poisson	$\alpha^k e^{-\alpha}/k!$	α	α	$e^{\alpha(v-1)}$	Discrete variable $x=k=0,1,\ldots;\alpha>0$
Exponential	$\alpha e^{-\alpha x}$	$1/\alpha$	$1/\alpha^2$	$\alpha/(\alpha-jv)$	$x \ge 0;\ \alpha>0$
Gaussian (normal)	$\dfrac{e^{-\frac{(x-m)^2}{2\sigma^2}}}{\sqrt{2\pi}\sigma}$	m	σ^2	$e^{-jmv-\frac{\sigma^2 v^2}{2}}$	$-\infty \le x \le \infty$
Chi-square ($N=2$) Exponential ($\alpha=1/2$)	$\dfrac{e^{-x/2}}{2}$	2	4	$(1-j2v)^{-1}$	$x \ge 0$
Chi-squared (N-degrees)	$\dfrac{x^{N/2-1}e^{-x/2}}{2^{N/2}(N/2-1)!}$	N	$2N$	$(1-j2v)^{-N/2}$	N-degrees of freedom $x \ge 0$
Rayleigh	$\dfrac{xe^{-x^2/2\sigma^2}}{\sigma^2}$	$\sqrt{\pi/2}\,\sigma$ as $\gamma\to\infty$	$\dfrac{(4-\pi)\sigma^2}{2}$ as $\gamma\to\infty$	$(1-jv/\beta)^\alpha$	$x > 0$
Ricean	$\dfrac{xe^{-\frac{(x^2-A^2)}{2\sigma^2}}}{\sigma^2}I_o\left(\dfrac{xA}{\sigma^2}\right)$	a	a	a	$x > 0$ $\begin{cases} A^2/2\sigma^2 \to \infty \\ A^2/2\sigma^2 = 0 \end{cases}$
Gamma	$\dfrac{\beta(\beta x)^{\alpha-1}}{\Gamma(\alpha)}e^{-\beta x}$	α/β	α/β^2	$\dfrac{1}{\left(1-j\frac{v}{\beta}\right)^\alpha}$	$x > 0$ $\beta > 0;\ \lambda > 0$
Lognormal	$\dfrac{e^{-\frac{(\ln(y)-m)^2}{2\sigma^2}}}{\sqrt{2\pi}y\sigma}$	$e^{m+\sigma^2/2}$	$e^{m+2\sigma^2}$ $-e^{m+\sigma^2}$	b	y is lognormal $y=e^x \ge 0$ $x = N(m,\sigma)$
Nakagami-m	$\dfrac{2m^m x^{2m-1}e^{-mx^2/\Omega}}{\Gamma(m)\Omega^m}$	c	c	c	$x \ge 0$ $m=\dfrac{E[x^2]^2}{E[x^2-E(x^2)]^2}$ $\ge 1/2$

Notes: $\gamma = A^2/(2\sigma^2)$ is the signal-to-noise ratio. $\gamma\to 0$ $f_X(x)$ = Rayleigh with $E[x] = \sqrt{\pi/2}\sigma$, $Var[x] = (4-\pi)\sigma^2/2$.
[a]$\gamma\to\infty$ $f_X(x)$ = Gaussian with $E[x] = A$, $Var[x] = \sigma^2$.
[b]Approximated using a series expansion of e^{jvy}.
[c]Refer to special cases in Section 1.5.7.2.
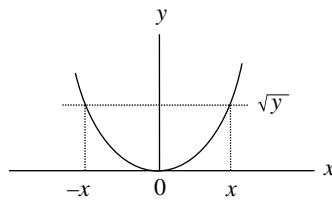
FIGURE 1.27 Transformation of the random x to $y = x^2$.

The *pdf* of y is determined using the incremental intervals $dy = 2xdx$ at $x = \pm\sqrt{y}$ such

$$p_Y(y) = p_X\left(x=\sqrt{y}\right)\left|\frac{dx}{dy}\right| + p_X\left(x=-\sqrt{y}\right)\left|\frac{dx}{dy}\right| \quad : U(y)$$

$$= \frac{1}{\sqrt{2\pi}\sigma_x}\left[e^{-y/2\sigma_x^2} + e^{-y/2\sigma_x^2}\right]\left|\frac{1}{2\sqrt{y}}\right| \quad : U(y)$$

$$= \frac{e^{-y/2\,\sigma_x^2}}{\sqrt{2\pi y}\sigma_x} \quad : U(y)$$

(1.276)

The characteristic function of (1.276) is evaluated as

$$C_Y^1(v) = E\left[p_Y(y)e^{jvy}\right] = \frac{1}{\left(1 - j2\,\sigma_x^2 v\right)^{1/2}} \qquad (1.277)$$

Consider now the random variable z resulting from the summation of N independent random variables y_i such that

$$z = \sum_{i=1}^{N} y_i = \sum_{i=1}^{N} x_i^2 \qquad (1.278)$$

The characteristic function of z is simply the N-th power of $C_Y(v)$ so that

$$C_Z^N(v) = \left[C_Y^1(v)\right]^N$$
$$= \frac{1}{\left(1 - j2\,\sigma_x^2 v\right)^{N/2}} \qquad (1.279)$$

Equation (1.279) transforms to the *pdf* of z, resulting in

$$p_Z(z) = \frac{z^{N/2-1}e^{-z/2\,\sigma_x^2}}{\left(2\,\sigma_x^2\right)^{N/2}\left(\dfrac{N}{2}-1\right)!} \quad : U(y) \qquad (1.280)$$

In conforming to the earlier definition, the chi-square distribution is expressed by letting $\sigma_x^2 = 1$ in (1.280) or, more formally, using the transformation $\chi = z/\sigma_x^2$; therefore, the *pdf* of the chi-square random variable χ with N degrees of freedom is

$$p_X(\chi) = \frac{\chi^{N/2-1}e^{-\chi/2}}{2^{N/2}\left(\dfrac{N}{2}-1\right)!} \quad : U(y) \;\; \text{Chi-square distribution}$$
$$(1.281)$$

and the corresponding characteristic, or moment generating, function is

$$C_X^N(v) = \frac{1}{\left(1-j2v\right)^{N/2}} \quad : \text{Chi-square characteristic function}$$
$$(1.282)$$

Equation (1.281) is occasionally referred to as the *central* χ^2 distribution because it is based on noise only, that is, the underlying zero-mean Gaussian random variables x_i

with distribution given by (1.275) do not contain a signal component.[*]

Special Case for N = 2   Under this special case $z = x_1^2 + x_2^2$ (1.280) reduces to the exponential distribution

$$p_Z(z) = \frac{e^{-z/2\,\sigma_x^2}}{2\,\sigma_x^2} \quad : U(y) \text{ exponential distribution} \quad (1.283)$$

So the resulting chi-square χ^2 distribution is obtained from (1.281) with $N = 2$. This is an important case because x_1 and x_2 can be thought of as orthogonal components in the complex description of a baseband data sample. Urkowitz [48] shows that the energy of a wide-sense stationary narrowband white noise Gaussian random process with bandwidth $–W$ to W Hz and measured over a finite interval of T seconds is approximated by $N = 2WT$ terms or degrees of freedom. The frequency W is the noise bandwidth of the narrowband baseband filter and the approximation error in the energy measurement decreases with increasing $2WT$. The factor of two can be thought of as the computation of complex orthogonal baseband functions $\tilde{z} = x_c^2 + jx_s^2$ so $N = 2$ degrees of freedom correspond to $WT = 1$. For example, the *rect(t/T)* function observed over the interval T seconds has a noise bandwidth of $W = 1/T$ Hz corresponding to $WT = 1$ resulting in 2 degrees of freedom.

Upon letting $w = |\tilde{z}| = \sqrt{x_c^2 + x_s^2}$, the random variable w is described in terms of the Rayleigh distribution

$$p_W(w) = \frac{w}{\sigma_x^2}e^{-w^2/2\sigma_x^2} \quad : U(y) \text{ Rayleigh distribution} \quad (1.284)$$

So the Rayleigh distribution is derived from the magnitude of the quadrature zero-mean Gaussian distributed random variables, $x = N(0,\sigma)$.[†]

1.5.7.2 *Relationship between Nakagami-*m*, Gaussian, Rayleigh, and Ricean Distributions*   The Nakagami-*m* distribution [49] was initially derived from experimental data to characterize HF fading; however, subsequent experimental observations demonstrate its application to rapid fading at carrier frequencies from 200 MHz to 4 GHz. It is considered to be a generalized distribution from which other distributions can be derived, for example, $m = 1$ results in the Rayleigh power distribution, $m = \frac{1}{2}$ results in the one-sided

---

[*]When the underlying Gaussian distributed random variable is composed of signal plus noise, the signal amplitude represents the mean value of the distribution. An analysis, similar to that of (1.276) through (1.280), containing a mean value, results in a noncentral χ^2 distribution with 1 through N degrees of freedom. The noncentral χ^2 distribution is developed and discussed in Appendix C.

[†]The notation $N(m,\sigma)$ is used to denote the distribution of a Gaussian, or normal, random variable with mean value m and standard deviation σ.

zero-mean Gaussian distribution, and as $m \to \infty$ the m-distribution approaches the Gaussian distribution with a unit mean value. In the region $1 \leq m \leq \infty$, the Nakagami-m distribution behaves much like the Ricean distribution; however, the normalized distributions are subtly different when plotted for various signal-to-noise ratios less than about 10 dB. The Ricean distribution, referred to as the n-distribution by Nakagami, is derived from concepts involving narrowband filtering of a continuous wave (CW) signal with additive Gaussian noise, whereas the Nakagami-m distribution is derived from experimental data involving multipath communication links.

1.5.8 Order Statistics

Communication systems analysis and performance evaluations often involve a large number of random samples taken from an underlying continuous or discrete probability distribution function. The various parameters, used to characterize the system performance, result in limiting distributions with associated means, variances, and confidence levels as dictated, for example, by an underlying distribution. Order statistics [31, 50, 51], on the other hand, involves a *distribution-free* or *nonparametric* analysis that requires only that the probability distribution functions be continuous and not necessary related to the underlying distribution from which the samples are taken. However, the randomly drawn samples are considered to be statistically independent.

Consider that the n random samples $\{X_1, X_2, \ldots, X_n\}$ are taken from the continuous *pdf* $f_X(x)$ over the range $a \leq x \leq b$. Now consider reordering the random variables $X_i : i = 1, \ldots, n$ to form the random variables $\{Y_1, Y_2, \ldots, Y_n\}$ arranged in ascending order of magnitude, such that, $a \leq Y_1 < Y_2 < \cdots < Y_n \leq b$ where $f_{Y_i}(y_i) = 1/(b-a)$ is uniformly distributed over the interval $b - a$. The joint *pdf* of the ordered samples [52] is expressed as

$$g_{Y_1, Y_2, \ldots, Y_n}(y_1, y_2, \ldots, y_n) = n! \prod_{i=1}^{n} f_{Y_i}(y_i) \qquad (1.285)$$

for $a \leq y_1 < y_2 < \cdots < y_n \leq b$ and $n!$ is the number of mutually disjoint sets of $x_1, x_2, \ldots, x_n$. For example, for $n = 4$ the set x_1, x_2, x_3, x_4 results in $n! = 24$ mutually disjoint sets determined as shown in Table 1.9. The first six mutually disjoint sets are determined by cyclically left shifting the indicated subsets of original set x_1, x_2, x_3, x_4; a cyclic left shift of a subset is obtained by shifting each element of the subset to the left and replacing the leftmost element in the former position of the rightmost element. Following the first six sets shown in the figure, the original set is cyclically shifted three more times each leading to six mutually disjoint sets by shifting subsets resulting in a total of 24 mutually disjoint sets.

TABLE 1.9   Example of Mutually Disjoint Sets ($n = 4$, 24 Mutually Disjoint Sets)

No.	Mutually Disjoint Sets	Shifting[a]
1	x_1, x_2, x_3, x_4	Original set
2	x_1, x_2, x_4, x_3	Shift subset x_3, x_4
3	x_1, x_3, x_4, x_2	Shift subset x_2, x_3, x_4
4	x_1, x_3, x_2, x_4	Shift subset x_4, x_2
5	x_1, x_4, x_2, x_3	Shift subset x_3, x_4, x_2
6	x_1, x_4, x_3, x_2	Shift subset x_2, x_3
7	x_2, x_3, x_4, x_1	Shift original set
8	x_2, x_3, x_1, x_4	Shift subset x_4, x_1
9	x_2, x_4, x_1, x_3	Shift subset x_3, x_4, x_1
. . .	. . .	. . .

[a]*Shift* denotes a cyclic left shift of a previous set or subset.

The ordered sample Y_i is referred to as the i-th order statistic of the sample set. The marginal *pfd* of the n-th order statistic Y_n, that is, the maximum of $\{X_1, X_2, \ldots, X_n\}$, is evaluated using (1.285) by performing the integrations in the ascending order $i = 1, 2, \ldots, n - 1$ as follows[*]:

$$g_{Y_n}(y_n) = n! \int_a^{y_n} \cdots \int_a^{y_4} \int_a^{y_3} \left[\int_a^{y_2} f(y_1) dy_1 \right] f(y_2) \cdots f(y_n) dy_2 \cdots dy_{n-1}$$

$$= n! \int_a^{y_n} \cdots \int_a^{y_4} \left[\int_a^{y_3} F(y_2) f(y_2) dy_2 \right] f(y_3) \cdots f(y_n) dy_3 \cdots dy_{n-1}$$

$$= n! \int_a^{y_n} \cdots \left[\frac{1}{2} \int_a^{y_4} F^2(y_3) f(y_3) dy_3 \right] f(y_4) \cdots f(y_n) dy_4 \cdots dy_{n-1}$$

$$\cdots$$

$$= n! f_{Y_n}(y_n) \left[\frac{1}{(n-2)!} \int_a^{y_n} F^{n-2}(y_{n-1}) f(y_{n-1}) dy_{n-1} \right] \qquad (1.286)$$

The solution (see Problem 15) to (1.286) is

$$g_{Y_n}(y_n) = n[F(y_n)]^{n-1} f_{Y_n}(y_n) \quad : \; a < y_n \leq b \qquad (1.287)$$

where $F^{n-1}(y_n)$ is the *cdf* evaluated as

$$F^{n-1}(y_n) = (n-1) \int_a^{y_n} F^{n-2}(y_{n-1}) f_Y(y_{n-1}) dy_{n-1} = \frac{(y_n - a)^{n-1}}{(b-a)^{n-1}} \qquad (1.288)$$

Using the marginal *pdf* of Y_n given by (1.287), the probability of selecting the maximum of value Y_n is determined as

$$P(y') = n \int_a^{y'} F^{n-1}(y_n) f_Y(y_n) dy_n \Bigg|_{y' = b} = 1 \qquad (1.289)$$

[*]For notational simplicity $f(y)$ is used to denote $f_Y(y)$.

TABLE 1.10   Order Statistics False-Detection Probability for Gaussian Distributed Random Variables

Ordered $S + N$ and N Statistics (j,k)	False-Detection Probability (P_{fd})		
	$\gamma_{dB} = 10$	$\gamma_{dB} = 15$	$\gamma_{dB} = 20$
1,1	$2.440e^{-2}$	$6.645e^{-5}$	$1.408e^{-12}$
1,2	$4.226e^{-2}$	$1.308e^{-4}$	$2.815e^{-12}$
1,4	$6.980e^{-2}$	$2.547e^{-4}$	$5.629e^{-12}$
1,8	$1.089e^{-1}$	$4.874e^{-4}$	$1.126e^{-11}$

These results are distribution free, in that, the *pdf* has not been defined; however, from a practical point of view (1.289) can be evaluated for any continuous *pdf*.

The distributions from which the x_i are taken need not be identical[*]; for example, the samples x_1 through x_j can be taken from a distribution involving signal plus noise (or clutter) and those from x_{j+1} through x_n corresponding to noise (or clutter) only. Using this example the distribution in (1.287) is expressed as

$$f_{Y_n}(y_n) = \frac{n!}{(j-1)!(n-j)!} \left[F_{sn}(y_j) \right]^{j-1} \left[1 - F_n(y_j) \right]^{n-j} f_{Y_n}(y_n)$$

$$(1.290)$$

where $F_{sn}(y)$ is the distribution corresponding to signal plus noise and $F_n(y)$ is the noise-only distribution.

Example distributions used to evaluate the performance of communication and radar systems are Gaussian, Ricean, lognormal, and Weibull distributions. Table 1.10 lists the false-detection probabilities, for the indicated signal-to-noise ratios γ_{dB}, associated with the detection of $j = 1$ signal-plus-noise event and $k = n - j = (1,2,4,$ and $8)$ noise-only events.

1.5.9   Properties of Correlation Functions

Correlation processing is used in nearly every aspect of demodulator signal detection from energy detection, waveform acquisition, waveform tracking, parameter estimation, and information recovery processing. With this wide range of applications, the theoretical analyst, algorithm developer, software coder, and hardware developer must be thoroughly familiar with the properties and implementation of waveform correlators. An equally important processing function is that of convolution or linear filtering. The equivalence between matched filtering and correlation is established in Section 1.7.2 and involves a time delay in the correlation response; with this understanding, the properties of correlation can be applied to convolution or filtering. The correlation

response can be exploited to determine the signal signature regarding the location of a signal in time and frequency, the duration and bandwidth of the signal, the shape of the modulated signal waveform, and the estimate of the information contained in the modulated waveform.

The correlation function[†] is evaluated for the complex functions $\tilde{x}(t)$ and $\tilde{y}(t)$ as the integral

$$R_{\tilde{x}\tilde{x}}(\tau) = \int_{-\infty}^{\infty} \tilde{x}(t)\tilde{x}^*(t-\tau)dt \quad : \text{autocorrelation} \quad (1.291)$$

and

$$R_{\tilde{x}\tilde{y}}(\tau) = \int_{-\infty}^{\infty} \tilde{x}(t)\tilde{y}^*(t-\tau)dt \quad : \text{cross-correlation} \quad (1.292)$$

where the asterisk denotes complex conjugation.

Autocorrelation processing examines the correlation characteristics of a single random process with the maximum magnitude corresponding to the zero-lag condition $R_{\tilde{x}\tilde{x}}(\tau = 0)$ that is equal to the maximum energy over the correlation interval. The correlation response $R_{\tilde{x}\tilde{x}}(\tau)$ is indicative of the shape of $\tilde{x}(t)$ and the duration, τ_d, of the principal correlation response is indicative of the correlation time. For deterministic signals, the correlation time (τ_o) is usually characterized in terms of the one-sided width of the principal correlation lobe; however, for stochastic processes the correlation interval is defined when $|R_{\tilde{x}\tilde{x}}(\tau)|$ decreases monotonically from $R_{\tilde{x}\tilde{x}}(0)$ to a defined level; for example, when the *normalized correlation response* first reaches the level $R_{\tilde{x}\tilde{x}}(\tau_o)/R_{\tilde{x}\tilde{x}}(0) = e^{-1}$. The normalized correlation response is referred to as the correlation coefficient as defined in (1.295) or (1.296). The parameters related to the correlation of the function $\tilde{x}(t)$ have equivalent Fourier transform frequency-domain definitions. In the case of stochastic processes, the Fourier transform of $R_{\tilde{x}\tilde{x}}(\tau)$ is defined as the PSD of the process.

Expanding (1.292) in terms of the real and imaginary with $\tilde{x}(t) = x_r(t) + jx_i(t)$ and $\tilde{y}(t) = y_r(t) + jy_i(t)$ results in

$$R_{\tilde{x}\tilde{y}}(\tau) = \int_{-\infty}^{\infty} x_r(t)y_r(t-\tau)dt + \int_{-\infty}^{\infty} y_i(t)y_i(t-\tau)dt$$
$$+ j\left(\int_{-\infty}^{\infty} x_i(t)y_r(t-\tau)dt - \int_{-\infty}^{\infty} x_r(t)y_i(t-\tau)dt \right)$$

$$(1.293)$$

This evaluation requires four real multiplies and integrations for each lag, whereas, if $\tilde{x}(t)$ and $\tilde{y}(t)$ were real functions only one multiplication and integration is required for each

---

[*]Equation (1.286) allows for different distributions; however, (1.287) through (1.289) are based on independent identically distributed (*iid*) random variables.

[†]A stationary stochastic processes is characterized by the first- and second-order moments corresponding to the mean $E[\tilde{x}(t)] = m_{xr} + jm_{xi}$ and autocorrelation response $R_{\tilde{x}\tilde{x}}(\tau) = E[\tilde{x}(t)\tilde{x}^*(t-\tau)]$.

lag. With discrete-time sampling, the integrations are replaced by summations over the finite sample values $\tilde{x}_n$ and $\tilde{y}_n$ where $t = nT_s$: $n = 0, \ldots, N - 1$ and T_s is the sampling interval; in this case, the computational complexity is proportional to N^2. The computation complexity can be significantly reduced by performing the correlation in the frequency domain using FFT [53], in which case, for a radix-2 FFT with $N = 2^k$, the computation complexity is proportional to $N\log_2(N)$. Brigham [54] provides detailed descriptions of the implementation and advantages of FFT correlation and convolution processing. The correlation results throughout the following chapters use the direct and FFT approaches without distinction.

Referring to (1.291) the zero-lag correlation is expressed as

$$R_{\tilde{x}\tilde{x}}(0) = \int_{-\infty}^{\infty} \tilde{x}(t)\tilde{x}^*(t)dt + \int_{-\infty}^{\infty} |\tilde{x}(t)|^2 dt \tag{1.294}$$

$$= E_x$$

where E_x is the total energy in the received signal. Using (1.294), the normalized correlation is defined in terms of the *normalized autocorrelation coefficient* as

$$\rho_x(\tau) \triangleq \frac{R_{\tilde{x}\tilde{x}}(\tau)}{E_x} \quad : \text{normalized autocorrelation coefficient} \tag{1.295}$$

with $|\rho_x(\tau)| \leq 1$. From (1.292), the normalized cross-correlation coefficient is defined as

$$\rho_{xy}(\tau) \triangleq \frac{R_{\tilde{x}\tilde{y}}(\tau)}{\sqrt{E_x E_y}} \quad : \text{normalized cross-correlation coefficient} \tag{1.296}$$

with $|\rho_{xy}(\tau)| \leq 1$.

The correlation may also be defined in terms of the long-term average over the interval T as

$$R_{\tilde{x}\tilde{x}}(\tau) = \lim_{T \to \infty} \frac{1}{T} \int_{-T/2}^{T/2} \tilde{x}(t)\tilde{x}^*(t - \tau)dt \quad : \text{autocorrelation} \tag{1.297}$$

However, most practical waveforms are limited to a finite duration $T_c = NT_s$ and, in these cases, $\tilde{x}(t)$ is zero outside of the range T_c. Therefore, dividing the zero-lag correlation by T_c results in the second-order moment $E(|\tilde{x}|^2) = \sigma_x^2 + m_x^2$ where m_x^2 is the DC or mean signal power. Removing the mean signal level prior to performing the correlation results in the autocovariance with $E(|\tilde{x}|^2) = \sigma_x^2$. Table 1.11 summarized several properties of correlation functions.

TABLE 1.11   Correlation Function Properties of Deterministic and Stochastic Processes

Property	Comments
$R_{\tilde{x}\tilde{x}}(-\tau) = R_{\tilde{x}\tilde{x}}^*(\tau)$	Autocorrelation
$R_{xx}(-\tau) = R_{xx}(\tau)$	$x(t)$ is real
$C_{\tilde{x}\tilde{x}}(-\tau) = R_{\tilde{x}\tilde{x}}(\tau) - |m_x|^2$	Autocovariance
$C_{xx}(-\tau) = R_{xx}(\tau) - m_x^2$	$x(t) \in \text{real}$
$R_{xx}(\tau) = R_{yy}(\tau)$	$x(t) = m(t)\cos(\omega_c t)$ $y(t) = m(t)\sin(\omega_c t)$
$R_{xy}(\tau) = -R_{yx}(\tau)$	$x(t) = m(t)\cos(\omega_c t)$ $y(t) = m(t)\sin(\omega_c t)$
$R_{\tilde{x}\tilde{y}}(-\tau) = R_{\tilde{y}\tilde{x}}^*(\tau)$	$x(t), y(t) \in \text{complex}$
$C_{\tilde{x}\tilde{y}}(\tau) = R_{\tilde{x}\tilde{y}}(\tau) - \tilde{m}_x \tilde{m}_y^*$	Cross-covariance
$C_{xy}(\tau) = R_{xy}(\tau) - m_x m_y$	$x(t), y(t) \in \text{real}$
$R_{\tilde{z}\tilde{z}}(\tau) = R_{\tilde{x}\tilde{x}}(\tau) + R_{\tilde{y}\tilde{y}}(\tau) + R_{\tilde{x}\tilde{y}}(\tau) + R_{\tilde{y}\tilde{x}}(\tau)$	$\tilde{z}(t) = \tilde{x}(t) + \tilde{y}(t)$

Consider, for example, that $\tilde{y}(t) = \tilde{x}(t) + \tilde{n}(t)$ is a received signal plus AWGN, the correlation $R_{\tilde{x}\tilde{y}}(\tau)$ is performed in the demodulator using the known reference signal $\tilde{x}(t)$. The dynamic range of the demodulator detection processing is minimized by the normalization in (1.296) and the optimum signal detection corresponds to $\rho_{xy}(0)$. On the other hand, if the optimum timing is not known, near optimum detection can be achieved by choosing the maximum correlation output over the uncertainty range of the correlation lag about $\tau = 0$. During initial signal acquisition, the constant false-alarm rate (CFAR) threshold, described in Section 11.2.2.1, is an effective algorithm for signal presence detection and coarse synchronization.

1.6   RANDOM PROCESSES

Many of the signal descriptions and processing algorithms in the following chapters deal exclusively with the signal and neglect the additive noise under the reasoning that the noise detracts from the fundamental signal processing requirements and complicates the notation which has the same effect. On the other hand, understanding the impact of the noise on the system performance is paramount to the waveform selection and adherence to the system performance specifications. To this end, the performance evaluation is characterized by detailed analysis of the signal-plus-noise conditions and confirmed by computer simulations.

The following descriptions of noise and signal plus noise are provided to illustrate the assumptions and analysis associated with the inclusion of the most basic noise source—AWGN. The reference to narrowband Gaussian noise simply means that the carrier frequency f_c is much greater than

the signal modulation Nyquist bandwidth B_N so that the $2f_c$ heterodyning or homodyne mixing terms are completely eliminated through filtering. In such cases, the white noise in the baseband demodulator bandwidth is denoted by the single-sided noise density N_o watts/Hz, where *single-sided* refers to positive frequencies.

1.6.1 Stochastic Processes

The subject of stochastic processes is discussed in considerable detail by Papoulis [55] and Davenport and Root [56] and the following definitions are often stated or implied in the applications discussed in throughout the following chapters. A stochastic process is defined as a random variable that is a function of time and the random events χ in S as depicted in Figure 1.14. In this context the random variable is characterized as $x(t,\chi)$. For a fixed value of $t = t_i$, $x(t_i,\chi)$ is a random variable and $\chi = \chi_i$, $x(t,\chi_i)$ denotes as the real random process $x(t)$ such that $x(t_i)$ is a random variable with *pdf* $f_X(x{:}t_i)$; in general, the *pdf* of $x(t)$ is defined as $f_X(x{:}t)$.

1.6.1.1 Stationarity   There are several ways to define the stationarity of a stochastic process, for example, stationarity of finite order, asymptotic stationary, and periodic stationarity; however, the following two are the most frequently encountered.

Strict-Sense Stationary Process   The stochastic process $x(t)$ is strict-sense stationary, or simply stationary, if the statistics are unaltered by a shift in the time axis. Furthermore, two random variables are jointly stationary if the joint statistics are unaltered by an equal time shift of each random variable, that is, the probability density function $f(x\,;\,t)$ is the same for all time shifts τ. This is characterized as

$$f(x_1,x_2,\ldots;\,t_1,t_2,\ldots) = f(x_1,x_2,\ldots;\,t_1+\tau,\,t_2+\tau,\ldots)$$
$$(1.298)$$

Wide-Sense Stationary Process   The stochastic process $x(t)$ is wide-sense stationary (WSS) if its expected value is constant and autocorrelation function is a function of the time shift $\tau = t_2 - t_1 \,\forall\, t_1$ and t_2. WSS stationarity is characterized as

$$E[x(t)] = m_x = \text{constant} \qquad (1.299)$$

and

$$E[x(t)x(t-\tau)] = R_x(\tau) \qquad (1.300)$$

Because wide-sense stationarity depends on only the first and second moments it is also referred to as *weak* stationarity. A function of two random processes is wide-sense stationary

if each process is wide-sense stationary and their cross-correlation function is dependent only the time shift, that is,

$$E[x(t_1)y(t_2)] = R_{xy}(t_1-t_2) = R_{xy}(\tau) \qquad (1.301)$$

1.6.1.2 Ergodic Random Process   The random process $x(t)$, defined earlier, is an ergodic random process if the statistics of $x(t)$ are completely defined by the statistics of $x(t,\chi)$. Denoting the random process $x(t_i,\chi)$ as an ensemble of $x(t,\chi)$, then ergodicity ensures that the statistics $x(t_i)$ are identical to those of the ensemble; in short, the time statistics are identical to the ensemble statistics.[*] Ergodicity of the mean, of the stochastic process $x(t,\chi)$, exists under the condition

$$\langle x(t,\chi_i)\rangle = E[x(t_i,\chi)] \quad : \forall i \qquad (1.302)$$

where the time average is defined as

$$\langle x(t,\chi_i)\rangle \triangleq \lim_{T\to\infty} \frac{1}{2T}\int_{-T}^{T} x(t,\chi_i)dt \qquad (1.303)$$

and the ensemble average is defined as

$$E[x(t_i,\chi)] \triangleq \int_{-\infty}^{\infty} \chi f_\chi(t_i,\chi)d\chi \qquad (1.304)$$

Since the mean value of a random process must be a constant, the *ergodic of the mean* theorem states that the equality condition in (1.302) is satisfied when $E[x(t_i,\chi)] = \eta : \forall i$ where η is a constant. This is a nontrivial task to prove, however, following the discussion by Papoulis [57], the *ergodic of the mean theorem* states that

$$\lim_{T\to\infty} \frac{1}{2T}\int_{-T}^{T} x(t)dt = E[x(t)] = \eta$$
$$: iff \lim_{T\to\infty} \frac{1}{2T}\int_{-T}^{T} R_x(\tau)d\tau = \eta^2$$
$$(1.305)$$

The *iff* condition in (1.305) is formally expressed in terms of the autocovariance function for which the limit $T \to \infty$ is expressed as the variance $\sigma_x^2 = \eta^2 - E[x(t)]^2$. However, from (1.305), the expectation $E[x(t)] = \eta$ resulting in $\sigma_x^2 = 0$. Therefore, the limit $T \to \infty$ of the autocovariance function *converges in probability* with the conclusion that $E[x(t,\chi_i)] = E[x(t_i,\chi)]$[†] proving *ergodicity of the mean*. Demonstration of *ergodicity of the autocorrelation function*

---

[*]Papoulis (Reference 8, Chapter 9) discusses the ergodicity of a stochastic process with respect to certain parameters.
[†]Convergence in probability is also discussed by Davenport and Root (Reference 6, pp. 66–71).

is considerably more involved, requiring the fourth-order moments.

1.6.2 Narrowband Gaussian Noise

Consider the noise described by the narrowband process [58] with bandwidth $B << f_c$ expressed as

$$n(t) = N(t)\cos(\omega_c t + \theta(t)) - N(t)\sin(\omega_c t + \theta(t)) \quad (1.306)$$

where $N(t)$ and $\theta(t)$ represent, respectively, the envelop and phase of the noise and $\omega_c = 2\pi f_c$ is the angular carrier frequency. Upon expanding the trigonometric functions, (1.306) can also be expressed as

$$n(t) = n_c(t)\cos(\omega_c t) - n_s(t)\sin(\omega_c t) \quad (1.307)$$

where

$$n_c(t) = N(t)\cos(\theta(t)) \quad (1.308)$$

and

$$n_s(t) = N(t)\sin(\theta(t)) \quad (1.309)$$

The noise terms $n_c(t)$ and $n_s(t)$ are uncorrelated with spectrum $S(f)$ and bandwidth B, such that $S(f) = 0$ for $|f - f_c| > B/2$. This is the general characterization of a narrowband noise process; however, in the following analysis, $n_c(t)$ and $n_s(t)$ are also considered to be statistically independent, stationary zero-mean white noise Gaussian processes with one-sided spectral density N_o watts/Hz.

Because of the stationarity, the noise autocorrelation is dependent only on the correlation lag τ and is evaluated as

$$R_{nn}(\tau) = E[n(t)n(t-\tau)]$$

$$= E[\{n_c(t)\cos(\omega_c t) - n_s(t)\sin(\omega_c t)\}$$

$$\{n_c(t-\tau)\cos(\omega_c(t-\tau)) - n_s(t-\tau)\sin(\omega_c(t-\tau))\}]$$

$$\quad (1.310)$$

Upon evaluating the product in (1.310) and distributing the expectation, it is found that the conditions for stationarity require[*] $R_{ss}(\tau) = R_{cc}(\tau)$ and $R_{cs}(\tau) = -R_{sc}(\tau)$ so that (1.310) reduces to

$$R_{nn}(\tau) = R_{cc}(\tau)\cos(\omega_c \tau) - R_{ss}(\tau)\sin(\omega_c \tau) \quad (1.311)$$

The noise power is evaluated using (1.311) with $\tau = 0$ with the result $R_{nn}(0) = R_{cc}(0) = \sigma_n^2$. This evaluation can be carried

[*]See Problem 29.

further using the Wiener–Khinchin theorem[†] which states that the power spectral density of a WSS random process is the Fourier transform of the autocorrelation function, that is,

$$S_n(f) = \int_{-\infty}^{\infty} R_{nn}(\tau)e^{-j2\pi f\tau}d\tau \quad (1.312)$$

From (1.312) the inverse Fourier transform is

$$R_{nn}(\tau) = \int_{-\infty}^{\infty} S_n(f)e^{j2\pi f\tau}df \quad (1.313)$$

and, substituting the condition that the single-sided noise spectral density is defined as N_o watts/Hz, (1.313) becomes

$$R_n(\tau) = \frac{N_o}{2}\int_{-\infty}^{\infty} e^{j2\pi f\tau}df = \frac{N_o}{2}\delta(\tau) \quad (1.314)$$

In (1.314) the single-sided noise density is divided by two because of the two-sided integration, that is, the integration includes negative frequencies. In this case, the noise power, defined for $\tau = 0$, is infinite, however, when the ideal band-limited filter, with bandwidth B, is considered the noise power in the filter centered at f_c is computed as

$$R_n(0) = N_o \int_{f_c-B/2}^{f_c+B/2} df = N_o B \quad (1.315)$$

In this case the one-sided noise density N_o is used instead of $N_o/2$ because the one-sided integration is over positive frequencies.

If a linear filter with impulse response $h(t)$ is used, the frequency response is given by

$$H(f) = \int_{-\infty}^{\infty} h(t)e^{-j2\pi ft}dt \quad (1.316)$$

The corresponding unit gain normalizing factor is $|H(0)|$. With the stationary noise process $n(t)$ applied to the input of the filter, the output is determined using the convolution integral and the result is as follows:

$$n_o(t) = \int_{-\infty}^{\infty} n(t-\lambda)h(\lambda)d\lambda \quad (1.317)$$

[†]Leon-Garcia (Reference 29, p. 404) refers to this theorem as the Einstein–Wiener–Khinchin theorem based on the discovery of an earlier paper by Albert Einstein.

Using (1.317) it can be shown (see Problem 33) that the normalized spectrum of the output noise is expressed, in terms of the input noise PSD $S_n(f)$, as

$$S_{no}(f) = S_n(f)\left|\frac{H(f)}{H(0)}\right|^2 \qquad (1.318)$$

where $|H(0)|$ is the normalizing gain of the filter. Using (1.318), with $S_n(f) = N_o/2$ corresponding to white noise, the output noise power is evaluated as

$$
\begin{aligned}
R_{no}(0) &= \int_{f_c-B/2}^{f_c+B/2} S_n(f)\frac{|H(f)|^2}{|H(f_c)|^2}df \\
&= \frac{N_o}{2}\int_{f_c-B/2}^{f_c+B/2}\frac{|H(f)|^2}{|H(f_c)|^2}df \qquad (1.319) \\
&= N_o B_n
\end{aligned}
$$

where the second integral in (1.319) is recognized as the definition of the noise bandwidth of the bandpass filter with low-pass bandwidth B_n.

1.7   THE MATCHED FILTER

The problem in the detection of weak signals in noise is one of deciding whether the detection filter output is due to the signal and noise or simply noise only. The matched filter [59, 60], provides for the optimum signal detection in AWGN noise based on the maximum instantaneous signal-to-noise ratio when sampled at the optimum time.[*] The matched filter, for an AWGN channel, is characterized as having an impulse response equal to the delayed time-reverse replica of the received signal. To maximize the signal detection probability the matched filter output must be sampled at T_o as defined in the following analysis. The matched filter can be implemented at a convenient receiver IF or in the demodulator using quadrature baseband-matched filters.

Considering the received signal, $s_r(t)$, the matched filter impulse response depicted in Figure 1.28 is expressed as

$$h(t) = Gs_r(T_o - t) \qquad (1.320)$$

The gain G is selected for convenience; however, it must be a constant value. The delay T_o is required to result in a causal impulse response, that is, the response of $h(t \leq 0) = 0$ for $h(t)$ to be realizable; consequently, $s_r(t \geq T_o)$ must be zero. Usually the selection of T_o is not an issue since many symbol modulation functions are time limited or can be truncated without a significant impact on the transmitted signal

[*]The matched filter was first derived by D.O. North [59] and is also referred to as the North filter.
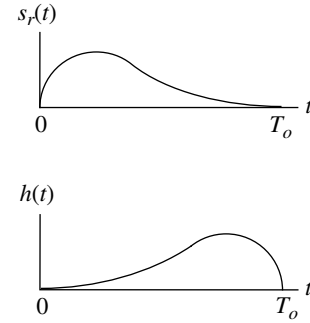

FIGURE 1.28   Example received signal and corresponding matched filter.

spectrum; however, the matched filter delay results in a throughput delay. To the extent that the impulse approximates (1.320) a detection loss will be encountered.

The criterion of the matched filter is to provide the maximum signal-to-noise ratio in the AWGN channel when sampled at the optimum time T_o. The following matched filter analysis follows that of Skolnik [61]. The signal-to-noise ratio of interest is

$$\gamma_f = \frac{|s_r(t)|^2_{max}}{N} \qquad (1.321)$$

where $|s_r(t)|^2_{max} = |s_r(T_o)|^2$ is evaluated as

$$|s_o(T_o)|^2 = \left|\int_{-\infty}^{\infty} S(f)H(f)e^{j2\pi fT_o}df\right|^2 \qquad (1.322)$$

and N is the noise power evaluated as

$$N = \int_{-\infty}^{\infty} N(f)|H(f)|^2df = \frac{N_o}{2}\int_{-\infty}^{\infty}|H(f)|^2df \qquad (1.323)$$

In these expressions, the filter spectrum $H(f)$ is normalized, such that $H(0) = 1$, and the last equality in (1.323) results because the channel noise is white with one-sided constant power density of N_o watts/Hz. Substituting (1.322) and (1.323) into (1.321) results in the expression for the signal-to-noise ratio

$$\gamma_f = \frac{\left|\displaystyle\int_{-\infty}^{\infty} S(f)H(f)e^{j2\pi fT_o}df\right|^2}{(N_o/2)\displaystyle\int_{-\infty}^{\infty}|H(f)|^2df} \qquad (1.324)$$

The maximum signal-to-noise ratio is evaluated by applying Schwarz's inequality (see Section 1.14.5, Equation 5) to the numerator of (1.324). Upon substituting $f^*(f) = S(f)e^{j2\pi fT_o}$ and $g(f) = H(f)$ into the Schwarz inequality, (1.324) is expressed as

$$\gamma_f \leq \frac{\int_{-\infty}^{\infty}|S(f)|^2 df \int_{-\infty}^{\infty}|H(f)|^2 df}{(N_o/2)\int_{-\infty}^{\infty}|H(f)|^2 df} = \frac{\int_{-\infty}^{\infty}|S(f)|^2 df}{N_o/2}$$

(1.325)

The equality condition of the signal-to-noise ratio in (1.325) applies when $f(f) = cg(f)$, where $c > 0$ is a conveniently selected constant resulting in the matched filter frequency response expressed as

$$H(f) = GS^*(f)e^{-j2\pi fT_o} \quad \text{: matched filter frequency response}$$

(1.326)

where $G = 1/c$ is an arbitrarily selected constant gain greater that zero. Upon applying Parseval's theorem and recognizing that the numerator of the second equality in (1.325) is the signal energy, E, the optimally sampled matched filter output signal-to-noise ratio is simply expressed as

$$\gamma_f(\max) = \frac{2E}{N_o} \quad \text{: baseband modulated signal}$$

(1.327)

Therefore, for the AWGN channel, the optimally sampled matched filter output results in a signal-to-noise ratio that is a function the signal energy and noise density and is independent of the shape of the signal waveform. The factor of two in (1.327) results from the analytic or baseband signal description in the derivation of the matched filter. Typically, the received signal spectrum is modulated onto a carrier frequency with an average power equal to one-half the peak carrier power. In this case, the signal-to-noise ratio at the output of the matched filter is one-half of that in (1.327) resulting in

$$\gamma_f(\max) = \frac{E}{N_o} \quad \text{: carrier moduated signal}$$

(1.328)

Referring to (1.326), the inverse Fourier transform of the complex conjugate of the signal spectrum results in the filter impulse response corresponding to the time reverse of the signal. In addition, the inverse Fourier transform of the exponential function in (1.326) results in a signal time delay of T_o seconds, so the resulting filter impulse response, $h(t)$, corresponds to the example depicted in Figure 1.28. Consequently, the matched filter impulse response can be expressed in the time domain by (1.320) or in the frequency domain by (1.326).

The detection loss associated with a filter that is not matched to the received signal is evaluated as

$$\rho_f \triangleq \frac{\gamma_f}{\gamma_f(\max)} = \frac{|s_o'(t)|^2_{max}/N_o'}{2E/N_o}$$

(1.329)

where $s_o'(t)$ and N_o' are the output signal and mean noise power density at the output of the unmatched filter. Typically

the matched filter is based on the transmitted waveform; however, the received signal into the matched filter may be distorted by the channel or receiver filtering[*] resulting in a detection loss. The matched filter implementation may also result in design compromises that result in a detection loss.

1.7.1   Example Application of Matched Filtering

In this example, a BPSK-modulated received signal is considered with binary source data bits $b_i = \{0,1\}$ expressed as the unipolar data $d_i = (1 - 2b_i) = \{1,-1\}$ over the data intervals $iT \leq t \leq (i+1)T$ of the bit duration T. The received signal plus noise is expressed as

$$r(t) = d_i s(t) + n(t)$$

(1.330)

The signal is described as

$$s(t) = A\cos(\omega_c t)$$

(1.331)

The noise is zero-mean additive white Gaussian noise with one-sided spectral density N_o described as

$$n(t) = n_c(t)\cos(\omega_c t) - n_s(t)\sin(\omega_c t)$$

(1.332)

The receiver-matched filter impulse response and Fourier transform are given by

$$h(t) = As(T_o - t) \quad \underset{\mathfrak{I}}{\Leftrightarrow} \quad H(f) = GS^*(f)e^{-j2\pi fT_o}$$

(1.333)

In (1.333) the signal spectrum defined as $S(f)$ and the squared magnitude of the matched filter output at the optimum sampling point is

$$|s_o(T_o)|^2 = \int_{-\infty}^{\infty} S(f)H(f)e^{j2\pi fT_o} df$$
$$= \int_{-\infty}^{\infty} |S(f)|^2 df = E$$

(1.334)

where the gain $G = |H(0)|$ is normalized to one resulting in a unit gain-matched filter response $H(f)$.

Referring to the additive noise described by (1.332) and Section 1.6.2, the noise power at the output of the matched filter is expressed as

$$R_{no}(0) = \frac{N_o}{2}\int_{-B/2}^{B/2}|H(f)|^2 df$$

(1.335)

where $B/2$ is the baseband bandwidth of the matched filter.

---

[*]Adaptive channel equalizers are often used to compensate for the channel distortion.

The received signal, as expressed in (1.330), can be rewritten in terms of the optimally sampled matched filter output as

$$l(r(iT_o)) = \sqrt{E}d_i + \sqrt{\frac{N_o}{2}}\, n_i \qquad (1.336)$$

where n_i are *iid* zero-mean, unit variance, white Gaussian noise samples. Upon dividing (1.336) by $\sqrt{N_o/2}$ the sampled matched filter output is expressed as

$$l'(r_i) = \sqrt{\frac{2E}{N_o}}d_i + n_i \qquad (1.337)$$

The sampled values $l(r(iT_o))$ and $l'(r_i)$ are referred to as *sufficient statistics*, in that, they contain all of the information in $r(t)$, expressed in (1.330), to make a maximum-likelihood estimate $\hat{d}_i$ of the source-bit d_i. The normalized form in (1.337) is used as the turbo decoder input discussed in Section 8.12. In Section 1.8 the sufficient statistic is seen to be a direct consequence of the log-likelihood ratio.

1.7.2 Equivalence between Matched Filtering and Correlation

Consider the receiver input as the sum of the transmitted signal plus noise expressed as

$$r(t) = s(t) + n(t) \qquad (1.338)$$

The cross-correlation of $r(t)$ with a replica of the received signal is computed as

$$R(\tau) = \int_{-\infty}^{\infty} r(t)s(t-\tau)dt \quad : \text{cross-correlation} \qquad (1.339)$$

Defining the matched filter impulse response as $h(t)$, the matched filter output response to the input $r(t)$ is

$$y_o(t) = \int_{-\infty}^{\infty} r(\lambda)h(t-\lambda)d\lambda \quad : \text{convolution} \qquad (1.340)$$

However, referring to the preceding matched filter discussion, the matched filter response is equal to the delayed image of the signal, such that,

$$h(t) = s(T_o - t) \qquad (1.341)$$

As mentioned previously, the delay T_o ensures that the filter response is causal and, therefore, realizable. To substitute (1.341) into (1.340) first let $t' = t - \lambda$ so that $h(t-\lambda) = s(T_o - (t-\lambda)) = s(\lambda - (t-T_o))$ and substitute this result in (1.340) to get

$$y_o(t) = \int_{-\infty}^{\infty} r(\lambda)h(t-\lambda)d\lambda$$
$$= \int_{-\infty}^{\infty} r(\lambda)s(\lambda - (t-T_o))d\lambda \qquad (1.342)$$
$$= R(t-T_o)$$

So that the convolution response is equal to the cross-correlation response delayed by T_o. If the input noise is zero, so that $r(t) = s(t)$, the same conclusion can be drawn regarding the autocorrelation response.

1.8 THE LIKELIHOOD AND LOG-LIKELIHOOD RATIOS

Bayes criterion is based on two events, referred to as hypothesis H_1 and H_0, that are dependent upon a priori probabilities P_1 and P_0 and the, respective, associated costs (C_{01},C_{11}) and (C_{10},C_{00}). Letting m correspond to the decision and n correspond to the hypothesis, the range of the cost is $0 \leq C_{mn} \leq 1$ with $C_{mn} + C_{nn}|_{m \neq n} = 1$. The cost of a correct decision is C_{nn} and an incorrect decision is $C_{mn}|_{m \neq n}$. For communication links the cost of incorrect decision is typically higher than a correct decision so that $C_{mn}|_{m \neq n} > C_{nn.}$ For example, when $C_{mn}|_{m \neq n} = 1$ and $C_{nn} = 0$ the decision threshold minimizes the probability of error which is the goal of communication demodulators. In summary,

$$C_{mn} = \begin{cases} m = n & : \text{cost of correct decision} \\ m \neq n & : \text{cost of decision error} \end{cases} \qquad (1.343)$$

and the a priori probabilities are typically known and equal.

In the following example, the hypotheses correspond to selecting $d_i = \{1, -1\}$, such that, under the two hypotheses

$$\begin{aligned} H_1 &\; : \; d_i = +1 \text{ with a prioi probability } P_1 \\ H_0 &\; : \; d_i = -1 \text{ with a prioi probability } P_0 \end{aligned} \qquad (1.344)$$

with the observations

$$r_i = d_i + n_i \quad : t = iT_o \qquad (1.345)$$

corresponding to the optimally sampled outputs of the matched filter. In terms of the a priori, the transition probabilities, and the cost functions, the hypothesis H_1: with $d_i = 1$ is chosen if the following inequality holds,

$$P_{r|H_1}(r|H_1)\, P_1(C_{01} - C_{11}) \geq P_{r|H_0}(r|H_0)\, P_0(C_{10} - C_{00}) \qquad (1.346)$$

otherwise, chose H_0 with $d_i = -1$. The decisions are made explicit under the following rearrangement of (1.346)

$$\frac{P_{r|H_1}(r|H_1)}{P_{r|H_0}(r|H_0)} \underset{H_0}{\overset{H_1}{\gtrless}} \frac{P_0(C_{10}-C_{00})}{P_1(C_{01}-C_{11})} \qquad (1.347)$$

Left and right sides of (1.347) are defined as the likelihood ratio (LR) $\Lambda(r)$ and decision threshold η or, alternately, as the log-likelihood ratio (LLR) $\ln\Lambda(r)$ with the threshold $\ln\eta$, so (1.347) is also expressed as

$$\Lambda(\boldsymbol{r}) \underset{H_0}{\overset{H_1}{\gtrless}} \eta \quad \text{or} \quad \ln\Lambda(\boldsymbol{r}) \underset{H_0}{\overset{H_1}{\gtrless}} \ln\eta \quad : \text{alternate decisions thresholds}$$

$$(1.348)$$

1.8.1 Example of Likelihood and Log-Likelihood Ratio Detection

Consider the two hypotheses H_1 and H_0 mentioned earlier with $d_i = \{1,-1\}$ and the observation r_i in (1.345) with the additive noise n_i characterized as *iid* zero-mean white Gaussian noise, denoted as $N(0,\sigma_n)$. The transition probabilities are expressed in terms of the Gaussian noise *pdf* as

$$p(n) = \frac{1}{\sqrt{2\pi}\sigma_n} e^{-(r-\bar{m})^2/2\sigma_n^2} \qquad (1.349)$$

Upon forming the likelihood ratio and recognizing that $\bar{m} = \pm d_i$, the likelihood ratio decision simplifies to

$$\exp\left(\frac{2r_i}{\sigma_n^2}\right) \underset{H_0}{\overset{H_1}{\gtrless}} \frac{P_0(C_{10}-C_{00})}{P_1(C_{01}-C_{11})} \qquad (1.350)$$

and the log-likelihood ratio decision simplifies to

$$\frac{2}{\sigma_n^2}r_i \underset{H_0}{\overset{H_1}{\gtrless}} \ln\left(\frac{P_0(C_{10}-C_{00})}{P_1(C_{01}-C_{11})}\right) \qquad (1.351)$$

Recognizing that $l(r_i)$ is a sufficient statistic, (1.351) is rewritten as

$$l(r_i) \underset{H_0}{\overset{H_1}{\gtrless}} \frac{\sigma_n^2}{2}\ln\left(\frac{P_0(C_{10}-C_{00})}{P_1(C_{01}-C_{11})}\right) \qquad (1.352)$$

When $C_{10} = C_{01} = 1$, $C_{00} = C_{11} = 0$, and $P_0 = P_1$ the LLR simplifies to

$$l(r_i) \underset{H_0}{\overset{H_1}{\gtrless}} 0 \quad : \ln(\eta = 1) = 0 \qquad (1.353)$$

Therefore, the data estimate is $\hat{d}_i = 1$ when $l(r_i) > 0$, otherwise, $\hat{d}_i = -1$. Recall that observations $r_i : t = iT_o$ are made at the output of the matched filter. These concepts involving the LR and LLR surface again in Section 3.2 and the notion of the natural logarithm of the transitions probabilities is discussed in the following section involving parameter estimation.

1.9   PARAMETER ESTIMATION

The subject of optimum signal detection in noise was examined in the preceding section in terms of a pulsed-modulated carrier and it resurfaces throughout the following chapters in the context of a number of different waveform modulations. However, signal detection is principally based on the signal energy without regard to specific signal parameters, although frequency and range delay must be estimated to some degree to declare signal presence and subsequently detection. Signal detection uses concepts involving *direct probabilities*, whereas the subject of parameter estimation uses concepts involving *inverse probabilities* as discussed by Feller [32], Slepian [62], Woodward and Davies [63], and others. The distinction between these concepts is that *direct probability* is based on the probability of an event happening, whereas *inverse probability* formulates the best estimate of an event that has already occurred. With this distinction, it is evident that parameter estimation involves inverse probabilities. The major characteristic of inverse probability is the use of a priori information associated with the available knowledge of each source event. At the receiver the a posteriori probability is expressed in terms of the inverse probability using Bayes rule that associates the transition probability and a priori knowledge of the source events.

The subject of this section is signal parameter estimation and, although the major parameter of interest in communications is the estimation of the source information, the estimation of parameters like, frequency, delay, and signal and noise powers are important parameters that aid in the estimation of the source information. For example, estimation of the received signal and noise powers form the basis for estimating the receiver signal-to-noise ratio that is used in the network management to improve and maintain communication reliability. Furthermore, characterizing the theoretical limits in the parameter estimates provides a bench mark or target for the accuracy of the parameter estimation during the system design.

The following discussion of statistical parameter estimation is largely based on the work of Cramér [64], Rao [65], Van Trees [66], and Cook and Bernfeld [67]. The received signal is expressed in terms of the transmitted signal with M unknown parameters $a_1, a_2, \ldots, a_M$ and additive noise, as

$$r(t) = s(t; a_1, a_2, \ldots, a_M) + n(t) \qquad (1.354)$$

Considering that N discrete samples of the received signal and additive noise are used to estimate the parameters, the joint probability density function (*pdf*) of the samples is

$$p_{\mathbf{r}}(r_1, r_2, \ldots, r_N | a_1, a_2, \ldots, a_M) = p_{\mathbf{n}}(r_1 - s_1, r_2 - s_2, \ldots, r_N - s_N)$$
(1.355)

where the noise samples $n_i = r_i - s_i$ are substituted into the joint *pdf* of the noise. The noise samples are statistically independent and the statistical characteristics of the noise are assumed to be known. Therefore, based on the received signal-plus-noise samples r_i, the receiver must determine the estimates $\hat{a}_1, \hat{a}_2, \ldots, \hat{a}_M$ of the M unknown parameters. The probability density function $p_r(r_1, \ldots | a_1, \ldots)$ in (1.355) is called the *likelihood function*.

Van Trees discusses several estimation criteria[*] and the following focuses on the optimum estimates for the *mean-square* (MS) error[†] and *maximum a posteriori probability* (MAP) criterion that are defined, respectively, for a single parameter a as

$$\hat{a}_{ms}(\mathbf{r}) = \int_{-\infty}^{\infty} a p_{a|r}(a|\mathbf{r}) da \quad : \text{MS estimate} \qquad (1.356)$$

and

$$\left. \frac{\partial}{\partial a} \ln p_{a|r}(a|\mathbf{r}) \right|_{a = \hat{a}_{map}(\mathbf{r})} = 0 \quad : \text{MAP equation} \qquad (1.357)$$

The estimate $\hat{a}_{ms}(\mathbf{r})$ is optimum in the sense that it results in the minimum MS error over all s_i and a. The MAP estimate $\hat{a}_{map}(\mathbf{r})$ is the solution to (1.357) and is optimum in the sense that it locates the maximum of the *a posteriori* probability density function; however, the solution must be checked to determine if it corresponds to the global maximum in the event of a multimodal distribution.

By applying Bayes rule to (1.357), the MAP estimate is expressed in terms of the a priori *pdf*, $p_{\mathbf{a}}(a)$, and the likelihood function, $p_{r|a}(\mathbf{r}|a)$, as

$$\left. \frac{\partial}{\partial a} \ln p_{r|a}(\mathbf{r}|a) + \frac{\partial}{\partial a} \ln p_a(a) \right|_{a = \hat{a}_{map}(\mathbf{r})} = 0 \qquad (1.358)$$

When the a priori probabilities are unknown, that is, as the a priori knowledge approaches zero, (1.358) becomes the *maximum-likelihood equation* and $\hat{a}_{ml}(\mathbf{r})$ is the *maximum-likelihood* estimate, evaluated as the solution to

$$\left. \frac{\partial}{\partial a} \ln p_{r|a}(\mathbf{r}|a) \right|_{a = \hat{a}_{ml}(\mathbf{r})} = 0 \quad : \text{ML estimate} \qquad (1.359)$$

To make use of these estimates it is necessary to determine the bias and the variance of the estimate. The mean value of the estimate is computed as

$$E[\hat{a}(\mathbf{r})] = \int_{-\infty}^{\infty} \hat{a}(\mathbf{r}) p_{r|a}(\mathbf{r}|a) d\mathbf{r} \qquad (1.360)$$

The bias of the estimate is defined as $B(a) = E[\hat{a}(\mathbf{r})] - a$. If, as indicated, the bias is a function of a, the estimate has an *unknown bias*, however, if the bias is B, independent of a, the estimate has a *known bias* that can be removed from the observation measurements r. In general, for any known biased estimate $\hat{a}(\mathbf{r})$ of the real random variable a, the variance is defined as

$$\sigma_{\hat{a}}^2 = Var[\hat{a}(\mathbf{r}) - a] \triangleq E\left[(\hat{a}(\mathbf{r}) - a)^2\right] - B^2 \qquad (1.361)$$

Although the bias and variance are often difficult to determine, the Cramér–Rao inequality provides a lower bound on the variance of the estimate. For a biased estimate of the random parameter a with a priori *pdf* $p_a(a)$, the variance is lower bounded by the Cramér–Rao inequality [64, 66]

$$\sigma_{\hat{a}}^2 \geq \frac{(\partial E[\hat{a}(\mathbf{r})]/\partial a)^2}{E\left[\left\{\dfrac{\partial \ln(p_{r|a}(\mathbf{r}|a))}{\partial a} + \dfrac{\partial \ln(p_a(a))}{\partial a}\right\}^2\right]} \quad : \text{biased; variable}$$
(1.362)

or, the equivalent result,

$$\sigma_{\hat{a}}^2 \geq \frac{(\partial E[\hat{a}(\mathbf{r})]/\partial a)^2}{-E\left[\dfrac{\partial^2 \ln(p_{r|a}(\mathbf{r}|a))}{\partial a^2} + \dfrac{\partial^2 \ln(p_a(a))}{\partial a^2}\right]} \qquad (1.363)$$
$$: \text{biased; variable}$$

When the estimate is unbiased, that is, when $E[\hat{a}(\mathbf{r})] = a$, the estimation variance of the random variable a simplifies to

$$\sigma_{\hat{a}}^2 \geq \frac{1}{E\left[\left\{\dfrac{\partial \ln(p_{r|a}(\mathbf{r}|a))}{\partial a} + \dfrac{\partial \ln(p_a(a))}{\partial a}\right\}^2\right]} \qquad (1.364)$$
$$: \text{unbiased; variable}$$

or, the equivalent result,

$$\sigma_{\hat{a}}^2 \geq \frac{1}{-E\left[\dfrac{\partial^2 \ln(p_{r|a}(\mathbf{r}|a))}{\partial a^2} + \dfrac{\partial^2 \ln(p_a(a))}{\partial a^2}\right]} \qquad (1.365)$$
$$: \text{unbiased; variable}$$

The Cramér–Rao bound in these relationships is formulated in terms of the Schwarz inequality and the equality condition applies when

$$\frac{\partial \ln\left(p_{r|a}(\boldsymbol{r}|a)\right)}{\partial a} + \frac{\partial \ln\left(p_a(a)\right)}{\partial a} = k(\hat{a}(\boldsymbol{r}) - a) \tag{1.366}$$

: MAP efficient estimate condition

where k is a constant. Therefore, (1.366) guarantees that the equality condition for the variance applies in (1.362) through (1.365); in this case, the MAP estimate is defined as an efficient estimate. Furthermore, an unbiased estimate, excluding the trivial case $k = 0$, requires that $\hat{a}(\boldsymbol{r}) = a$ leading to (1.358).

When the a priori knowledge $p_a(a)$ is constant, that is, the parameter a is nonrandom, or unknown, then (1.359) also requires that $\hat{a} = a$ or $\hat{a}_{ml}(\boldsymbol{r}) = a$. Under the maximum-likelihood (ML) criteria Schwarz's equality condition applies when

$$\frac{\partial \ln\left(p_{r|a}(\boldsymbol{r}|a)\right)}{\partial a} = k(a)(\hat{a}(\boldsymbol{r}) - a) \tag{1.367}$$

: ML efficient estimate condition

In this case, the constant $k(a)$ may be a function of a; this condition only applies when parameter a is a constant which corresponds to the ML estimate.

Van Trees lists three principles based on the forgoing results:

1 The mean-square (MS) error estimate is always the mean of the a posteriori density, that is, the conditional mean.

2 The MAP estimate corresponds to the value of a for which the a posteriori density is maximum.

3 For a large class of cost functions, the optimum estimate is the conditional mean whenever the a posteriori density is a unimodal function which is symmetric about the conditional mean. The Gaussian *pdf* is a commonly encountered example.

By way of review, the estimates are evaluated using the a posteriori *pdf*; however, if the parameter is a random variable, the a posteriori *pdf* must be expressed in terms of the transition distribution and the a priori *pdf* of the random parameter using Bayes rule. If the estimate is unbiased, that is, if $B = E[\hat{a}(\boldsymbol{r})] - a = 0$, evaluation of the Cramér–Rao bound simplifies to (1.364); it is sometimes necessary to use the equivalent expression in (1.365). The Cramér–Rao equality condition is established if the left-hand side of (1.366) can be expressed in terms of the right-hand side where k is a constant parameter resulting from Schwarz's condition for equality.

If the a priori knowledge is unknown then the maximum-likelihood equation given in (1.359) is used to determine maximum-likelihood estimate. In this case, the Cramér–Rao bound is established by omitting the dependence of $p_a(a)$ in, (1.362) through (1.365) and the equality condition is established if the left-hand side of (1.367) can be expressed in terms of the right-hand side where, in this case, the constant $k(a)$ is a function of the parameter a. With either the MAP or ML estimates, if the bias is zero and the equality condition applies, the estimate is referred to as an efficient estimate.

Van Trees shows that for the MS estimate to be an efficient estimate, the a posteriori probability density $p_{a|r}(a|r)$ must be Gaussian for all r and, for efficient MAP estimates, $\hat{a}_{ms}(r) = \hat{a}_{map}(r)$. However, it may be easier to solve the MAP equation than to determine the conditional mean as required by the MS estimation procedure.

1.9.1 Example of MS and MAP Parameter Estimation

As an example application of the parameter estimation procedures discussed earlier, consider the Poisson distribution that is used to predict population growth, telephone call originations, gamma ray emissions from radioactive materials, and is central in the development of queueing theory [68]. For this example, the Poisson distribution is characterized as

$$p_a(a|n) = \frac{a^n}{n!} e^{-a} \quad : a \geq 0; \ n = 0, 1, 2, \ldots \tag{1.368}$$

In the application of (1.368) to queueing theory, $a = \lambda t$ is the average number of people entering a queueing line in the time interval 0 to t and λ is the arrival rate. The a posteriori distribution $p_{a|n}(a|n)$ is the probability of a conditioned on exactly n arrivals occurring in the time interval. A fundamental relationship in the Poisson distribution is that the time interval *between* people entering the queueing line is exponentially distributed and is characterized by the a priori distribution

$$p_a(a) = e^{-a} \quad : a \geq 0 \tag{1.369}$$

The a posteriori *pdf* in (1.368) is expressed in terms of the a priori and transition *pdfs* as

$$p_{a|n}(a|n) = \frac{p_{n|a}(n|a) p_a(a)}{p_n(n)} = \frac{k}{n!} a^n e^{-2a} \tag{1.370}$$

where the constant k is a normalizing constant that includes $1/p_n(n)$. Integrating of the second equality in (1.370) with respect to da over the range 0 to ∞ and setting the result equal to one, the value of k is found to be $k = 2^{n+1}$ and (1.370) becomes

$$p_{a|n}(a|n) = \frac{2^{n+1}}{n!}a^n e^{-2a} \qquad (1.371)$$

Using (1.356) and (1.371) the MS estimate is evaluated as

$$\hat{a}_{ms}(n) = \frac{2^{n+1}}{n!}\int_0^\infty a^{n+1}e^{-2a}da = \frac{n}{2} \qquad (1.372)$$

Also, using (1.357) and (1.371) the MAP estimate is evaluated as

$$\frac{\partial}{\partial a}\left(\ln\left\{\frac{2^{n+1}}{n!}a^n e^{-2a}\right\}\right) = \frac{\partial}{\partial a}\left(\ln\left\{\frac{2^{n+1}}{n!}\right\} + n\ln(a) - 2a\right)$$

$$= \frac{n}{a} - 2\bigg|_{a=\hat{a}_{map}(n)} = 0 \qquad (1.373)$$

and solving the second equality in (1.373) for a results in $\hat{a}_{map}(n) = n/2$. As is typical in many cases, the MS and MAP estimation procedures result in the same estimate. It is left as an exercise (see Problem 38) to determine the bias of the estimates, compute the Cramér–Rao bound, and using (1.366), determine if the estimates are efficient, that is, if the Cramér–Rao equality condition applies.

1.9.2 Constant-Parameter Estimation in Gaussian Noise

To simplify the description of the estimation processing, the analysis in this section considers the single constant-parameter case with zero-mean narrowband additive Gaussian noise. Under these conditions, the estimation is based on the solution to the maximum-likelihood equation with the joint *pdf* of the received signal and noise written as

$$p_{\mathbf{r}}(r_1, r_2, \ldots, r_N; a) = p_{\mathbf{n}}(r_1 - s_1, r_2 - s_2, \ldots, r_N - s_N)$$

$$= \prod_{i=1}^N p_{\mathbf{n}}(r_i - s_i) \qquad (1.374)$$

where a is the constant parameter to be estimated and $r_i = s_i + n_i$ represents the received signal samples. The sampling rate satisfies the Nyquist sampling frequency and the second equality in (1.374) recognizes that the noise samples are independent. The following analysis is based on the work of the Woodard [24] and Skolnik [61] and uses the maximum-likelihood estimate of (1.359) with the Cramér–Rao bound expressed by (1.365).

Using (1.374) with zero-mean AWGN, the minimum Cramér–Rao bound on the variance of the estimate is expressed as

$$\sigma\hat{a}^2(\min) = -E\left[\frac{\partial^2}{\partial a^2}\ln\left\{\prod_i^N \frac{1}{\sqrt{2\pi}\sigma_n}\exp\left(-\frac{(r_i - s_i)^2}{2\,\sigma_n^2}\right)\right\}\right]^{-1}$$

$$= -E\left[\frac{\partial^2}{\partial a^2}\ln\left\{k\exp\left(\frac{-1}{2N_o}\sum_{i=1}^N (r_i - s_i)^2\Delta t\right)\right\}\right]^{-1}$$

$$= -E\left[\frac{\partial^2}{\partial a^2}\ln\left\{k\exp\left(\frac{-1}{2N_o}\int_0^{T_e}(r(t) - s(t))^2 dt\right)\right\}\right]^{-1}$$

$$(1.375)$$

In arriving at the third equality in (1.375) the factor k is independent of the parameter a and, it is recognized that, $\sigma_n^2 = N_o B$ where $B = 1/T_e$ is the bandwidth corresponding to the estimation time. The integral is formed by letting $\Delta t \to 0$ as the number of samples $N \to \infty$ over the estimation interval T_e. Upon taking the logarithm of the product $k\exp(-)$ and performing the partial derivatives on the integrand, (1.375) simplifies to

$$\sigma\hat{a}^2(\min) = E\left[\frac{-1}{N_o}\int_0^{T_e}\left\{(r(t) - s(t))\frac{\partial^2 s(t)}{\partial a^2} - \left(\frac{\partial s(t)}{\partial a}\right)^2\right\}dt\right]^{-1}$$

$$= \left[\frac{1}{N_o}\int_0^{T_e}\left(\frac{\partial s(t)}{\partial a}\right)^2 dt\right]^{-1}$$

$$(1.376)$$

The last equality in (1.376) is the basis for determining the variance and is obtained by moving the expectation inside of the integral and recognizing that $E[r(t) - s(t)] = E[n(t)] = 0$. The following example outlines the procedures for estimating the variance of the estimate using the ML procedures.

1.9.2.1 Example of ML Estimate Variance Evaluation
Consider the signal $s(t)$ expressed as

$$s(t) = A\cos\left(\omega_o t + \dot{\omega}t^2/2 + \phi\right) \qquad (1.377)$$

where A is the peak carrier voltage, ω_o is the IF angular frequency, $\dot{\omega}$ is the angular frequency rate, and ϕ is a constant phase angle; the signal power is defined $P_s = A^2/2$.

The variance of the frequency estimate is determined by squaring the partial derivative of $s(t)$ respect to ω_o and integrating over the estimation interval T_e as indicated in (1.376). Under these conditions the analysis of the Cramér–Rao lower bound is performed as follows.

$$\sigma_{\hat{\omega}_o}^2(\min) = \left[\frac{A^2}{N_o}\int_0^{T_e}t^2\sin^2\left(\omega_o t + \dot{\omega}t^2/2 + \phi\right)dt\right]^{-1}$$

$$= \left[\frac{P_s}{N_o}\int_0^{T_e}t^2\left(1 - \cos\left(2\omega_o t + \dot{\omega}t^2 + 2\phi\right)\right)dt\right]^{-1}$$

$$(1.378)$$

Upon neglecting the term involving $2\omega_o$ and performing the integration, (1.378) becomes

$$\sigma_{\hat{\omega}_o}^2(\min) = \frac{3}{T_e^2 \gamma_e} \quad : \mathrm{rad}^2/\mathrm{s}^2 \tag{1.379}$$

where $\gamma_e = P_s T_e/N_o$ is the signal-to-noise ratio in the estimation bandwidth of $1/T_e$. In terms of the carrier frequency f_o in hertz, the standard deviation of the estimate is

$$\sigma_{\hat{f}_o}(\min) = \frac{\sqrt{3}}{2\pi T_e \sqrt{\gamma_e}} \quad : \mathrm{Hz} \tag{1.380}$$

In a similar manner, the standard deviation of the frequency rate and phase are evaluated as

$$\sigma_{\hat{f}}(\min) = \frac{\sqrt{5}}{\pi \, T_e^2 \sqrt{\gamma_e}} \quad : \mathrm{Hz/s} \tag{1.381}$$

and

$$\sigma_{\hat{\phi}}(\min) = \frac{1}{\sqrt{\gamma_e}} \quad : \mathrm{rad} \tag{1.382}$$

The evaluation of the standard deviation of the signal amplitude (A) estimation error is left as an exercise (see Problem 39).

1.9.3 Received Signal Delay and Frequency Estimation Errors

Accurate estimation of the signal delay and frequency are essential in aiding the signal acquisition processing by minimizing the overall time and frequency search ranges. The delay estimation accuracy (σ_{Td}) is inversely related to the signal bandwidth (B) and the signal frequency estimation accuracy (σ_{fd}) is inversely related to the time duration (T) of the signal. Neglecting the signal-to-noise dependence of each measurement, these inverse dependencies are evident, in that, the product $\sigma_{Td}\sigma_{fd} \propto 1/TB$ where TB is the time-bandwidth product of the waveform. For typical modulated waveforms T and B are inversely related so that simultaneous accurate time and frequency estimates are not attainable. However, the use of spread-spectrum (SS) waveform modulation provides for arbitrarily large BT products with simultaneous accurate estimates of T_d and f_d. The analysis of delay and frequency estimation errors in the following sections is based on the work of Skolnik [61] and can be applied to conventional or SS-modulated waveforms. In Section 1.9.3.3 delay and frequency estimation is examined using a DSSS-modulated waveform.

1.9.3.1 Delay Estimation Error Based on Effective Bandwidth   The signal delay measurement accuracy using

the effective signal bandwidth was introduced by Gabor [69] and is discussed by Woodward [24] and defined as the standard deviation of the delay measurement expressed as[*]

$$\sigma_{T_d} = \frac{1}{\beta\sqrt{2\gamma_e}} \quad : \mathrm{second} \tag{1.383}$$

where $\gamma_e = P_s/N_oW = E/N_o$ is the signal-to-noise ratio[†] measured in the two-sided bandwidth W, N_o is the one-sided noise density, P_s is the signal power, and β is the effective bandwidth of the signal. β^2 is the normalized second moment of the waveform spectrum $|S(f)|^2$, defined as

$$\beta^2 \triangleq \frac{\displaystyle\int_{-\infty}^{\infty} (2\pi f)^2 |S(f)|^2 df}{\displaystyle\int_{-\infty}^{\infty} |S(f)|^2 df} \tag{1.384}$$

The denominator in (1.384) is the signal energy and the integration limits extend over the frequency range $f \leq |W/2|$ corresponding to the nonzero signal spectrum. The one-way range error corresponding to (1.383) is $\sigma_{rng} = c\sigma_{T_d}$ meters where c is the free-space velocity of light in meter/second.

For the rectangular symbol modulation function $rect(t/T)$, band limited to W Hz with $\beta^2 \cong W/T$ and large time-bandwidth products $WT/2$, (1.383) is evaluated as

$$\sigma_{T_d} = \frac{T}{\sqrt{WT\gamma_e}} \quad : \text{band-limited } rect(t/T) \text{ symbol}; \; WT/2 \gg 1 \tag{1.385}$$

1.9.3.2 Frequency Estimation Error Based on Effective Signal Duration   In a manner similar to the analysis of

the delay estimation error in the preceding section, Manasse [70] shows that the, minimum root-mean-square (rms) error in the frequency estimate is given by[‡]

$$\sigma_{f_d} = \frac{1}{\alpha\sqrt{2\gamma_e}} \quad : \mathrm{Hz} \tag{1.386}$$

where $\gamma_e = E/N_o$ is the signal-to-noise ratio measured in the two-sided bandwidth W, N_o is the one-sided noise density, P_s is the signal power, and α is the effective time duration of the

---

[*]Woodward refers to the delay error as the standard deviation of the error. Slepian's analysis [62] is based on the likelihood function and also arrives at (1.383).

[†]The factor of two in γ_e results because N_o is the one-sided noise density and W is the two-sided bandwidth.

[‡]The notation σ_{fd} is used to denote the standard deviation of the frequency estimation error.
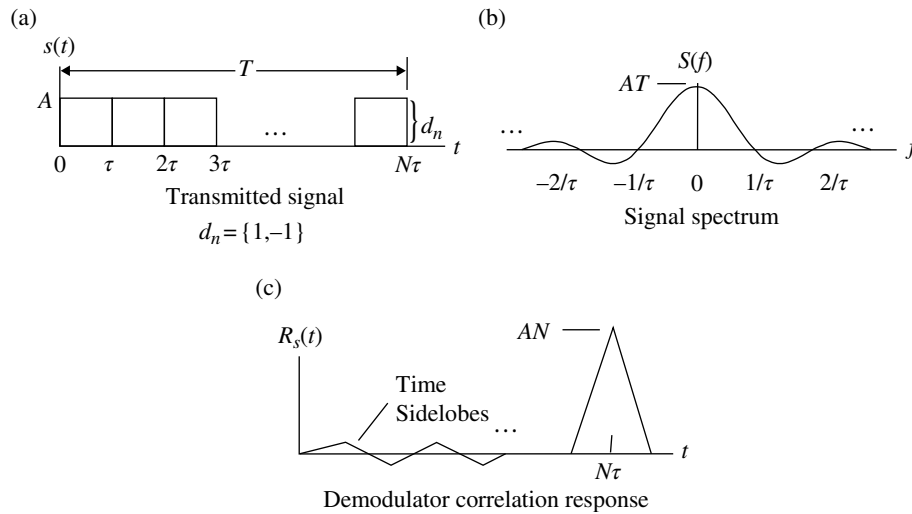
FIGURE 1.29 Time–frequency estimation using DSSS waveform.

received signal. The parameter α^2 is the normalized second moment of the waveform $s(t)$ and is defined as

$$\alpha^2 \triangleq \frac{\int_{-\infty}^{\infty} (2\pi t)^2 s^2(t) dt}{\int_{-\infty}^{\infty} s^2(t) dt} \qquad (1.387)$$

The Doppler frequency results from the velocity (v) and the carrier frequency (f_c) and is expressed as $f_d = (v/c)f_c$. Frequency errors resulting from hardware oscillators are usually treated separately and combined as the root-sum-square (RSS) of the respective standard deviations.

For the band-limited $rect(t/T)$ symbol modulation used in the preceding section, the normalized second moment is evaluated as $\alpha^2 \cong (\pi T)^2/3$ and (1.386) is expressed as

$$\sigma_{f_d} = \frac{\sqrt{3}}{\pi T \sqrt{2\gamma_e}} \quad : \text{band-limited } rect(t/T) \text{ symbol}; \ WT/2 \gg 1$$

$$(1.388)$$

Comparison of (1.385) and (1.388) demonstrates the inverse relationship between the estimation accuracy of the range-delay and frequency errors for conventional (unspread) modulations. For example, for a given time bandwidth (WT) product and signal-to-noise ratio (γ_e), the delay estimate error decreases with decreasing symbol duration; however, the frequency estimate error increases. The issue resolves about the signal-to-noise ratio in the estimation bandwidth. For example, with conventional waveform modulations, $WT = 2BT = 2$ so $BT = 1$ and the bandwidth changes inversely with the symbol duration. Consequently, by decreasing symbol duration, the bandwidth increases resulting in a signal-to-noise γ_s,

measured in the symbol bandwidth, degradation of B/B' where $B' > B$. Therefore, in the previous example, to maintain a constant signal-to-noise ratio γ_e the estimation interval must be appropriately adjusted. As mentioned previously, the solution to simultaneously obtaining accurate estimates of range delay and frequency while maintaining a constant γ_s, involves the use of a SS-modulated signals with an inherently large WT product as discussed in the following section.

1.9.3.3 Improved Frequency and Time Estimation Errors Using the DSSS Waveform

The DSSS waveform uses a pseudo-noise (PN) sequence of chips with and instantaneous bandwidth (W) over the estimation interval (T) as shown in Figure 1.29.[*] The resulting large WT product signal provides for arbitrarily low time and frequency estimation errors. This is accomplished by the respective selection of a high bandwidth (short duration) chip interval (τ) and the low bandwidth (long duration) estimation interval T. The estimation interval can be increased to improve the frequency estimate; conversely, the chip interval can be decreased to improve the range-delay estimate; however, to maintain the accuracy of the other, the number of chips per estimation interval (N) must be increased. These relationships are described in terms of the pulse compression ratio, defined as $\rho = T/\tau = N$. In Figure 1.29 the chips are depicted as appropriately delayed $Ad_n rect((t-n)/\tau - 0.5): n = 0, \ldots, N-1$ functions and, because of the equivalence between the correlator and matched filter, the peak correlator output is a triangular function with a peak value[†] of AN. When sampled at $t = N\tau$, the correlator output

[*]Although not shown in the figure, the chips are ± binary pulses which suggest that the received signal carrier frequency is BPSK modulated.
[†]This suggests that the local reference is an identical unit amplitude PN sequence that is synchronized with the received PN sequence.

results in the maximum signal-to-noise ratio measured in the bandwidth of $1/T$ Hz.

Based on the fundamental principles for jointly achieving accurate time and frequency estimates as stated earlier, the triangular shape of the wide bandwidth correlator output is related to the accuracy of the time estimate and the low bandwidth sampled output at interval of $T = N\tau$ determines the accuracy of the frequency estimate. Therefore, evaluation of the time and frequency estimation accuracies of the DSSS waveform involves evaluating, respectively, the effective bandwidth (β) of the triangular function and the effective time duration (α) of the $rect(t/T - 0.5)$ function.

Delay Estimation Error of the DSSS Waveform   The delay estimation error is based on detecting the changes in the leading and trailing edge of wideband signals. This does not require that the signal has a short duration but that the bandwidth is sufficiently wide to preserve the rapid rise and fall times of the correlator response. On the other hand, received signals with additive noise must be detected and the parameters estimated under the optimum signal-to-noise conditions as provided by matched filtering or correlation. In this regard, the correlator output in Figure 1.29 is examined in the context of the signal delay estimate error.

The triangular function, corresponding to the correlator output, is an isosceles triangle with base and height equal to 2τ and AN, respectively, and is described as

$$R_s(\xi) = AN(1 - |\xi|/\tau) \quad : |\xi| \le \tau \qquad (1.389)$$

where, for convenience, $\xi = t - N\tau$ such that the time axis is shifted so that the isosceles triangle is symmetrical about $\xi = 0$. The effective bandwidth of $R_s(\xi)$ is evaluated (see Problem 41) as

$$\beta = \frac{\sqrt{3}}{\tau} \quad : \text{triangular function} \qquad (1.390)$$

and the corresponding standard deviation of the delay estimate is

$$\sigma_{T_d} = \frac{\tau}{\sqrt{3}\sqrt{2\gamma_e}} \quad : \text{triangular function} \qquad (1.391)$$

Frequency Estimation Error of the DSSS Waveform   The frequency estimation error is based on the interval T of the PN sequence under the conditions corresponding to the local PN reference being exactly synchronized with and multiplied by the received signal; in other words, with zero frequency and phase errors, the integrand of the correlation integral is constant over the interval T. However, with a frequency error of f_ε Hz the correlator response is computed as

$$R_s(T; f_\varepsilon) = A \int_0^T e^{j2\pi f_\varepsilon \xi} d\xi$$

$$= ATe^{j\pi f_\varepsilon T} \frac{\sin(\pi f_\varepsilon T)}{\pi f_\varepsilon T} \quad : \text{correlator response with } f_\varepsilon$$

$$(1.392)$$

The principal frequency error in the main lobe of the *sinc* ($f_\varepsilon T$) function corresponds to $|f_\varepsilon| \le 1/T$ which defines the fundamental resolution accuracy of the frequency estimate. However, the effective duration of the correlator of length $T = N\tau$ is evaluated (see Problem 42) as

$$\alpha = \frac{2\pi T}{3} \quad : \text{rectangular function} \qquad (1.393)$$

and the corresponding standard deviation of the frequency estimate is

$$\sigma_{f_d} = \frac{\sqrt{3}}{2\pi T \sqrt{2\gamma_e}} \quad : \text{rectangular function} \qquad (1.394)$$

Considering the SS pulse compression ratio, or processing gain, $\rho = T/\tau$, the correlator output signal-to-noise ratio (γ_e) in (1.391) and (1.394) is measured in the bandwidth of $1/T$. The product of the estimation accuracies of the SS waveform is

$$\sigma_{T_d}\sigma_{f_d} = \frac{\tau}{2\pi T\gamma_e} = \frac{1}{2\pi\rho\gamma_e} \qquad (1.395)$$

Therefore, the time and frequency estimates accuracies can be made arbitrarily low, even in low signal-to-noise ratio environments, by designing a SS waveform with a sufficiently high pulse compression ratio.

1.9.3.4 Effective Bandwidth of SRRC and SRC Waveforms
In view of the increasing demands on bandwidth, the spectral containment of the spectral raised-cosine (SRC) waveform meets the corresponding need for spectrum conservation. Although the spectral root-raised-cosine (SRRC) waveform has a slightly wider bandwidth than the SRC waveform, it is preferred because of the improved matched filter detection[*] and, in the context of range delay estimation, provides for a somewhat better range delay estimate. The spectrum of the SRC waveform is characterized, in the context of a spectral windowing function, in Section 1.11.4.1 and the spectrum of the SRRC is characterized in Section 4.3.2 in the context of the optimum transmitted waveform for root-raised-cosine (RRC) waveform modulation. The following analysis compares the effective

---

[*]The optimally sampled SRRC matched filter output results in the maximum signal energy and orthogonal symbol samples resulting in zero intersymbol interference.

bandwidth of the SRC and SRRC waveforms with the understanding that the SRC delay estimate is based on the matched filter out samples taken symmetrically about the optimum matched filter sample at $t = T_o$.

The dependence of the effective bandwidth of the SRRC and SRC waveforms on the excess bandwidth parameter α is expressed as

$$\beta T = \pi \sqrt{\frac{1}{3} + \left(\frac{\pi^2 - 8}{\pi^2}\right)\alpha^2} \quad :\text{SRRC waveform} \qquad (1.396)$$

and

$$\beta T = \pi \sqrt{\frac{4 - 3\alpha + 12\alpha^2 - \alpha^3}{3(4-\alpha)} - \frac{8\alpha^2(16-\alpha)}{(2\pi)^2(4-\alpha)}} \quad :\text{SRC waveform} \qquad (1.397)$$

Equations (1.396) and (1.397) are plotted in Figure 1.30 that demonstrates the advantages of the wider bandwidth SRRC waveform in providing short rise-times symbols with the associated improvement in range-delay detection. In this regard, the $rect(t/T)$ modulated received symbol, as characterized by the BPSK-modulated waveform, has zero rise-time and results in perfect range-delay detection in a noise-free channel and receiver; however, infinite bandwidth is required to achieve this performance. The *dashed* curve in Figure 1.30 shows the normalized effective bandwidth of the $rect(t/T)$ modulated symbol after passing through an ideal $(1/B)rect$ (f/B) filter with one-sided bandwidth $B/2$ Hz; this is referred to a *filtered* BPSK and is discussed in the following section.
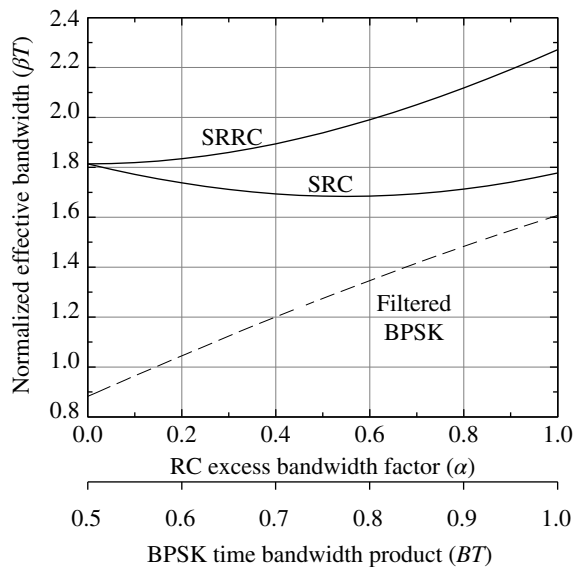
The noise bandwidth of the SRRC frequency function is significant, in that, it corresponds to the demodulator-matched filter response used in the detection of the SRRC-modulated waveform. On the other hand, the interest in the noise bandwidth of the SRC is more academic in nature because of its application as a windowing function. In either event, the noise bandwidth of the SRRC and SRC frequency functions is examined in Problem 44.

1.9.3.5 Effective Bandwidth of the Ideally Filtered rect (t/T) Waveform   In this case the effective bandwidth of the ideal symbol modulation, characterized by $rect(t/T)$, is evaluated after passing through an ideal filter with frequency response $(1/B)rect(f/B)$ where $B/2$ is the one-sided or low-pass bandwidth of the filter. The filter response is examined in Section 1.3 and the normalized effective bandwidth of the filtered symbol is characterized by Skolnik [71] as

$$\beta T = \sqrt{\frac{\pi BT - \sin(\pi BT)}{Si(\pi BT) + (\cos(\pi BT) - 1)/\pi BT}} \qquad (1.398)$$
$$:\text{ideally filtered } rect(t/T) \text{ waveform}$$

This result is plotted in Figure 1.31 as a function of BT where T is the symbol duration. From this plot it is evident that as BT approaches infinity the standard deviation of the range-delay estimate approaches zero resulting in an exact estimate of the true range delay. A practical application is to define a finite bandwidth which is sufficiently wide so as not to degrade the symbol detection through intersymbol interference.

Defining the excess bandwidth factor for the ideal filter as $\alpha' = B/R_s = BT$, where $R_s = 1/T$ is the $rect(t/T)$ symbol rate, in
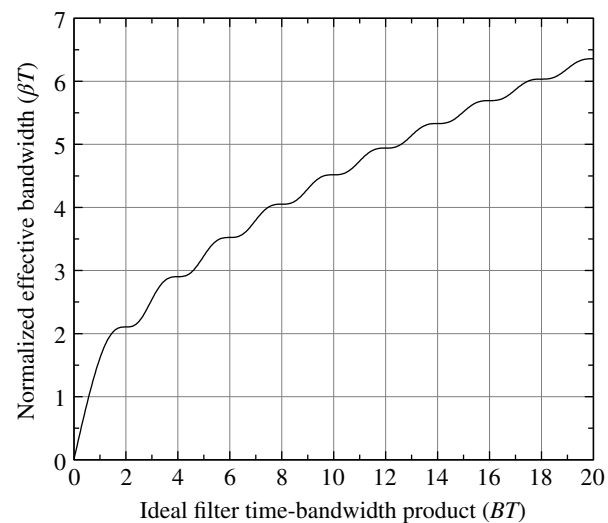

FIGURE 1.30   Normalized effective bandwidths for SRRC and SRC waveforms.

FIGURE 1.31   Normalized effective bandwidth for filtered $rect(t/T)$ waveform.

terms of the excess bandwidth factor α of the raised-cosine (RC) waveform, $\alpha' = (1+\alpha)/2$. The corresponding range of BT is $1/2 \le BT \le 1$; this range of the filtered $rect(t/T)$ effective bandwidth from Figure 1.31 is plotted as the *dashed* curve in Figure 1.30. The range of BT results in significant intersymbol interference and received symbol energy loss even under the ideal conditions of symbol time and frequency correction. However, under the same conditions, if the SRRC waveform and matched filter responses are sufficiently long, the intersymbol interference and symbol energy loss will be negligible. At the maximum SRRC normalized effective bandwidth of $\beta T = 2.27$, the filter time bandwidth product corresponds to $BT = 2.64$ or a 32% increase with the filter bandwidth spanning the main signal spectral lobe and 16% of the adjacent sidelobes. In other words, the one-sided filter bandwidth spans 1.32 lobes and, referring to Appendix A, this results in a performance loss of about 1.25 dB for BPSK waveform modulation; for a loss of less than 0.3 dB the BT product should be greater than 5 with a resulting effective bandwidth of $\beta T = 3.23$ corresponding to a $(3.23/2.27 - 1)100 = 42\%$ improvement relative to the best SRRC range-delay estimation error; however, the required bandwidth is 150% wider. The bandwidth and range-delay estimation accuracy are design trade-off in the waveform selection.

1.10 MODEM CONFIGURATIONS AND AUTOMATIC REPEAT REQUEST

The three basic modulator and demodulator configurations are simplex, half-duplex, and full-duplex. The definition of simplex communications involves communication in one direction between a modulator/transmitter and a remote receiver/demodulator. Examples of simplex communications include broadcasting from radio and television stations or from various types of monitoring devices. Half-duplex communications is a broader definition including two-way communications but only in one direction at a time. In these cases, transceivers and modems are required at each location. A common application of half-duplex operation is the *push-to-talk* handheld radios. Full-duplex communications provide the capability to communicate in both directions simultaneously. In these cases the bidirectional communications may use identical transceivers and modems operating at the same symbol rate; however, as is often the case, the communication link in one direction may be designated as the reverse channel and operated at a lower symbol rate. In either event, the forward and reverse channels must operate at different, noninterfering, frequencies.

The transfer of data is often performed using information frames or packets, each containing a cyclic redundancy check (CRC) code for error checking. If an error is detected the receiving terminal requests that the frame be retransmitted, otherwise an acknowledgment may be returned indicating that the frame was received without error. These protocols are referred to as automatic repeat request [72] (ARQ). The ARQ protocol requires either a half-duplex or full-duplex communication capability. The two commonly used variations of the ARQ protocol are generally referred to as idle-repeat request (RQ) and continuous-RQ.[*] However, more complex variations involving point-to-point and multipoint protocols are also defined.[†]

The remainder of this section analyzes the idle-RQ protocol which is the simplest ARQ system to implement and evaluate, in that, when a data frame is transmitted a timer is initiated and a new frame is transmitted only after acknowledgment (ACK) that the current frame was received without errors and/or the timer has not exceeded a maximum timeout T_{max}. However, the current frame is retransmitted if the timer exceeds T_{max}, a negative acknowledgment (NAK) is received, indicating the receipt of an incorrect frame, or the ACK or NAK code is received in error. The timer limit is based on the information bits per frame, the bits in the ACK and NAK codes, the date rates, and the expected two-way link propagation delay through the media. The idle-RQ implementation also has the advantage of requiring less data storage compared to the continuous-RQ protocol and the Go-back-N protocol [73]. However, the performance cost of these advantages is that the end-to-end transmission efficiency is lower and more sensitive to the link propagation delay. The end-to-end transmission efficiency is defined as

$$\eta_{trans} \triangleq \frac{\bar{R}_{bf}}{R_{bf}} \qquad (1.399)$$

where $\bar{R}_{bf}$ is the average bit rate over the forward channel and R_{bf} is the uninterrupted forward channel bit rate.

The idle-RQ is modeled as shown in Figure 1.32 with the delays and other parameters defined in Table 1.12.

Using the parameters described earlier, the average time associated with the transmission and acknowledgment is described as

$$\bar{T} = \bar{N}\left(\left(T_{df} + T_{sf}\right) + 2T_p + T_{cs} + \left(T_{dr} + T_{sr}\right) + T_{cp} \right) \qquad (1.400)$$

where $\bar{N}$ is the average number of frame repetition based on the specified bit-error probability and the number of frame information and CRC bits N_B. The computation of $\bar{N}$ is based on *iid* additive white Gaussian channel noise over all of the N_B bits. This provides for the probability of a correct message to be expressed in terms of the discrete binomial distribution[‡] given the bit-error probability P_{bef}; the result is expressed as

---

[*]Reference 72, Chapter 4, Protocol Basics.
[†]Reference 72, Chapter 5, Data Link Control Protocols.
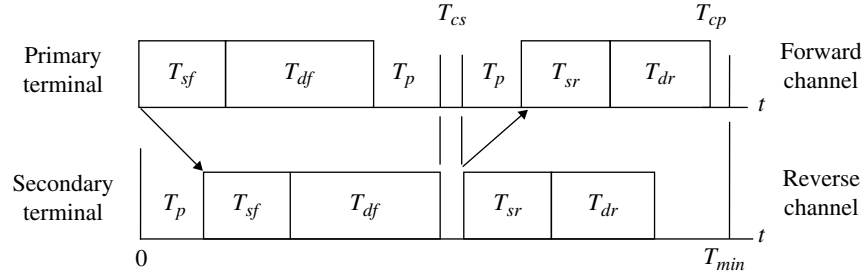[‡]See Table 1.42.

FIGURE 1.32 Model of idle-RQ implementation.

TABLE 1.12 Idle-ARQ Parameter Definitions

Delay	Value	Description
T_{df}	$(N_b + N_{crc})/R_{bf}$	Forward message duration
T_{sf}	N_{sf}/R_{bf}	Forward synchronization duration
T_p	$range/c$	Propagation delay between terminals
T_{dr}	$(N_{br}+N_{chk})/R_{br}$	Reverse message duration
T_{sr}	N_{sr}/R_{br}	Reverse synchronization duration
T_{cs}	0	Secondary terminal computational delay (ms)[a]
T_{cp}	0	Primary terminal computational delay (ms)[a]
T_{max}	$>T_{min}$	Idle-RQ maximum idle time (ms)
N_B	Variable	Message bits: (N_b = info) + (N_{crc} = CRC)
N_{sf}	30	Forward synchronization bits
R_{bf}	100	Forward bit rate (kbps)
$range$	Parameter	One-way: 18.5, 200, 600, 35,800 (km)
c	3×10^8	Free-space velocity (m/s)
N_{brt}	30	ARQ bits:(N_{br}=ACK) + (N_{chk} = parity)
N_{sr}	10	Reverse synchronization bits
R_{br}	$= R_{bf}$	Reverse bit rate (kbps)
P_{bef}	Parameter	Forward channel bit-error probability: 10^{-4}, 10^{-5}
P_{ber}	$= P_{bef}$	Reverse channel bit-error probability

[a]The CRC and parity check codes provide instantaneous error decisions.

$$P_{cm} = \left(1 - P_{bef}\right)^{N_B} \qquad (1.401)$$

Therefore, using (1.401), the average number of transmissions required to obtain an error-free frame with N_B bits is evaluated as

$$\bar{N} = P_{cm}^{-1} = \left(1 - P_{bef}\right)^{-N_B} \qquad (1.402)$$

The idle-RQ transmission efficiency, as defined in (1.399), is expressed as

$$\eta_{trans} = \frac{T_{df} + T_{sf}}{\bar{\bar{T}}} \qquad (1.403)$$
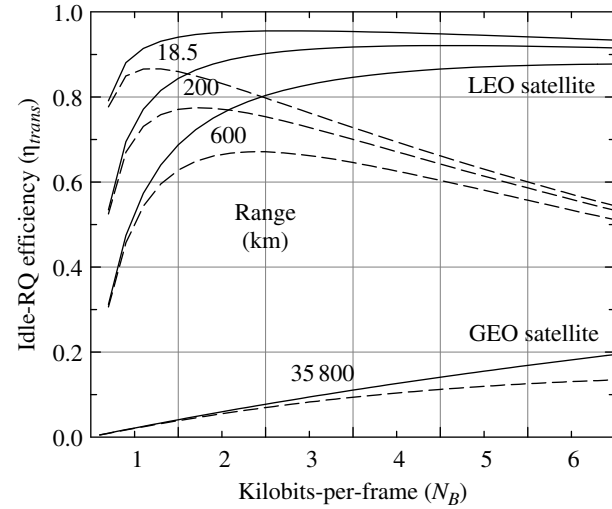
FIGURE 1.33 Idle-RQ efficiency as function of bits/frame (R_{bf} = 100 kbps, $P_{bef} = 10^{-5}$ *solid*, 10^{-4} *dashed* curve).

The number of forward channel bits per frame is defined as[*]

$$N_B \triangleq \left(T_{df} + T_{sf}\right)R_{bf} \qquad (1.404)$$

With this definition, the transmission efficiency is expressed explicitly in terms of N_B, by substituting (1.400) and (1.402) into (1.403) and, after some simplifications, the efficiency is expressed as

$$\eta_{trans} = \frac{N_B\left(1 - P_{bef}\right)^{N_B}}{N_B + K_B} \qquad (1.405)$$

where K_B is defined as

$$K_B \triangleq \left(2Tp + Tcr + \left(Tdr + Tsc\right) + Tcf\right)R_{bf} \qquad (1.406)$$

The idle-RQ efficiency expressed in (1.405) is plotted in Figure 1.33 for several one-way communication link ranges;

[*]Inclusion of the synchronization bits $N_{sf} = T_{sf} R_{bf}$ in the definition of N_B is optional.

TABLE 1.13   Optimum $N_B{}^a$ Corresponding to the Maximum Efficiency Conditions in Figure 1.33

	Range (km)			
P_{bef}	18.5	200	600	35,800
1e−3	204	338	478	960
1e−4	697	1,232	1,889	7,589
1e−5	2,261	4,077	6,416	38,380
1e−6	7,208	13,079	20,757	143,125
1e−7	22,850	41,546	66,112	477,137

$^a N_B$ in bits.

the *solid* curves correspond to $P_{bef} = 10^{-5}$ and the *dashed* curves correspond to $P_{bef} = 10^{-4}$. The impact of the link propagation delay (T_p) is significant and results in long idle times for the ACK/NAK response. The performance is also dependent on the link bit-error probabilities, the bit rate, and the number of bits per frame.

The optimum number of forward channel bits per frame, N_B, corresponding to the maximum efficiency, $\eta_{trans}(\text{max})$, is evaluated by differentiating (1.405) with respect to N_B and setting the result equal to zero and then solving for $N_B(opt)$. Following this procedure, the optimum N_B, corresponding to the maximum efficiency, is evaluated as the solution to the quadratic equation

$$N_B^2 + N_B K_B - K_B/\lambda = 0 \qquad (1.407)$$

where $\lambda = \ln(1/(1-P_{be}))$. The solution to (1.407) is

$$N_B(opt) = -\frac{K_B}{2} + \sqrt{\left(\frac{K_B}{2}\right)^2 + \frac{K_B}{\lambda}} \qquad (1.408)$$

Using the example parameters, $N_B(opt)$ is listed in Table 1.13 for the conditions shown in Figure 1.33.

Optimizing the message frame size using $N_B(opt)$ has limited practical appeal because the resulting maximum efficiency may be unacceptable or because of the broad range of N_B over which the slope around $\eta_{trans}(\text{max})$ is virtually unchanged; this latter point is seen in Figure 1.33 corresponding to $P_{bef} = 10^{-5}$. Selecting N_B from a range that satisfies an acceptable minimum transmission efficiency is a preferable criterion and operating at low bit-error probabilities offers a wider range of selections.

1.11   WINDOWS

Windows have been characterized and documented by a number of researchers [74, 75], and this section focuses on the windows that are used in the simulation codes in the following chapters to enhance various performance objectives. Windows are applied in radar and communication systems to achieve a variety of objectives including antenna sidelobe reduction, improvements in range resolution and target discrimination, spectral control for adjacent channel interference (ACI) reduction [76], ISI control, design of linear phase filters, and improvements in parameter estimation algorithms. Windows can be applied as time or frequency functions to achieve complementary results depending on the application.

Windows are described in terms of the discrete-time samples[*] $w(n)$ where n is indexed over the finite window length of N samples. When the window is applied as a discrete-frequency sampled window the notation $W(n)$ is used. The discrete-time sampled rectangular window, defined, for example, as $w(n) = 1$ for $|n| \le N/2$ and zero otherwise, is typically used as the reference window by which the performance measures of other windows are compared. The spectrum of the time-domain rectangular window is described in terms of the *sinc(x)* function as $S(f) = sinc(nf/N)$. The rectangular window is also referred to as a uniformly weighted or simply as an unweighted window.

Several window parameters [75] that are useful in selecting a window for a particular application are the gain, the noise bandwidth, and the scalloping loss. The window voltage gain is defined as

$$G_v \triangleq \sum_n w(n) \qquad (1.409)$$

The noise bandwidth of the window follows directly from the definition of the noise bandwidth defined by Equation (1.46). In terms of the discrete-time sampling and application of Parseval's theorem, the normalized noise bandwidth is expressed as

$$B_n' = \frac{\sum_n w^2(n)}{\left(\sum_n w(n)\right)^2} \qquad (1.410)$$

In terms of Hertz, the bandwidth is given by

$$B_n(\text{Hz}) = \frac{B_n'}{T_w} \qquad (1.411)$$

where $1/T_w$ Hz is the fundamental frequency resolution of the window with duration T_w seconds. The theoretical normalized noise bandwidth of the rectangular window is $B_n' = 1$, so the noise bandwidth is $B_n = 1/T_w$ Hz. Harris [75] defines the scalloping loss (SL) of a time-domain window, as the frequency domain loss, relative to the maximum level, mid-way between two maximum adjacent DFT outputs. The scalloping loss is expressed as

[*]The notation $w(n)$ is a time-normalized sample corresponding to $w(nT_s)$ where T_s is the sampling interval. Similarly, the frequency-domain samples $W(n)$ are normalized by $f_s/N = 1/NT_s$.

TABLE 1.14   Summary of Window Performance Results

Window	Max. Sidelobe (dB)	At $\pm fT_w$	Scalloping Loss (dB) with T_w Zero-Padding			
			0	1	2	3
Rectangular	−13.26	1.5	3.92	0.91	0.4	0.18
Bartlett	−26.4	3.0	1.81	0.44	0.20	0.09
Blackman	−58.2	3.6	1.09	0.27	0.12	0.05
Blackman–Harris	−92.0	4.52	0.82	0.20	0.09	0.04
Hamming	−42.6	4.5	1.74	0.43	0.19	0.09
Cosine $k = 1$	−23.0	1.89	2.08	0.51	0.22	0.10
$k = 2$	−31.5	2.4	1.41	0.35	0.15	0.07
$k = 3$	−39.3	2.83	1.06	0.26	0.12	0.05
$k = 4$	−46.7	3.33	0.85	0.21	0.09	0.04

Using $N = 200$ samples/window.

$$SL \triangleq \frac{|W(\pi/N)|}{W(0)} = \frac{\left|\sum_n w(n)e^{-j\pi n/N}\right|}{\sum_n w(n)} \tag{1.412}$$

The characteristics of the various windows considered in the following sections are summarized in Tables 1.14 and 1.15. The maximum sidelobes correspond to those adjacent to the central, or main, lobe, and apply to the time (or frequency) domains depending on whether the window is applied, respectively, in the frequency (or time) domains. The scalloping loss results from the frequency or time domain ripple resulting from contiguous repetitions of the window functions. Harris has compiled an extensive table of windows and their performance characteristics.

The duration of the window and the manner in which it is sampled is dependent upon the application. In the following descriptions, the sampling is applied to windows that are symmetrical and asymmetrical about $t = 0$ as described by (1.413) using the $rect(x)$ window. The $rect(x)$ window is a uniformly weighted window[*] that is used to describe the window delay[†] and duration T_w for all arbitrarily weighted windows.

$$w(t) = \begin{cases} rect\left(\dfrac{t - T_d}{T_w} - m - \dfrac{1}{2}\right) & : \text{asymmetrcial about } t = 0 \\[4mm] rect\left(\dfrac{t - T_d}{T_w} - m\right) & : \text{symmetrical about } t = 0 \end{cases} \tag{1.413}$$

The parameter T_d introduces a delay and m is an integer corresponding to a contiguous sequence of windows; in the following analysis T_d and m are zero. Considering N to be an integer number of samples over the window duration with the sampling interval of $T_s = T_w/N$ seconds, the windows are characterized, with a maximum value of unity, in terms of the sample index n. In the following examples, the Bartlett or triangular window[‡] is used and the respective odd and even values of N are 9 and 8. For odd integers N, the asymmetrical triangle window is expressed as

$$w(n)|_{N \in odd} = 1 - \frac{|n - (N-1)/2|}{(N-1)/2} : 0 \leq n \leq N-1, \text{ asymmetrical} \tag{1.414}$$

and the symmetrical triangle window is expressed as

$$w(n)|_{N \in odd} = 1 - \frac{|n|}{(N-1)/2} \quad : |n| \leq (N-1)/2, \text{ symmetrical} \tag{1.415}$$

For the even integers, the asymmetrical triangle window is expressed as

$$w(n)\Big|_{\substack{N \in even \\ n = n' + .5}} = \begin{cases} \dfrac{2n'+1}{N} & : 0 \leq n' < N/2 \\[3mm] 2 - \dfrac{2n'+1}{N} & : N/2 \leq n' \leq N-1 \end{cases}, \text{ asymmetrical} \tag{1.416}$$

and the symmetrical triangle window is expressed as

$$w(n)\Big|_{\substack{N \in even \\ n = n' + .5}} = \begin{cases} 1 + \dfrac{1 - 2|n'|}{N} & : -N/2 \leq n' < 0 \\[3mm] 1 - \dfrac{1 + 2|n'|}{N} & : 0 \leq n' \leq N/2 - 1 \end{cases}, \text{ symmetrical} \tag{1.417}$$

Equations (1.414) through (1.417) are plotted in Figure 1.34 with the *circles* indicating the window sampling instances. The distinction between the symmetrical and asymmetrical sampling is evident and must be applied commensurately to the sampled data. In this regard, the windows can be applied, for example, to the transmitted data-modulated symbols for spectrum control, to the received data symbol for detection, or to the FFT window for spectrum evaluation. With minimum shift keying (MSK) modulation, discussed in Section 4.2.3.4, a cosine window is applied to each quadrature rail that are delayed, or offset, by one-half symbol period, so the notion of symmetrical and asymmetrical windows applies.[§] The examples using an odd number of window samples, shown in Figure 1.34a and b, include the first and last window samples that are zero and increase

---

[*]Since the weighting is constant over T_w, the uniformly weighed window is also referred to as an unweighted window.
[†]The application of a window to a sequence of received symbols prior to spectral analysis requires the window to be appropriately delayed.

[‡]The triangular window is used to emphasize the sampling with respect to a nonuniformly weighted window.
[§]Windows applied to transmitter symbols for spectral control are generally referred to as symbol shaping functions and denoted as $p(t)$.

TABLE 1.15   Summary of Window Performance Results

Samples (N)	Bartlett		Blackman		Blackman–Harris		Hamming	
	B'_n	G_v	B'_n	G_v	B'_n	G_v	B'_n	G_v
1000	1.3357	0.4995	1.728	0.4196	2.006	0.3584	1.364	0.5395
500	1.335	0.499	1.730	0.419	2.008	0.358	1.365	0.539
200	1.340	0.498	1.735	0.418	2.014	0.357	1.368	0.538
100	1.347	0.495	1.744	0.416	2.025	0.355	1.373	0.535
50	1.361	0.490	1.762	0.412	2.045	0.352	1.383	0.531
25	1.394	0.480	1.799	0.403	2.088	0.344	1.403	0.522
12	1.467	0.455	1.884	0.385	2.186	0.329	1.450	0.502
	Cosine $k = 1$		Cosine $k = 2$		Cosine $k = 3$		Cosine $k = 4$	
1000	1.235	0.636	1.502	0.4995	1.737	0.424	1.946	0.3746
500	1.236	0.635	1.503	0.499	1.738	0.4236	1.948	0.3742
200	1.240	0.633	1.507	0.498	1.744	0.422	1.954	0.373
100	1.246	0.630	1.515	0.495	1.752	0.420	1.964	0.371
50	1.260	0.624	1.531	0.490	1.770	0.416	1.984	0.368
25	1.290	0.610	1.562	0.480	1.807	0.407	2.026	0.360
12	1.364	0.580	1.636	0.458	1.892	0.389	2.121	0.344

Noise bandwidth and voltage gain.

(a) $N_{odd} = 9$: symmetrical

(b) $N_{odd} = 9$: asymmetrical

(c) $N_{even} = 8$: symmetrical
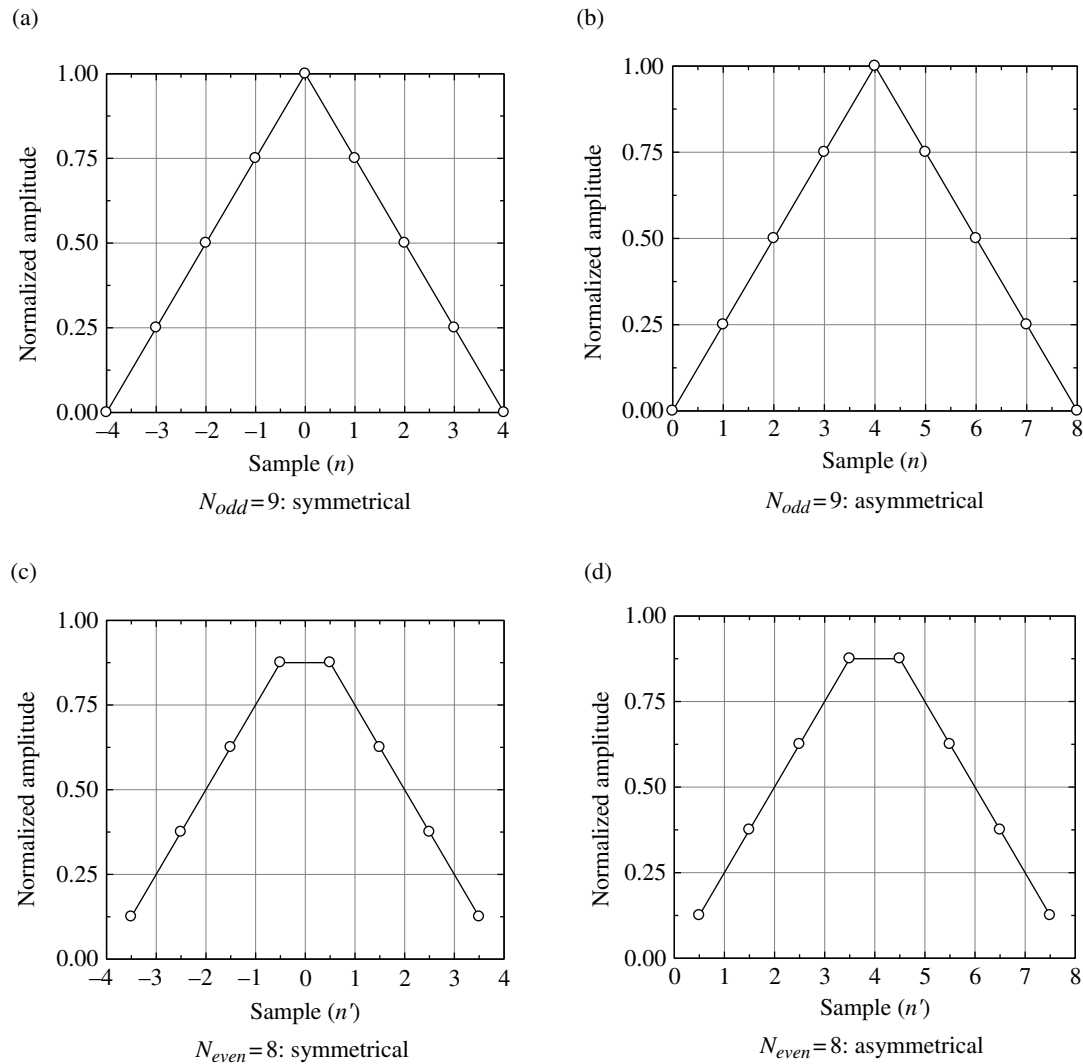
(d) $N_{even} = 8$: asymmetrical

FIGURE 1.34   Examples of triangular window sampling.

symmetrically to the peak value. Although these cases are visually appealing, the sampled windows in Figure 1.34c and d use an even number of samples per window and result in same performance commensurate with the Nyquist sampling rate. Furthermore, using an even number of samples is suitable for analysis using the efficient FFT.

The case for using an even number of samples can be made based on the down-sampled output of a high sample rate analog-to-digital converter. For example, relative to a received data-modulated symbol, the down-sampled, or rate-reduced, output is the average symbol amplitude of the down-sampled interval from nT_s to $(n + 1)T_s$, so the window weighting should be applied to the point midway between the two samples as is often done using rectangular integration. This is accommodated by the even number of samples over the window interval shown in Figure 1.34c and d, with the understanding that the data sample at $n = n' + 0.5$ results from the linear interpolation of the data between sample n' and $n' + 1$. In addition to applying the correctly aligned window with interpolated data samples, this sampling arrangement also removes the delay estimation bias thereby improving the symbol tracking performance. Of course, the roles of the odd and even sampling can be reversed; however, it is convenient to use an even number of samples per symbol into the detection-matched filter for symbol tracking and the detection of quadrature symbol offset modulations. However, as long the Nyquist sampling criterion is satisfied the symbol information can be extracted in either case. In the following sections, the spectrums of the various windows are evaluated using both symmetrically and asymmetrically sampled windows with an odd number of samples. The reason for this choice is simply based on esthetics or eye appeal which is particularly noticeable when only a few number of samples is used.

1.11.1 Rectangular Window

In the time domain, the rectangular window is a uniformly weighted function described by the $rect(t/T_w)$ function with amplitude equal to unity over the range $|t/T_w| \leq 1/2$ and zero otherwise. Expressing the time in terms of the discrete samples $t = nT_s$, where T_s is the sampling interval, results in the sample range $|n| \leq (N - 1)/2$ for the symmetrical window and $0 \leq n \leq N - 1$ for the asymmetrical window, where $N = T_w/T_s$ is the total number of samples per window.

The spectrum of the rectangular window is described in terms of the $sinc(fT_w)$ function and, upon letting $f = n\delta f$ and $\delta f = \Delta f/L$, where $\Delta f = 1/T_w$ is the fundamental frequency resolution of the window, the spectrum is expressed as

$$W(n) = \frac{\sin(\pi n/L)}{\pi n/L} = sinc\left(\frac{n}{L}\right) \qquad (1.418)$$

Defining the frequency increment in this way allows for L samples per spectral sidelobe. The Fourier transforms relationship between the time and frequency domains is discussed in Section 1.2. Special applications involving the *rect* (x) window in the time and frequency domains are discussed in Sections 1.11.4, 4.4.1, 4.4.4, and 4.4.5.

1.11.2 Bartlett (Triangular) Window

The sampling of the Bartlett or triangular window is discussed earlier under a variety of conditions that depend largely on the application and signal processing capabilities. The Bartlett window is shown in Figure 1.35 for $N = 21$ samples per symbol. Considering the frequency dependence of the spectral attenuation, expressed as $sinc^2(fT_w/2)$, the spectral folding about the Nyquist band $f_N = f_s/2 = N/2T_w$ is negligible for $N = 201$ and the peak spectral sidelobes are virtually identical to the theoretical Bartlett spectrum over the range of frequencies shown in Figure 1.36b, although the sidelobe level at $fT_w = 29$ is −65.8 dB and the theoretical value is −66.5 dB. Furthermore, upon close examination, the peak values of the sidelobe are progressively shifted to the right with increasing fT_w. These observations are more evident for the case involving $N = 21$ where the first sidelobe level is −26.8 dB (1 dB higher that theory) and the sidelobe at $fT_w = 9$ is significantly skewed to the right with a level 6 dB higher than the theoretical value. The sidelobe skewing is a direct result of the odd symmetry of the folded spectrum about $2kfT_w : k = 1, 2, …$ which does not occur when N is even. However, with even values of N, the sidelobes are still altered by the folded spectral sidelobes. This phenomenon is a direct result of the sampling and the implicit periodicity of the window when using the discrete Fourier transform. These observations do not alter the utility of windows for spectral control; however, they may influence the spectral detail in applications involving spectral analysis.
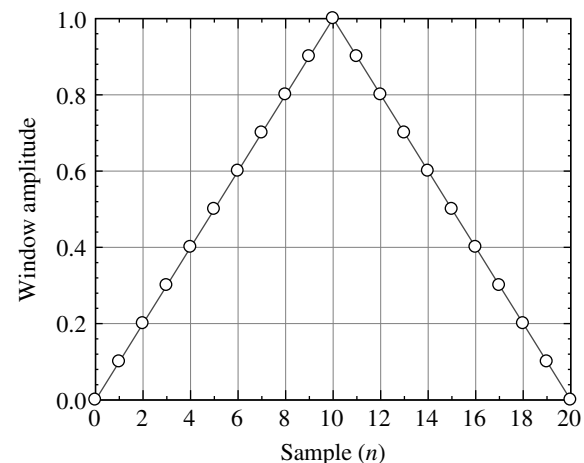

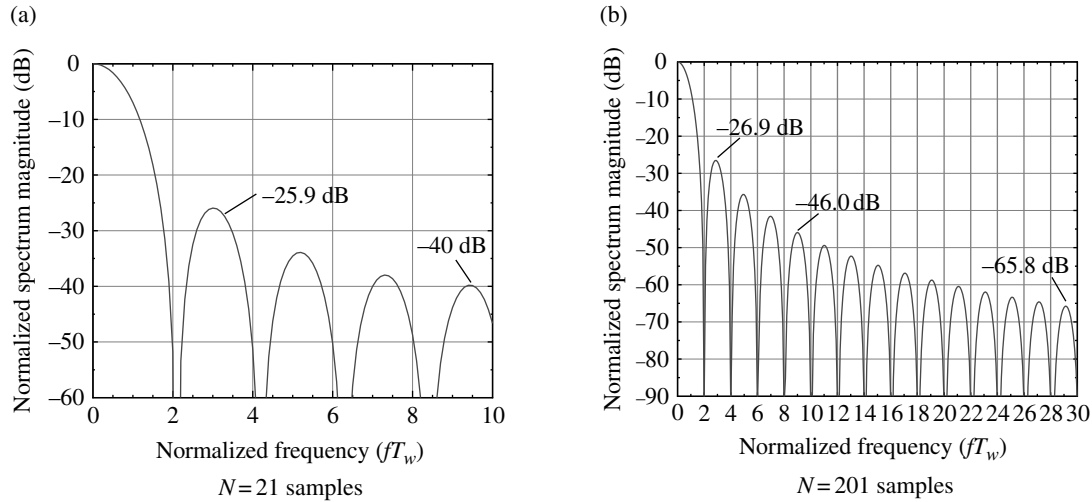**FIGURE 1.35** Bartlett window with $N = 21$ samples.

(a)   (b)

FIGURE 1.36   Bartlett (triangular) window spectrums.

1.11.3   Cosine Window

The sidelobes of the window spectrum can be reduced by providing additional shaping or tapering of the window function at the expense of a wider main spectral lobe that results in a higher noise bandwidth. For example, the rectangular window has an abrupt change in amplitude leading to a first sidelobe level of -13 dB, a spectral roll-off proportional to $1/f^2$ (6-dB/octave), and a noise bandwidth of $1/T_w$ Hz. On the other hand, the Bartlett window has an abrupt change in the slope of the amplitude leading to a first sidelobe level of -26.9 dB, a spectral roll-off of $1/f^4$ (12-dB/octave), and a noise bandwidth of $1.336/T_w$. The cosine window results in the k-th derivative of the amplitude, that is, the slope of the amplitude at the edges of the window is zero resulting in even greater spectral sidelobe roll-off.

The cosine window is characterized as

$$w(n) = \cos^k(\phi_n + \delta_1) \tag{1.419}$$

where $\delta_1 = 0$ when $|n| \le \lfloor (N-1)/2 \rfloor$ and $\delta_1 = -\pi/2$ when $n = 0, \ldots, N-1$; this corresponds to a $\sin^k(\phi_n)$ window function. The phase function in (1.419) is expressed as

$$\phi_n = \frac{\pi}{N-1}(n + \delta_0) \quad : |n| \le \lfloor (N-1)/2 \rfloor \tag{1.420}$$

where $\delta_0 = 0$ when $n \in$ odd and $\delta_0 = 0.5$ when $n \in$ even. The cosine window is shown in Figure 1.37 for $n > 0$ and $k = 1, \ldots, 4$. In the following subsections, the cosine windows for various values of k are described for the conditions $\delta_0 = \delta_1 = 0$.

The gain for the finite sampled cosine window with $k = 1$ and N samples per window is given by

$$G_v = \frac{2}{\pi}\left(\frac{N-1}{N}\right) \tag{1.421}$$
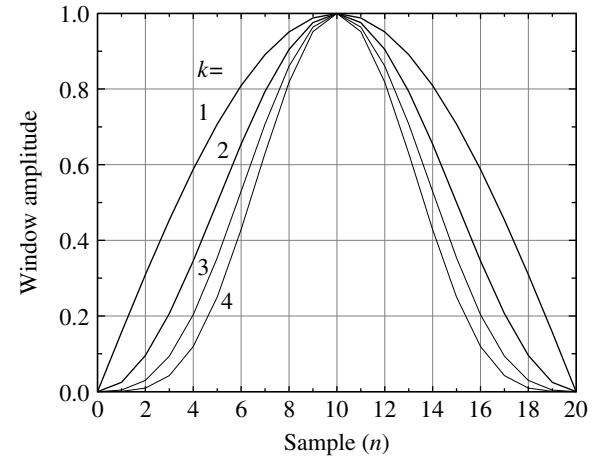
FIGURE 1.37   Cosine windows ($\delta_0 = 0$, $\delta_1 = -\pi/2$).

and the normalized noise bandwidth is given by

$$B'_n = \frac{\pi^2}{8}\left(\frac{N}{N-1}\right) \tag{1.422}$$

G_v and B'_n are recorded in Table 1.15 for various values of N. Equations (1.421) and (1.422) approach their theoretical limits as $N \to \infty$.

1.11.3.1   Cosine Window (k = 1)   With $k = 1$ the cosine window is expressed as

$$w(n) = \cos(\phi_n) \tag{1.423}$$

This window is used as the symbol weighting function for MSK modulation and, in terms of the window duration T_w, the theoretical spectrum is given by

$$W(f) = \left(\frac{4T_w}{\pi}\right)\frac{\cos(\pi f T_w)}{1-(2fT_w)^2} \qquad (1.424)$$

The spectrum shown in Figure 1.38a is based on computer simulation with $N = 200$ samples per window.

1.11.3.2 Cosine-Squared (Hanning) Window (k = 2)   The cosine-squared window with $k = 2$ is referred to as a Hanning window [74]. Applying trigonometric identities, this window is expressed as

$$w(n) = 0.5 + 0.5\cos(2\phi_n) \qquad (1.425)$$

and the spectrum is shown in Figure 1.38b for $N = 200$ samples per window.

1.11.3.3 Cosine Window (k = 3 and 4)   Applying trigonometric identities, the cosine windows for $k = 3$ and 4 are expressed as

$$w(n) = 0.75\cos(\varphi_n) + 0.25\cos(3\varphi_n) \quad :k=3 \qquad (1.426)$$

and

$$w(n) = 0.375 + 0.5\cos(2\phi_n) + 0.125\cos(4\phi_n) \quad :k=4 \qquad (1.427)$$

The spectrums for these two cases are shown in Figure 1.38c.

1.11.4 Temporal Raised-Cosine (TRC) Window

The temporal raised-cosine (TRC) window applies a cosine shaping function symmetrically about each end of the
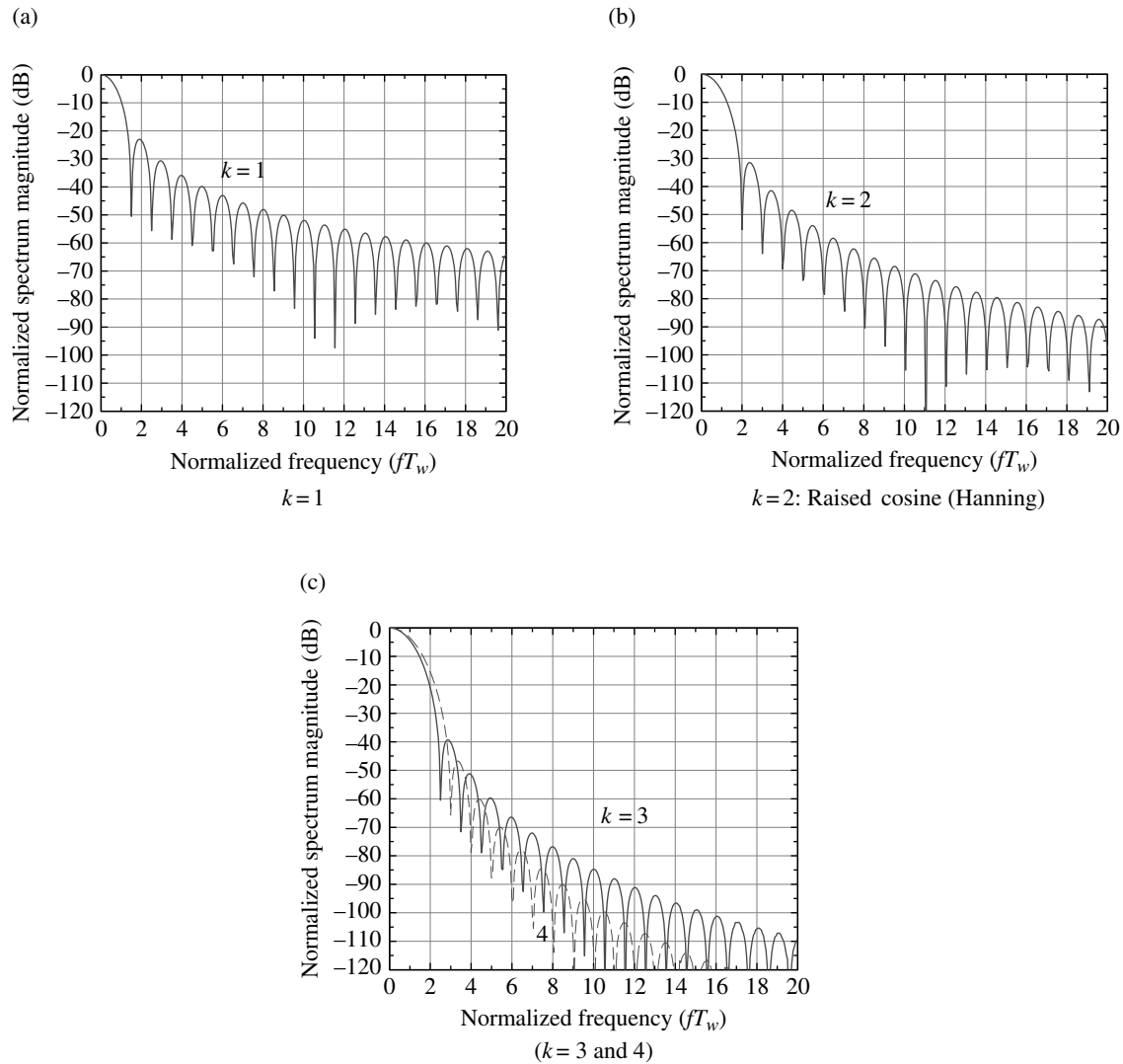
(a)

(b)

$k = 1$

$k = 2$: Raised cosine (Hanning)

(c)

$(k = 3$ and 4$)$

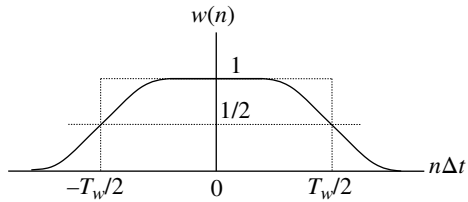**FIGURE 1.38**   Cosine window spectrums.

FIGURE 1.39   Temporal raised-cosine window.

rectangular window function, $rect(n\Delta t/T_w)$, as shown in Figure 1.39. In this case, the integer n corresponds to the samples N over the interval T_w such that $N = T_w/\Delta t$.

The TRC window is expressed as

$$w(n') = \begin{cases} 1 & : |n'| < \dfrac{1-\alpha}{2} \\ \dfrac{1}{2}\left\{1 - \sin\left(\dfrac{\pi}{\alpha}\left(|n'| - \dfrac{1}{2}\right)\right)\right\} & : \dfrac{1-\alpha}{2} \le |n'| \le \dfrac{1+\alpha}{2} \end{cases}$$

(1.428)

where $n' = t/T_w = n\Delta t/T_w$ is the normalized sample index and α is a design parameter limited to $0 \le \alpha \le 1$. The TRC window is applied to the phase function of PSK-modulated waveforms in Sections 4.2.8 and 4.4.3.9 to improve the waveform spectral containment while maintaining a constant signal amplitude; in this application α is referred to as the excess phase factor.

Letting $m = f/T_w$, the spectrum of the TRC amplitude window is evaluated as

$$W(m) = \frac{\sin(\pi m)}{\pi m}\left[\frac{\cos(\alpha \pi m)}{1 - (2\alpha m)^2}\right]$$

(1.429)

1.11.4.1 Spectral Raised-Cosine Window   The raised-cosine window when applied in the frequency domain is referred to as the spectral RC (SRC) window and the parameter α is referred to as the excess bandwidth. With $m = fT_w$, the SRC frequency response is expressed as

$$W(m) = \begin{cases} T_w & : |m| < \dfrac{1-\alpha}{2} \\ \dfrac{T_w}{2}\left\{1 - \sin\left(\dfrac{\pi}{\alpha}\left(|m| - \dfrac{1}{2}\right)\right)\right\} & : \dfrac{1-\alpha}{2} \le |m| \le \dfrac{1+\alpha}{2} \end{cases}$$

(1.430)

and upon letting $n = t/T_w$, the SRC impulse response is evaluated as

$$w(n) = \frac{\sin(\pi n)}{\pi n}\left[\frac{\cos(\alpha \pi n)}{1 - (2\alpha n)^2}\right]$$

(1.431)
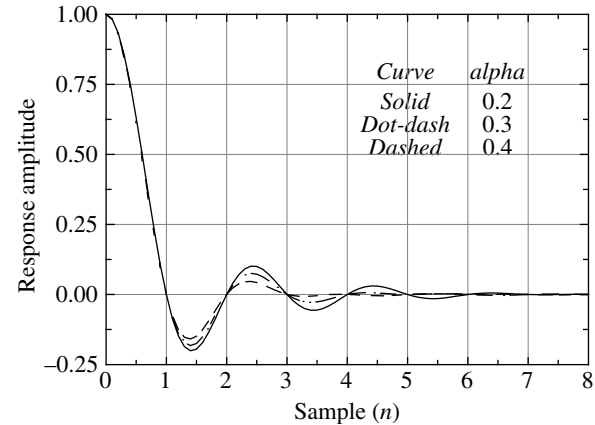
FIGURE 1.40   Impulse response of SRC window.

This response has indeterminate solutions of the form 0/0 at $n = 0$ and $1/(2\alpha)$ that are evaluated as $w(0) = 1$ and

$$w\left(\frac{1}{2\alpha}\right) = \frac{\alpha}{2}\sin\left(\frac{\pi}{2\alpha}\right)$$

(1.432)

Using these results, (1.431) is plotted in Figure 1.40 for several values of the excess bandwidth factor. The SRRC window, associated with spectral shaping of a modulated symbol, is discussed in detail in Section 4.3.2. In this application the symbol duration is $T = T_w$ and the transmitted symbol and demodulator-matched filter spectrums have a square-root RC, or simply root RC, frequency response of $\sqrt{W(n)}$. The matched filter output results in the SRC impulse response shown in Figure 1.40 with symbol spacing corresponding to integer values of n that results in zero ISI $\forall n \ne 0$. With an AWGN channel and optimum matched filter sampling the demodulator performance corresponds to maximum-likelihood detection.

1.11.5 Blackman Window

The Blackman window uses three terms to provide more tapering of the window at the expense of a narrower time response and a wider noise bandwidth. The Blackman window is expressed as

$$w(n) = 0.42 - 0.5\cos(\phi_n) + 0.08\cos(2\phi_n)$$

(1.433)

where the phase function in (1.433) is expressed as

$$\phi_n = \frac{2\pi}{N-1}n \qquad : 0 \le n \le N-1$$
$$= \frac{2\pi}{N-1}(n + \lfloor N/2 \rfloor) \qquad : -\lfloor N/2 \rfloor \le n \le \lfloor N/2 \rfloor$$

(1.434)

(a)

Window (N = 21)

(b)

Spectrum (N = 200)

FIGURE 1.41   Blackman window and spectrum.

TABLE 1.16   Blackman–Harris Window Coefficients[a]

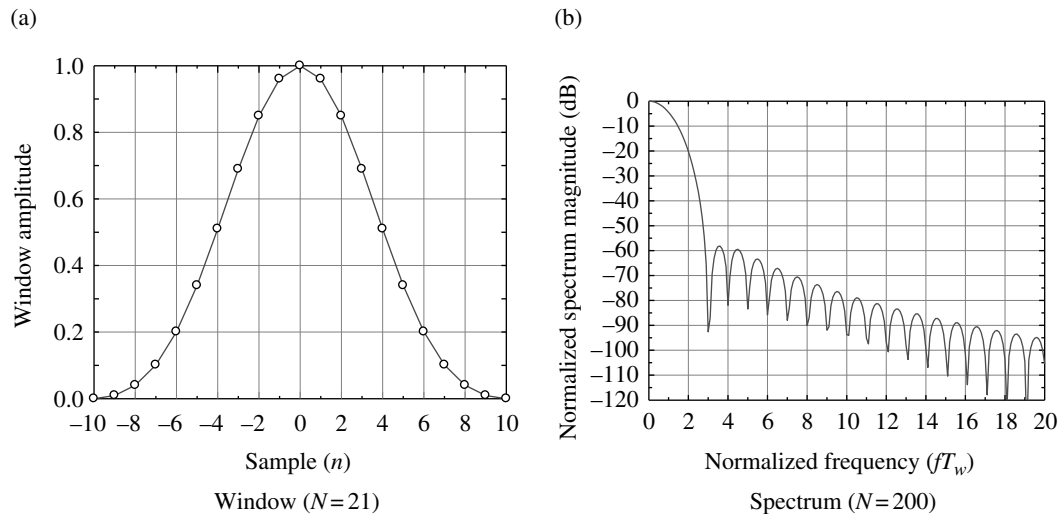| Coefficient	3-Term 67 dB	4-Term 92 dB
c_0	0.42323	0.35875
c_1	0.49755	0.48829
c_2	0.07922	0.14128
c_3	0.0	0.01168

[a]Harris [75]. Reproduced by permission of the IEEE.

This definition of the phase function results in a symmetrical window for all values of N with indexing over $\pm \lfloor N/2 \rfloor$ as shown in Figure 1.41a for $N = 21$. The spectrum of the Blackman window corresponding to $N = 200$ samples per window is shown in Figure 1.41b.

1.11.6   Blackman–Harris Window

The Blackman–Harris window is expressed as

$$w(n) = c_o - c_1 \cos(\phi_n) + c_2 \cos(2\phi_n) - c_3 \cos(3\phi_n) \quad (1.435)$$

Harris [75] performed a gradient search on the coefficients c_i to minimize spectral sidelobe level and the results are given in Table 1.16 for a three- and four-term window.

The Blackman–Harris window, as formulated by Harris, divides the phase function by N that results in an asymmetrical window. To provide a symmetrical window for all N, the phase function ϕ_n is divided by $N - 1$ and expressed as
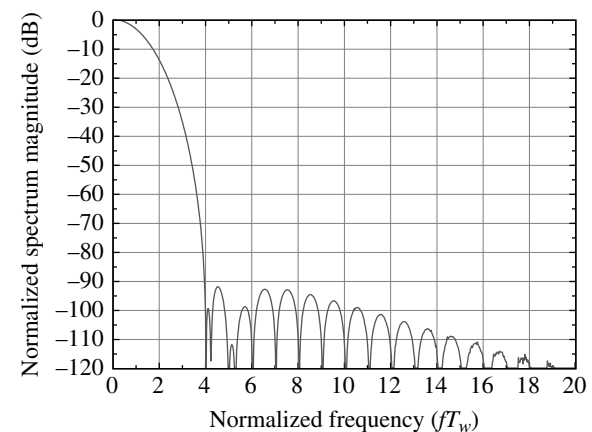
FIGURE 1.42   Blackman–Harris window spectrum ($N = 200$, 92 dB, 4-Term).

$$\phi_n = \frac{2\pi}{N-1} n \qquad\qquad : 0 \le n \le N-1$$
$$= \frac{2\pi}{N-1}(n + \lfloor N/2 \rfloor) \quad : -\lfloor N/2 \rfloor \le n \le \lfloor N/2 \rfloor$$
(1.436)

The spectrum of the 4-Term 92 dB Blackman–Harris window is shown in Figure 1.42 for $N = 200$ samples per symbol and $L = 40$ samples in the bandwidth $1/T_w$ Hz.

The coefficients for the Blackman–Harris function, as given in Table 1.16, do not result in window values of zero for the first and last sample resulting in a window *pedestal* of 6×10^{-5}; this is a direct result of the coefficients not summing to zero at the window edges. The pedestal plays a critical role in the control of the sidelobes and noise bandwidth and windows with more dramatic pedestals are examined in the following sections.

1.11.7 Hamming Window

The Hamming window is expressed as

$$w(n) = 0.54 - 0.46\cos(\phi_n) \qquad (1.437)$$

where the phase function ϕ_n is expressed as

$$\phi_n = \frac{2\pi}{N-1}n \quad : 0 \le n \le N-1 \qquad (1.438)$$

The window is shown in Figure 1.43a with indexing over the range $0 \le n \le N-1$ and the spectrum is shown in Figure 1.43b.

1.11.8 Kaiser (Kaiser–Bessel) Window

The Kaiser window, also referred to as the Kaiser–Bessel window, is expressed as

$$w(n) = \frac{I_o\left(\pi\beta\sqrt{1-\left(\frac{n}{N/2}\right)^2}\right)}{I_o(\pi\beta)} \quad : |n| \le N/2 \qquad (1.439)$$

where $I_o(x)$ is the modified Bessel function of order zero and β is the time-bandwidth product equal to T_wB where T_w is the window duration and B is the corresponding baseband bandwidth. The Kaiser window is shown in Figure 1.44a, using $N = 51$ samples per window, as a
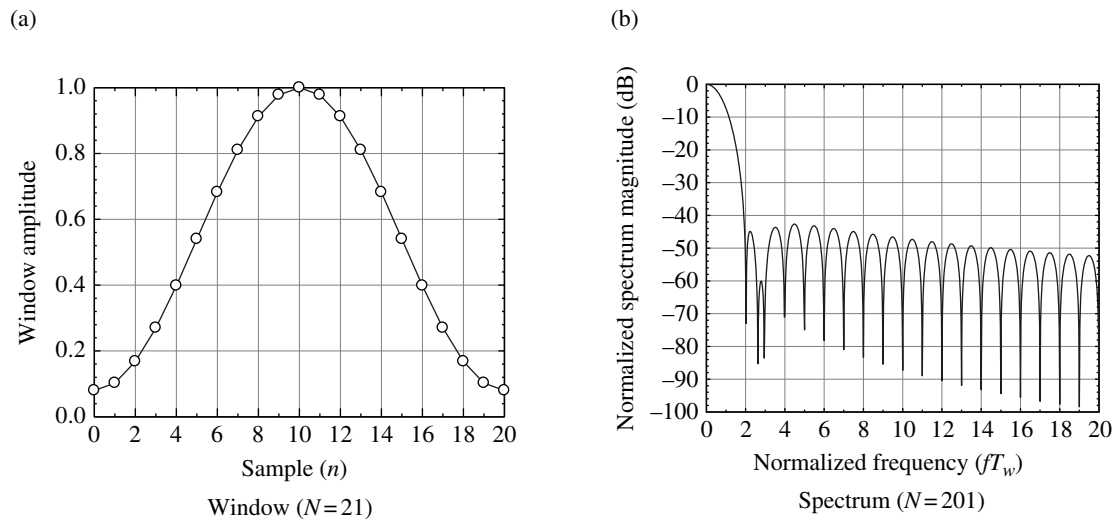

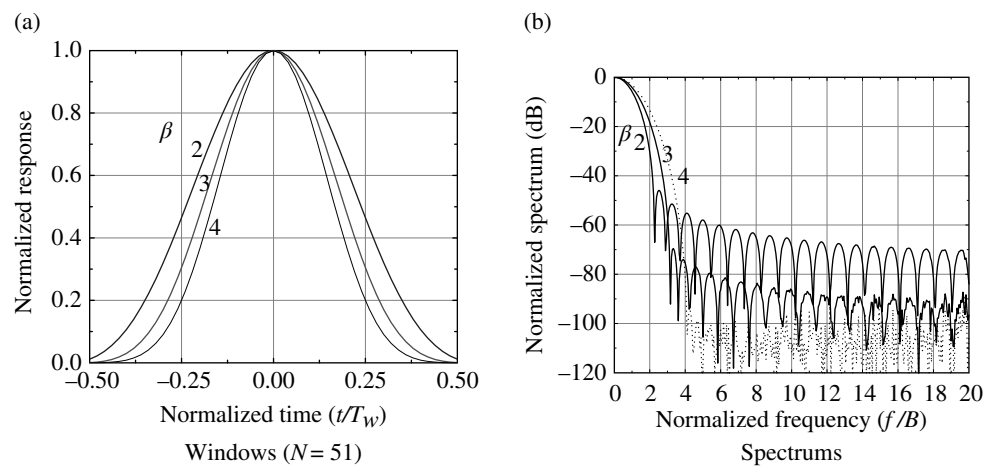**FIGURE 1.43** Hamming window and spectrum.

FIGURE 1.44 Kaiser windows and spectrums ($\beta = 2$, 3, and 4).

symmetrical window for $\beta = 2$, 3, and 4; the range $-N/2 \leq n \leq N/2$ corresponds to $-T_w/2 \leq t \leq T_w/2$. The corresponding spectrum of the Kaiser window is shown in Figure 1.44b.

1.12 MATRICES, VECTORS, AND RELATED OPERATIONS

A matrix is a convenient way to describe complicated linear systems and is used extensively in the analysis of control systems. For example, a large linear system is generally described in terms of the inputs x_j, outputs y_i, and the system coefficients a_{ij} as

$$
\begin{aligned}
y_1 &= a_{11}x_1 + a_{12}x_2 + \cdots + a_{1n}x_n \\
y_2 &= a_{21}x_1 + a_{22}x_2 + \cdots + a_{2n}x_n \\
&\vdots \\
y_m &= a_{m1}x_1 + a_{m2}x_2 + \cdots + a_{mn}x_n
\end{aligned}
\tag{1.440}
$$

and using matrix and vector notations (1.440) is described as

$$
\begin{pmatrix} y_1 \\ y_2 \\ \vdots \\ y_m \end{pmatrix} = \begin{bmatrix} a_{11} & a_{12} & \cdots & a_{1n} \\ a_{21} & a_{22} & \cdots & a_{2n} \\ \vdots & \vdots & \vdots & \vdots \\ a_{m1} & a_{m2} & \cdots & a_{mn} \end{bmatrix} \begin{pmatrix} x_1 \\ x_2 \\ \vdots \\ x_n \end{pmatrix}
\tag{1.441}
$$

where the 1 by n inputs x_j, and the 1 by m outputs y_i are described by vectors and the coefficients a_{ij} are described by the m by n matrix. The notation of an m by n matrix refers, respectively, to the number of rows and columns of the matrix. The linear system may include time-varying inputs, outputs, and coefficients as found in control systems and time-varying parameter estimation and tracking applications. The following descriptions of matrices and vectors are introductory and targeted to the description of adaptive systems in Chapter 12. More in-depth discussions on the subject and applications are given by Derusso, Roy, and Close [77], Haykin [78], Sage and White [79], and Gelb [80].

1.12.1 Definitions and Types of Matrices

- A $m \times n$ matrix A contains m rows and n columns of elements a_{ij} and is denoted as

$$
A = \begin{bmatrix} a_{11} & \cdots & a_{1n} \\ \vdots & \cdots & \vdots \\ a_{m1} & \cdots & a_{mn} \end{bmatrix}
\tag{1.442}
$$

- A *diagonal matrix* (Λ) is a $m \times m$ *square matrix* with $a_{ij} = 0$: $i \neq j$, otherwise, the elements on the principal diagonal are identified as a_{ii} with $\Lambda = \mathrm{diag}(a_{ii}) \; \forall \; i$.
- The *unit matrix* (I) is similar to the diagonal matrix with $a_{ij} = 0$: $i \neq j$, and $a_{ii.} = 1$.
- A *null matrix* or *zero matrix* (O) is a matrix for which all of the elements are zero.
- A *symmetric matrix* is a square matrix of real elements if $A = A^T$, that is, $a_{ji} = a_{ij} \; \forall \; i,j$.
- A *skew matrix* is a square matrix of real elements if $A = -A^T$, that is, $a_{ij} = -a_{ji} \; \forall \; i,j$.
- A *nonsingular matrix* A has an inverse A^{-1}.
- A *complex matrix* is denoted as $\tilde{A}$ and has complex elements $\tilde{a}_{ij} = a_{cij} + ja_{sij}$ where a_{cij} and a_{sij} denote the respective real and imaginary values of the complex elements. Conjugation the complex matrix is denoted as $\tilde{A}^*$ with elements $\tilde{a}_{ij} = a_{cij} - ja_{sij}$.

The *transposition* of the matrix interchanges the row and columns and is denoted with the superscript T. For example, the transpose of the matrix A is the $n \times m$ matrix denoted as

$$
A^T = \begin{bmatrix} a_{11} & \cdots & a_{m1} \\ \vdots & \cdots & \vdots \\ a_{1n} & \cdots & a_{mn} \end{bmatrix}
\tag{1.443}
$$

The *Hermitian matrix* is a complex matrix with the elements below the principal diagonal equal to the complex conjugate of the those about the principal diagonal; satisfying the conditions $(A^*)^T = A^+ = A^H$ where the superscripts + and H denote the complex conjugate transposition. The superscript + generally denotes complex transposition and H is used to emphasize the Hermitian complex transposition.

The order, or rank, of an $(m \times n)$ matrix is denoted as m-by-n and the order, or rank, of the square $(m \times m)$ matrix is denoted as m.

1.12.2 The Determinant and Matrix Inverse

The determinant [81] of an $m \times m$ square matrix A is denoted as $|A|$ and defined in terms of the *cofactors*, A_{ij}, of A as

$$
|A| = \sum_{i=1}^{m} a_{ij}A_{ij} = \sum_{j=1}^{m} a_{ij}A_{ij}
\tag{1.444}
$$

The cofactors are defined as

$$
A_{ij} = (-1)^{i+j}M_{ij}
\tag{1.445}
$$

where M_{ij} is the determinant of the *minor matrix* of the element a_{ij}. The $m' \times m' : m' = m - 1$ minor matrix of a_{ij} is the matrix formed by the m' rows and columns of A

excluding the row and column containing a_{ij}. For example, considering the 4×4 square matrix A, the 3×3 minor matrix A' of the element a_{32}, and the determinant M_{32} are expressed in (1.446) as

$$A = \begin{bmatrix} a_{11} & a_{12} & a_{13} & a_{14} \\ a_{21} & a_{22} & a_{23} & a_{24} \\ a_{31} & a_{32} & a_{33} & a_{34} \\ a_{41} & a_{42} & a_{43} & a_{44} \end{bmatrix}, \quad A' = \begin{bmatrix} a_{11} & a_{13} & a_{14} \\ a_{21} & a_{23} & a_{24} \\ a_{41} & a_{43} & a_{44} \end{bmatrix}, \quad M_{32} = |A'|$$

(1.446)

Therefore, using (1.446), the cofactor A_{32} is evaluated as $A_{32} = (-1)^5 M_{32}$. Following the evaluation of the remaining $m-1$ cofactors $A_{i,2}$: $i = 1,2,4$ or the cofactors A_{3j}: $j = 1,3,4$, the determinant |A| is evaluated using, respectively, the first or second equality in (1.444).

For square matrices of order ≤ 3, the determinant can be computed in terms of the elements a_{ij} as expressed, for example, in the 3×3 matrix described in (1.447). In this example, the determinant is formed by summing the $n = 3$ products of the elements parallel to the principal diagonal elements (a_{11}, a_{22}, a_{33}) and subtracting the $n = 3$ products of the elements parallel to the diagonal elements (a_{13}, a_{22}, a_{31}). The three positive products are indicated by *solid arrows* pointing to the diagonal elements parallel to the principal diagonal and the three negative products are indicated by *dashed arrows* pointing to the diagonal elements parallel to the complement of the principal diagonal. In both cases, the elements below the diagonals are *wrapped around* to form the three element products. In general, this procedure does not give the correct results for orders > 3.

$$|A| = \begin{vmatrix} a_{11} & a_{12} & a_{13} \\ a_{21} & a_{22} & a_{23} \\ a_{31} & a_{32} & a_{33} \end{vmatrix} = \begin{cases} a_{11}a_{22}a_{33} + a_{12}a_{23}a_{31} + a_{13}a_{21}a_{32} \\ -a_{13}a_{22}a_{31} - a_{12}a_{21}a_{33} - a_{11}a_{23}a_{32} \end{cases}$$

(1.447)

Determinants are defined only for square matrices and if |A| = 0 the matrix A is referred to as a singular matrix, otherwise, A is nonsingular. The inverse of a *nonsingular* $n \times n$ matrix A, with elements a_{ij}, is expressed as

$$A^{-1} = \frac{[A_{ji}]}{|A|}$$

(1.448)

where the matrix $[A_{ji}]$ is defined as the adjoint of the matrix A. Considering the $n \times n$ matrix of cofactors $[A_{ij}]$ of the matrix A, with the cofactor of each element a_{ij} evaluated using (1.445), the adjoint matrix is the transpose of the matrix $[A_{ij}]$ so that

$$[A_{ji}] = [A_{ij}]^T$$

(1.449)

Premultiplication of A^{-1} by A results in the unit matrix, that is, $AA^{-1} = $ I

1.12.3   Definition and Types of Vectors

A *vector* is an $m \times 1$ column matrix with elements a_i and is denoted as

$$a = \begin{bmatrix} a_1 \\ \vdots \\ a_m \end{bmatrix}$$

(1.450)

A *complex vector* is denoted as $\tilde{a}$ with complex elements $\tilde{a}_k = a_{ck} \pm ja_{sk}$ where a_c and a_s denote the real and imaginary values of the complex element. The transposition of the matrix a is the $1 \times m$ complex row vector a^T. *Conjugation* and *conjugate transposition* are denoted by the respective superscripts $*$ and $+$.

1.12.4   Matrix and Vector Operations

Addition of two matrices of the same order $(m \times n)$ is

$C = A + B$: The elements of C are $c_{ij} = a_{ij} + b_{ij}$

Multiplication of the two matrices must conform to the following rule: $[m \times n][n \times m'] = [m \times m']$ where the inner dimension n must be identical.

$y = Ax$: Matrix postmultiplication by a vector results in a $[m \times n][n \times 1] = [m \times 1]$ vector

The element multiplication is $y_i = \sum_k^n a_{ik}x_k$: $i = 1, \ldots, m$

$y = x^T A$: Matrix premultiplication by a vector results in a $[1 \times n][n \times m] = [1 \times m]$ vector.

The element multiplication is $y_i = \sum_k^m a_{ki}x_k$: $i = 1, \ldots, n$

$C = AB$: Matrix multiplication results in a $[m \times \ell]$ $[\ell \times n] = [m \times n]$ matrix

The element multiplication is $c_{ij} = \sum_k^\ell a_{ik}b_{kj}$: $i = 1, m$; $j = 1, \ldots, n$

In general, multiplication is not communicative $AB \neq BA$

$A(BC) = (AB)C$: Associative

$A(B + C) = AB + AC$: Distributive

Multiplication by diagonal matrix D

$C = AD$: Postmultiplication of a real $(m \times m)$ matrix A by D results in a diagonal matrix C with the diagonal element of A scaled by those of D; the elements of C are $c_{ij} = a_{ij}d_{jj}$: $i,j = 1, \ldots, m$

$C = DA$: Premultiplication of a real $(m \times m)$ matrix A by D results in the same diagonal matrix C; the elements of C

are $c_{ij} = d_{ii}a_{ij} : i,j = 1, \ldots, m$. In this case multiplication is communicative.

Multiplication by unit matrix I

$IA = A$: Multiplication of a $(m \times m)$ matrix A by I does not alter the matrix A.

$IA = AI$: Multiplication by I is communicative.

Transposition of AB

$C = (AB)^T = A^T B^T$

Scalar, or inner, product of two $(m \times 1)$ complex vectors $\tilde{x}$ and $\tilde{y}$

$\tilde{y}^T \tilde{x}^* = \tilde{x}^+ \tilde{y} = \sum_i^m \tilde{y}_i \tilde{x}_i^*$ are complex values and $\tilde{y}^T \tilde{x}^* \neq \tilde{x}^T \tilde{y}^*$
$\tilde{x}^T \tilde{y}^* = \tilde{y}^+ \tilde{x} = \sum_i^m \tilde{x}_i \tilde{y}_i^*$

Scalar product of two $(m \times 1)$ real vectors x and y

$y^T x = \sum_i^m y_i x_i$ is   a   real   scalar   value   and $y^T x = x^T y = \sum_i^m x_i y_i$

Orthogonality of two vectors is defined if their scalar product is zero.

Length of a complex vector $\tilde{x}$ is defined as magnitude, denoted as $\|\tilde{x}\|$, of the inner product

$$||\tilde{x}|| = \sqrt{\sum_i^m \tilde{x}_i \tilde{x}_i^*} = \sqrt{\sum_i^m |\tilde{x}_i|^2} \tag{1.451}$$

Outer, or dyadic, product of two $(m \times 1)$ and $(1 \times n)$ complex vectors $\tilde{x}$ and $\tilde{y}$ forms an $(m \times n)$ complex matrix $\tilde{C} = xy^+$ with elements $c_{ij} = \sum_j^n x_i y_j^* : i = 1, \ldots, m$. The autocorrelation matrix of a complex vector is computed as the outer product.

Differentiation of Complex Matrices: Differentiation of a complex matrix $\tilde{A}(t)$ results in the complex matrix $\tilde{C} = (d/dt)\tilde{A}(t)$ with elements evaluated as $\tilde{c}_{ij} = (da_{cij}/dt) \pm j(da_{sij}/dt)$. The differentiation of sums and products of matrices is evaluated as

$$\frac{d}{dt}(\tilde{A}(t) + \tilde{B}(t)) = \frac{d}{dt}\tilde{A}(t) + \frac{d}{dt}\tilde{B}(t) \tag{1.452}$$

$$\frac{d}{dt}(\tilde{A}(t)\tilde{B}(t)) = \left(\frac{d}{dt}\tilde{A}(t)\right)\tilde{B}(t) + \tilde{A}(t)\left(\frac{d}{dt}\tilde{B}(t)\right) \tag{1.453}$$

Differentiation of a complex vector follows by considering the vector as a single column matrix. Therefore, differentiation of real matrices and vectors is identical with $a_{ij} = 0$.

Differentiation of quadratic transformation with the matrix $\tilde{Q}(t)$ expressed as

$$\tilde{Q}(t) = \tilde{x}^H(t)\tilde{A}(t)\tilde{x}(t) \tag{1.454}$$

where the elements of the $(m \times m)$ complex matrix $\tilde{A}(t)$ and the complex $(m \times 1)$ vector $\tilde{x}(t)$ are functions of t. The derivative of $\tilde{Q}(t)$ is evaluated as

$$\frac{d\tilde{Q}(t)}{dt} = \left(\frac{d}{dt}\tilde{x}^H(t)\right)\tilde{A}(t)\tilde{x}(t) + \tilde{x}^H(t)\left(\frac{d\tilde{A}(t)}{dt}\right)\tilde{x}(t)$$
$$+ \tilde{x}^H(t)\tilde{A}(t)\left(\frac{d}{dt}\tilde{x}(t)\right) \tag{1.455}$$

For a real matrix $A(t)$ and vector $x(t)$, the matrix $Q(t)$ is symmetric and the derivative of the quadratic function $Q(t)$ simplifies to

$$\frac{dQ(t)}{dt} = 2\left(\frac{d}{dt}x^T(t)\right)A(t)x(t) + x^T(t)\left(\frac{dA(t)}{dt}\right)x(t) \tag{1.456}$$

Bilinear transformation with the real $(m \times m)$ matrix $B(t)$, expressed in terms of the $(m \times 1)$ real vectors $x(t)$ and $y(t)$, is evaluated as

$$B(t) = x^T(t)A(t)y(t) \tag{1.457}$$

Differentiation of $B(t)$ with respect to t is evaluated as

$$\frac{dB(t)}{dt} = \left(\frac{d}{dt}x^T(t)\right)B(t)y(t) + x^T(t)\left(\frac{dB(t)}{dt}\right)y(t)$$
$$+ x^T(t)B(t)\left(\frac{d}{dt}y(t)\right) \tag{1.458}$$

1.12.5   The Quadratic Transformation

The quadratic matrix Q is similar to the bilinear matrix, expressed in (1.457), with the vector $y = x$. The following description is based on the $(n \times n)$ correlation matrix[*]

$$R = E\left[\tilde{u}\tilde{u}^H\right] \tag{1.459}$$

where $\tilde{u}$ is an $(n,1)$ complex vector of arbitrary data and $\tilde{u}^H$ is the complex conjugate transpose[†] of $\tilde{u}$. The n columns of the matrix Q represent the $(n,1)$ characteristic vectors of

---

[*]In Chapter 12 the data vector is denoted as $\tilde{x}$ and represents the discrete-time samples of a stationary stochastic process and $\tilde{w}$ is used to denote an arbitrary nonzero vector with $\tilde{y} = \tilde{w}^H \tilde{x}$.

[†]The Hermitian transpose $\tilde{u}^H$ is an alternate notation to $\tilde{u}^+$ denoting the complex conjugate transpose.

the correlation matrix R that is transformed to the diagonal matrix Λ as

$$Q^H R Q = \Lambda \qquad (1.460)$$

The diagonal elements of Λ are the characteristic values[*] of the matrix R.

The derivation of (1.460) follows the work of Haykin [82] and is based on the linear transformation of the $(n,1)$ complex vector $\tilde{x}$ to the vector $\lambda\tilde{x}$ using the transformation

$$R\tilde{x} = \lambda\tilde{x} \qquad (1.461)$$

where λ is a constant. Equation (1.461) can be expressed as $(R - \lambda I)\tilde{x} = O$ which has nontrivial solutions with $\tilde{x} \neq 0$, *iff* the determinant of $R - \lambda I$ is zero, that is,

$$|R - \lambda I|_{\det} = 0. \qquad (1.462)$$

Equation (1.462) is the characteristic equation of the matrix R and has n solutions corresponding to the λ_i characteristic values or roots of (1.462). In general, the characteristic values are distinct; however, for the correlation matrix R, with the complex vector $\tilde{u}$ based on samples of a discrete-time weakly stationary stochastic process, the mean-square value of the scalar $\tilde{y}' = \tilde{x}^H \tilde{u}$ is evaluated as

$$E\left[|\tilde{y}'|^2\right] = \tilde{x}^H R \tilde{x} \geq 0 \qquad (1.463)$$

Equation (1.463) corresponds to a nonnegative definite quadratic form and Haykin points out that the equality condition rarely applies in practice so that (1.463) is almost always positive definite.[†] Consequently, in these cases, characteristic values are real with and $\lambda_i > 0 \; \forall \; i$ and, for the weakly stationary stochastic process, the characteristic values are equal with $\lambda_i = \sigma^2 \; \forall \; i$.

Referring to (1.461), the n solutions to the characteristic equation are determined using

$$R\tilde{x}_i = \lambda_i\tilde{x}_i \qquad (1.464)$$

where $\tilde{x}_i$ are the characteristic vectors corresponding to the characteristic values λ_i. Based on the correlation matrix R, it can be shown [83] that the characteristic values are all real and nonnegative and the characteristic vectors are linearly independent and orthogonal to each other. A corollary to the proof of independence is that when the characteristic value is multiplied by a scalar constant the characteristic

vectors remain independent and orthogonal. This allows for the independent scaling of all characteristic values so that

$$\tilde{x}_i^H \tilde{x}_j = \begin{cases} 1 & : i = j \\ 0 & : i \neq j \end{cases} \qquad (1.465)$$

resulting in an orthonormal set of characteristic vectors satisfying (1.464). Recognizing that the matrix Q is a column of characteristic vectors with $Q = [\tilde{x}_1, \tilde{x}_2, \ldots, \tilde{x}_n]$ and Λ is a diagonal matrix of characteristic values $\Lambda = diag(\lambda_1, \lambda_2, \ldots, \lambda_n)$, (1.464) is expressed as

$$RQ = Q\Lambda \qquad (1.466)$$

and the orthonormal matrix Q satisfies the relationship $Q^H Q = I$, therefore, $Q^H = Q^{-1}$ and premultiplying both sides of (1.466) by Q^H results in (1.460) as stated. Also, by post-multiplying both sides of (1.466) the correlation matrix is expressed as

$$R = Q\Lambda Q^H = \sum_i^n \lambda_i \tilde{x}_i \tilde{x}_i^H \qquad (1.467)$$

Haykin states that there is no best way to compute the characteristic values and suggest that the use of the characteristic equation should be avoided except for the simple case involving the 2×2 matrix. However, a number of authors [77, 78, 84–89] describe computationally efficient methods for computing the characteristic values.

Consider the quadratic form $\tilde{Q} = \tilde{w}^H R \tilde{w}$ discussed in Section 12.3, where $\tilde{w}$ is a $(m \times 1)$ complex vector with elements $\tilde{w}_i = w_{ci} + jw_{si}$ and $R = E[\tilde{x}\tilde{x}^*]$ is a $(m \times m)$ Hermitian matrix with elements $\tilde{r}_{ji} = \tilde{r}_{ij}^*: i \neq j$ corresponding to the auto-correlation matrix of the $(m \times 1)$ complex vector $\tilde{x}$. The following derivatives with respect to the complex vector $\tilde{w}$ are evaluated as:

$$\frac{d}{d\tilde{w}}\tilde{Q} = \frac{d}{d\tilde{w}}\tilde{x}^H R \tilde{w} = 2R\tilde{w} \qquad (1.468)$$

$$\frac{d}{d\tilde{w}}\tilde{c}^H \tilde{w} = 0 \qquad (1.469)$$

and

$$\frac{d}{d\tilde{w}}\tilde{w}^H \tilde{c} = 2\tilde{c} \qquad (1.470)$$

where $\tilde{c}$ is a $(m \times 1)$ complex vector. The solutions to the derivative of the quadratic form with respect to the vector w are used in Chapter 12 in the analysis of adaptive systems. The proofs of (1.468), (1.469), and (1.470) are given by Haykin [78].

---

[*]The characteristic vectors and values are also referred to as the eigenvectors and eigenvalues.

[†]A quadratic form is positive definite *iff* the characteristic values of R are all positive.

1.13 OFTEN USED MATHEMATICAL PROCEDURES

This section outlines the processing and formulas encountered in several of the chapters throughout this book.

1.13.1 Prime Factorization and Determination of Greatest Common Factor and Least Common Multiple

Prime factors are used in various coding applications where polynomials are used as code generators. The greatest common factor (GCF) and least common multiple (LCM) are often used where signal processing sample-rate changes are required to improve performance or reduce processing complexity. They are also used in the implementation of mixed radix fast Fourier transforms. An integer p is prime if $p \neq \pm 1$ and the only divisors are $\pm p$ and ± 1. The procedures involved in determining the prime factors of a number and the GCF and LCM between two or more numbers are simply given by way of the following examples. The algorithms are easy to generalize and implement in a computer program.

1.13.1.1   Prime Factors of Two Numbers   The following examples, presented in Table 1.17, demonstrate the procedure for determining the prime factors of the numbers 120 and 200. The results are used in the following two examples to determine the GCF and LCM. The prime factors of a number are determined, starting with repeated division of the number by 2.

1.13.1.2   Determination of the Greatest Common Factor   This example outlines the procedures in determining the GCF of the two numbers 120 and 200 using the prime factors listed in Table 1.17; inclusion of more than more than two numbers is straightforward. The GCF is also referred to as the greatest common divisor (GCD). The GCF (or GCD) between 120 and 200 is determined as the product of the prime factors taken the *minimum* number of times that they occurred in any one of the prime factorizations, that is,

$$\text{GCF}(120,200) = 2^3 \times 3^0 \times 5^1 = 8 \times 1 \times 5 = 40.$$

TABLE 1.17   Example of Prime Factorization

Using 120	Using 200
$120 \div 2 = 60$	$200 \div 2 = 100$
$60 \div 2 = 30$	$100 \div 2 = 50$
$30 \div 2 = 15$	$50 \div 2 = 25$
$15 \div 3 = 5$	$25 \div 5 = 5$
$5 \div 5 = 1$	$5 \div 5 = 1$
The prime factors are:	
$2 \times 2 \times 2 \times 3 \times 5$	$2 \times 2 \times 2 \times 5 \times 5$

1.13.1.3   Determination of the Least Common Multiple   This example outlines the procedures in determining the LCM between 120 and 200. In this case, the LCM is determined as the product of the prime factors taken the *maximum* number of times that they occurred in any one of the prime factorizations, that is,

$$\text{LCM}(120,200) = 2^3 \times 3^1 \times 5^2 = 8 \times 3 \times 5 = 600.$$

1.13.2 Newton's Method

A transcendental equation involves trigonometric, exponential, logarithmic, and other functions that do not lend themselves to solutions by algebraic means. Newton's method [90] of solving transcendental equations is used extensively in arriving at solutions to problems characterized by nonalgebraic equations. The method provides a rapid and accurate solution to determine the value of functions having the form $f(x) = h(x)$, by finding the solution of the auxiliary function $g(x) = f(x) - h(x) = 0$. The solution begins by starting with an estimate $\hat{x}_o$ of the solution and performing iterative updates to the estimate, described as

$$x_{i+1} = x_i - \frac{g(x_i)}{g'(x_i)} \quad : i = 0, \ldots \tag{1.471}$$

where $g'(x_i) = \partial g(x_i)/\partial x_i$. The evaluation is terminated when $|f(x_{i+1}) - h(x_{i+1})| \leq \varepsilon$ where ε is an acceptable error in the solution and the corresponding x_{i+1} is the desired value of x satisfying $f(x) \cong h(x)$.

1.13.3 Standard Deviation of Sampled Population

When a finite number of samples n comprises the entire population, the standard deviation is computed as

$$\sigma = \sqrt{\frac{1}{n}\sum x^2 - \left(\frac{1}{n}\sum x\right)^2} \tag{1.472}$$

where the summation is over the entire population. However, when the samples n are a subset of the entire population, the standard deviation is computed as

$$s = \sqrt{\frac{1}{n-1}\sum x^2 - \frac{n}{n-1}\left(\frac{1}{n}\sum x\right)^2} \tag{1.473}$$

where the summations are over the sample size n of the subset.

1.13.4 Solution to the Indeterminate Form 0/0

The frequently encountered functional form

$$h(x) = \frac{f(x)}{g(x)} \tag{1.474}$$

evaluated at $x = a$ often results in the indeterminate form 0/0 resulting from $f(a) = g(a) = 0$. Application of L'Hospital's rule of repeated differentiation of $f(x)$ and $g(x)$ and evaluating the result as

$$h(x) = \lim_{x \to a} \frac{f^{(n)}(x)}{g^{(n)}(x)} \tag{1.475}$$

often leads to a solution for $n = 1$ or 2. Solutions to other indeterminate forms involving ∞/∞, $0*\infty$, $\infty-\infty$, 0^0, ∞^0, 0^∞, and 1^∞ may also be found using similar techniques [90, 91].

1.14 OFTEN USED MATHEMATICAL RELATIONSHIPS

In this section a number of mathematical relationships are listed as found in various mathematical handbooks. The references frequently referred to are as follows: Burington [92], Korn and Korn [93], Milton and Stegun [94], and Gradshteyn and Ryzhik [46].

1.14.1 Finite and Infinite Sums

1 $\displaystyle\sum_{m=1}^{M} m = \frac{M(M+1)}{2}$: summation of integers

2 $\displaystyle\sum_{m=1}^{M} (2m-1) = M^2$: summation of odd integers

3 $\displaystyle\sum_{m=1}^{M} 2m = M(M+1)$: summation of even integers

4 $\displaystyle\sum_{m=1}^{M} m^2 = \frac{M(M+1)(2M+1)}{6}$

5 $\displaystyle\sum_{m=0}^{M-1} x^m = \frac{1-x^M}{1-x}$: $|x| < 1$ finite geometric series

6 $\displaystyle\sum_{m=0}^{\infty} x^m = \frac{1}{1-x}$: $|x| < 1$ infinite geometric series

7 $\displaystyle\sum_{m=0}^{\infty} m x^m = \frac{x}{(1-x)^2}$: $|x| < 1$

8 $\displaystyle\sum_{m=0}^{M} \sin(m\alpha + \beta) = \frac{\sin\left(\frac{M+1}{2}\alpha\right)}{\sin(\alpha/2)} \sin\left(\frac{M}{2}\alpha + \beta\right)$
  : M = positive integer

9 $\displaystyle\sum_{m=0}^{M} \cos(m\alpha + \beta) = \frac{\sin\left(\frac{M+1}{2}\alpha\right)}{\sin(\alpha/2)} \cos\left(\frac{M}{2}\alpha + \beta\right)$
  : M = positive integer

10 $1 + 2\displaystyle\sum_{m=1}^{M} \cos(m\alpha) = \frac{\sin((M+1/2)\alpha)}{\sin(\alpha/2)}$

11 $\displaystyle\sum_{m=0}^{M} e^{j(m\alpha + \beta)} = \frac{\sin\left(\frac{M+1}{2}\alpha\right)}{\sin(\alpha/2)} e^{j\left(\frac{M}{2}\alpha + \beta\right)}$
  : M = positive integer

12 $\displaystyle\sum_{m=-M}^{M} e^{\pm jm\alpha} = \frac{\sin((M+1/2)\alpha)}{\sin(\alpha/2)}$

13 $(1 \pm x)^m = 1 \pm mx + \dfrac{m(m-1)}{2!}x^2 + \cdots$
   $+ (\pm 1)^n \dfrac{m(m-1)\dots(m-n+1)}{n!}x^n + \cdots$: $m > 0$

14 $(1 \pm x)^{-m} = 1 \mp mx + \dfrac{m(m+1)}{2!}x^2 + \cdots$
   $+ (\pm 1)^n \dfrac{m(m+1)\dots(m+n-1)}{n!}x^n + \cdots$: $m > 0$

1.14.2 Binomial Theorem and Coefficients

1 $(x \pm y)^m = x^m \pm \dbinom{m}{1}x^{m-1}y + \dbinom{m}{2}x^{m-2}y^2 \pm \cdots$
   $(\pm 1)^{m-2}\dbinom{m}{m-1}xy^{m-1}(\pm 1)^{m-1}\dbinom{m}{m}y^m$
   $= \displaystyle\sum_{i=0}^{m}(\pm 1)^i \dbinom{m}{i}x^{m-i}y^i$

2 $(1 \pm y)^m = 1 - \displaystyle\sum_{i=1}^{m}(\pm 1)^{i+1}\dbinom{m}{i}y^i$

3 $\dbinom{m}{n} = {}_mC_n = \dfrac{m!}{(m-n)!n!}$: coefficient evaluation

4 $\dbinom{m}{n} = \dbinom{m}{m-k}$: coefficient symmetry

5 $\displaystyle\sum_{n=0}^{m}\dbinom{m}{n} = 2^m$: coefficient summation

6 $\displaystyle\sum_{n=0}^{m}\dbinom{m}{n}(-1)^n = 0$: alternating sign coefficient summation

TABLE 1.18 Brief List of Binomial Coefficients

m \\ n	0	1	2	3	4	5	6	7	8	9	10
1	1	1									
2	1	2	1								
3	1	3	3	1							
4	1	4	6	4	1						
5	1	5	10	10	5	1					
6	1	6	15	20	15	6	1				
7	1	7	21	35	35	21	7	1			
8	1	8	28	56	70	56	28	8	1		
9	1	9	36	84	126	126	84	36	9	1	
10	1	10	45	120	210	252	210	120	45	10	1

7 $\displaystyle\sum_{n=1}^{m-1}\binom{m-1}{n}\frac{1}{n+1}=\frac{1}{m}\sum_{n=2}^{m}\binom{m}{n}$

: coefficient summation identity

1.14.3 Trigonometric Identities

1 $\sin(2\alpha)=2\sin(\alpha)\cos(\alpha)$

2 $\cos(2\alpha)=2\cos^2(\alpha)-1=1-2\sin^2(\alpha)=\cos^2(\alpha)-\sin^2(\alpha)$

3 $\sin^2(\alpha)=\dfrac{1}{2}(1-\cos(2\alpha))$

4 $\sin^3(\alpha)=\dfrac{1}{4}(3\sin(\alpha)-\sin(3\alpha))$

5 $\sin^4(\alpha)=\dfrac{1}{8}(3-4\cos(2\alpha)+\cos(4\alpha))$

6 $\cos^2(\alpha)=\dfrac{1}{2}(1+\cos(2\alpha))$

7 $\cos^3(\alpha)=\dfrac{1}{4}(3\cos(a)+\cos(3\alpha))$

8 $\cos^4(\alpha)=\dfrac{1}{8}(3+4\cos(2a)+\cos(4\alpha))$

9 $\sin(\alpha)+\sin(\beta)=2\sin((\alpha+\beta)/2)\cos((\alpha-\beta)/2)$

10 $\sin(\alpha)-\sin(\beta)=2\cos((\alpha+\beta)/2)\sin((\alpha-\beta)/2)$

11 $\cos(\alpha)+\cos(\beta)=2\cos((\alpha+\beta)/2)\cos((\alpha-\beta)/2)$

12 $\cos(\alpha)-\cos(\beta)=-2\sin((\alpha+\beta)/2)\sin((\alpha-\beta)/2)$

13 $\sin(\alpha)\sin(\beta)=\dfrac{1}{2}\cos(\alpha-\beta)-\dfrac{1}{2}\cos(\alpha+\beta)$

14 $\cos(\alpha)\cos(\beta)=\dfrac{1}{2}\cos(\alpha-\beta)+\dfrac{1}{2}\cos(\alpha+\beta)$

15 $\sin(\alpha)\cos(\beta)=\dfrac{1}{2}\sin(\alpha+\beta)+\dfrac{1}{2}\sin(\alpha-\beta)$

16 $\cos(\alpha)\sin(\beta)=\dfrac{1}{2}\sin(\alpha+\beta)-\dfrac{1}{2}\sin(\alpha-\beta)$

17 $\tan^{-1}(z_1)\pm\tan^{-1}(z_2)=\tan^{-1}\left(\dfrac{z_1\pm z_2}{1\mp z_1 z_2}\right)$

18 $\sinh(z)=\dfrac{1}{2}(e^z-e^{-z})=1/\operatorname{csch}(z)$

19 $\cosh(z)=\dfrac{1}{2}(e^z+e^{-z})=1/\operatorname{sech}(z)$

20 $\tanh(z)=\left(\dfrac{e^z-e^{-z}}{e^z+e^{-z}}\right)=\dfrac{\sinh(z)}{\cosh(z)}=1/\operatorname{ctnh}(z)$

1.14.4 Differentiation and Integration Rules

The notations u and v are functions of x

1 $\dfrac{d}{dx}(uv)=u\dfrac{dv}{dx}+v\dfrac{du}{dx}$

2 $\dfrac{d}{dx}(u/v)=\dfrac{v\dfrac{du}{dx}-u\dfrac{dv}{dx}}{v^2}$

3 $\dfrac{d}{dx}(u^v)=u^v\left(\dfrac{v}{u}\dfrac{du}{dx}+\ln(u)\dfrac{dv}{dx}\right)$

4 $\dfrac{d}{dx}\ln(u)=\dfrac{1}{u}\left(\dfrac{du}{dx}\right);\dfrac{d}{dx}\log_a(u)=\dfrac{\log_a(e)}{u}\left(\dfrac{du}{dx}\right)$

5 $\dfrac{d}{dx}a^u=a^u\log_e(a)\left(\dfrac{du}{dx}\right);\dfrac{d}{dx}e^u=e^u\left(\dfrac{du}{dx}\right)$

$6 \quad \dfrac{d}{dx}\sin(u) = \cos(u)\left(\dfrac{du}{dx}\right); \dfrac{d}{dx}\sin^{-1}(u) = \dfrac{1}{\sqrt{1-u^2}}\left(\dfrac{du}{dx}\right)$

$7 \quad \dfrac{d}{dx}\cos(u) = -\sin(u)\left(\dfrac{du}{dx}\right); \dfrac{d}{dx}\cos^{-1}(u) = \dfrac{-1}{\sqrt{1-u^2}}\left(\dfrac{du}{dx}\right)$

$8 \quad \dfrac{d}{dx}\tan(u) = \sec^2(u)\left(\dfrac{du}{dx}\right); \dfrac{d}{dx}\tan^{-1}(u) = \dfrac{1}{1+u^2}\left(\dfrac{du}{dx}\right)$

$9 \quad \dfrac{d}{dx}\sinh(u) = \cosh(u)\left(\dfrac{du}{dx}\right); \dfrac{d}{dx}\sinh^{-1}(u) = \dfrac{1}{\sqrt{1+u^2}}\left(\dfrac{du}{dx}\right)$

$10 \quad \dfrac{d}{dx}\cosh(u) = \sinh(u)\left(\dfrac{du}{dx}\right);$

$\quad \dfrac{d}{dx}\cosh^{-1}(u) = \dfrac{1}{\sqrt{-1+u^2}}\left(\dfrac{du}{dx}\right) \quad : u > 1$

$11 \quad \dfrac{d}{dx}\tanh(u) = \operatorname{sech}^2(u)\left(\dfrac{du}{dx}\right);$

$\quad \dfrac{d}{dx}\tanh^{-1}(u) = \dfrac{1}{1-u^2}\left(\dfrac{du}{dx}\right)$

$12 \quad \int u\,dv = uv - \int v\,du$: integration by parts with $u = f(x)$ and $dv = g(x)dx$

$13 \quad \displaystyle\int_0^\infty x^b e^{-ax}dx = \dfrac{\Gamma(b+1)}{a^{b+1}} \quad : a > 0, \ b > -1$

$\quad\quad\quad\quad = \dfrac{b!}{a^{b+1}} \quad\quad : a > 0, \ b = 0,1,2,\dots$

$14 \quad \displaystyle\int_0^\infty e^{-ax}dx = \dfrac{1}{a}$

$15 \quad \displaystyle\int_0^\infty \sqrt{x}\,e^{-ax}dx = \dfrac{\sqrt{\pi/a}}{2a}$

$16 \quad \displaystyle\int_0^\infty \dfrac{1}{\sqrt{x}}e^{-ax}dx = \sqrt{\dfrac{\pi}{a}}$

$17 \quad \displaystyle\int_0^\infty x^b e^{-ax^2}dx = \dfrac{\Gamma((b+1)/2)}{2a^{(b+1)/2}} \quad\quad : a > 0, \ b > -1$

$\quad\quad\quad\quad = \dfrac{1(3)\dots(b-1)\sqrt{\pi}}{2^{b/2+1}a^{(b+1)/2}} \quad : a > 0, \ b = 0,2,4,\dots$

$\quad\quad\quad\quad = \dfrac{((b-1)/2)!}{2a^{(b+1)/2}} \quad\quad : a > 0, \ b = 1,3,5,\dots$

$18 \quad \displaystyle\int_0^\infty e^{-a^2x^2}dx = \dfrac{\sqrt{\pi}}{2a}$

$19 \quad \dfrac{d}{dy}\displaystyle\int_{a(y)}^{b(y)} f(x,y)dx = \int_{a(y)}^{b(y)} \dfrac{\partial}{\partial y}f(x,y)dx$

$\quad\quad\quad\quad + f(b,y)\dfrac{db}{dy} - f(a,y)\dfrac{da}{dy}$: Leibniz's theorem

$20 \quad \displaystyle\int_{-\infty}^\infty |s(t)|^2 dt = \dfrac{1}{2\pi}\int_{-\infty}^\infty |F(\omega)|^2 d\omega$

$\quad\quad\quad\quad$: Parseval's Theorem

$21 \quad g(t) = \displaystyle\int_{-\infty}^\infty x(\lambda)h(t-\lambda)d\lambda$

$\quad\quad = \displaystyle\int_{-\infty}^\infty x(t-\lambda)h(\lambda)d\lambda \quad$: convolution

$22 \quad R(\tau) = \displaystyle\int_{-\infty}^\infty x(t)y(t-\tau)dt$

$\quad\quad = \displaystyle\int_{-\infty}^\infty x(t+\tau)y(t)dt \quad$: correlation

1.14.5 Inequalities

1 $\quad |a-b| \le |a \pm b| \le |a| + |b| \quad$: triangle inequality

2 $\quad \left|\displaystyle\sum_{n=1}^N a_n\right| \le \sum_{n=1}^N |a_n| \quad$: triangle inequality

3 $\quad \left(\displaystyle\prod_{n=1}^N b_n\right)^{1/N} \le \dfrac{1}{N}\sum_{n=1}^N a_n \quad$: geometric mean $\le$
arithmetic mean
$b_n > 0$; equality holds *iff* $b_n = a_n$

4 $\quad \left[\displaystyle\sum_{n=1}^N a_n b_n\right]^2 \le \sum_{n=1}^N a_n^2 \sum_{n=1}^N b_n^2 \quad$: Cauchy's inequality
Equality holds for c = constant > 0 *iff* $a_n = c\,b_n$

5 $\quad \left[\displaystyle\int_a^b f^*(x)g(x)dx\right]^2 \le \left[\int_a^b |f(x)|^2 dx\right] \left[\int_a^b |g(x)|^2 dx\right]$
: Schwarz's inequality
Equality holds for c = constant > 0 *iff* $f(x) = c\,g(x)$.

1.14.6 Relationships between Complex Numbers

For $A = M_a e^{j\alpha}$ and $B = M_b e^{j\beta}$

1 $\quad ||A| - |B|| \le |A \pm B| \le |A| + |B|$

2 $\quad |AB| = |A||B|; \ |A/B| = |A|/|B|$

3 $\quad A/B = AB/|B|^2$

4 $\quad \operatorname{Re}[A] = \dfrac{1}{2}[A + A^*]$

5 $\quad \operatorname{Re}[A]\operatorname{Re}[B] = \dfrac{1}{2}\operatorname{Re}[AB] + \dfrac{1}{2}\operatorname{Re}[AB^*]$

6 $\text{Re}[A]\text{Im}[B] = \dfrac{1}{2}\text{Im}[AB] - \dfrac{1}{2}\text{Im}[AB^*]$

$\qquad = \dfrac{1}{2}\text{Im}[AB] + \dfrac{1}{2}\text{Im}[A^*B]$

7 $\text{Im}[A]\text{Re}[B] = \dfrac{1}{2}\text{Im}[AB] + \dfrac{1}{2}\text{Im}[AB^*]$

$\qquad = \dfrac{1}{2}\text{Im}[AB] - \dfrac{1}{2}\text{Im}[A^*B]$

8 $\text{Im}[A]\text{Im}[B] = \dfrac{-1}{2}\text{Re}[AB] + \dfrac{1}{2}\text{Re}[AB^*]$

1.14.7   Miscellaneous Relationships [94]

1 $\Gamma(z) = \displaystyle\int_0^\infty t^{z-1}e^{-t}dt$: Euler's integral, $\text{Re}(z) > 0$

2 $\Gamma\left(\dfrac{1}{2}\right) = \left(\dfrac{-1}{2}\right)! = \sqrt{\pi}$

3 $\Gamma\left(\dfrac{3}{2}\right) = \left(\dfrac{1}{2}\right)! = \dfrac{\sqrt{\pi}}{2}$

4 $\Gamma(n+1) = n! = n(n-1)(n-2)\ldots 1$: integer factorial; $0! = 1$

5 $(2n+1)!! = 1\cdot3\cdot5\cdots(2n+1)$: odd integer factorial [95]

6 $(2n)!! = 2\cdot4\cdot6\cdots(2n)$: even integer factorial [95]

7 $\log_{10}(x) = \log(x)$: common logarithm of x

8 $\log_e(x) = \ln(x)$: natural logarithm of x

9 $\log_a(b) = \dfrac{1}{\log_b(a)}$

10 $\log_a(x) = \dfrac{\log_b(x)}{\log_b(a)}$

11 $a^{\log_a(x)} = x$

12 $r = \text{mod}(a,b) = a - \text{int}\left(\dfrac{a}{b}\right)b$: $r,a,b \neq 0$

are same type $\in$ real or integer[*]
Example: for $b = 3$: $a = \ldots -4\ -3\ -2\ -1\ 0\ 1\ 2\ 3\ 4\ \ldots$
$\qquad\qquad\qquad\qquad r = \ldots -1\ 0\ -2\ -1\ 0\ 1\ 2\ 0\ 1\ \ldots$

13 $r = \text{modulo}(a,b)$

$= \begin{cases} a - \lfloor a/b \rfloor b & : r,a,b \in \text{real} \\ \\ a - bq & \begin{aligned}&: r,a,b,q \in \text{integer with } q \text{ selected}^* \\ &\text{so that } r \text{ is nearer to zero than } b \end{aligned} \end{cases}$

Example: for $b = 3$: $a = \ldots -4\ -3\ -2\ -1\ 0\ 1\ 2\ 3\ 4\ \ldots$
$\qquad\qquad\qquad\qquad r = \ldots\ 2\ 0\ 1\ 2\ 0\ 1\ 2\ 0\ 1\ \ldots$

14 $sign(a,b) = \begin{cases} |a| & : b \geq 0 \\ -|a| & : b < 0 \end{cases}$: a,b are same type $\in$ real or integer[*]

15 The solutions to the quadratic equation $x^2 + bx + c = 0$ is

---

[*]Fortran 95 Language Reference, Revision D, Lahey Computer Systems, Inc., Incline Village, NV, 1994. The notations a modulo(b) and a modulo-b are also used.

$x_1, x_2 = -b/2 \pm \sqrt{(b/2)^2 - c}$

16 Completing the square of: $x^2 + bx = (x + b/2)^2 - (b/2)^2$

17 Completing the square of: $ax^2 + bx = \left(\sqrt{a}x + b/(2\sqrt{a})\right)^2 - (b/2)^2/a$

ACRONYMS

ACI	Adjacent channel interference
ACK	Acknowledgment (protocol)
AFSCN	U.S. Air Force Satellite Control Network
AM	Amplitude modulation
ARQ	Automatic repeat request
AWGN	Additive white Gaussian noise
BPSK	Binary phase shift keying
BT	Time bandwidth (product, low pass)
CFAR	Constant false-alarm rate
CRC	Cyclic redundancy check (code)
DC	Direct current
DFT	Discrete Fourier transform
DSB	Double sideband
DSSS	Direct-sequence spread-spectrum (waveform)
EHF	Extremely high frequency
ELF	Extremely low frequency
FFT	Fast Fourier transform
FM	Frequency modulation
FSK	Frequency shift keying
GCD	Greatest common divisor
GCF	Greatest common factor
HF	High frequency
I/Q	In-phase and quadrature (channels or rails)
IDFT	Inverse discrete Fourier transform
IF	Intermediate frequency
IFFT	Inverse Fast Fourier transform
ISI	Intersymbol interference
LCM	Least common multiple
LF	Low frequency
LLR	Log-likelihood ratio
LR	Likelihood ratio
MAP	Maximum a posteriori
MF	Medium frequency
ML	Maximum likelihood
MMSE	Minimum mean-square error
MS	Mean square
MSK	Minimum shift keying
NAK	Negative acknowledgment (protocol)
OQPSK	Offset quadrature phase shift keying
PM	Phase modulation
PN	Pseudo-noise (sequence)
PSD	Power spectral density
PSK	Phase shift keying
QAM	Quadrature amplitude modulation

QPSK	Quadrature phase shift keying
RC	Raised-cosine
RQ	Repeat request
RRC	Root-raised-cosine (temporal)
RSS	Root-sum-square
SHF	Super high frequency
SLF	Super low frequency
SRC	Spectral raised-cosine
SRRC	Spectral root-raised-cosine
SS	Spread-spectrum
TRC	Temporal raised-cosine
UHF	Ultra-high frequency
ULF	Ultra-low frequency
VLF	Very low frequency
WSS	Wide-sense stationary
WT	Time bandwidth (product, bandpass)

PROBLEMS

1. Show that the amplitude-modulated waveform given by (1.2), when heterodyned by a receiver local oscillator that is phase locked to the received carrier angular frequency ω_c, recovers the modulation function $s(t) = A(1 + m_I \sin(\omega_m t))$, except for a factor of 1/2.

   Hint: Mix (1.2) with $\sin(\omega_c t + \phi)$ and show that ϕ must be zero.

2. Show that the real signal given by (1.13) is a form of suppressed carrier modulation. Under what conditions of $M(t)$ and $\phi(t) + \psi(t)$ does (1.13) reduce to the form of the suppressed carrier modulation given by (1.12)? What can be said about the information capacity between the suppressed carrier modulations given by (1.12) and (1.13)?

3. Compute the Hilbert transform of $s_c(t) = \cos(\omega_c t)$ and $s_s(t) = \sin(\omega_c t)$.

4. Given that the bandwidth of the modulation function $A(t)$ satisfies the condition $B << f_c$, compute the Hilbert transform of $s(t) = A(t)\cos(\omega_c t + \phi(t))$.

5. Show that the Fourier coefficients C_n and C_{-n}, expressed in (1.30), form complex conjugate pairs when $f(t)$ is real.

6. Show that the real-valued function $f(t)$ can be expressed in terms of the Fourier series real coefficient $C_o = \alpha_o$ and the complex coefficients $C_n = \alpha_n + j\beta_n$: $1 \leq n \leq \infty$ as

$$f(t) = C_o + 2\sum_{n=1}^{\infty} |C_n|\cos(n\omega_o t + \phi_n)$$

where $|C_n| = \sqrt{\alpha_n^2 + \beta_n^2}$ and $\phi_n = \arctan(\beta_n/\alpha_n)$. Note: This solution is based on Problem 5.

7. Show that the finite summation $(1/T)\sum_{n=-N}^{N} e^{jn\omega_o t}$ is equal to the second equality in (1.52).

   Hint: Expand the summation and combine the exponential terms to yield a series involving $\cos(n\omega_o T)$ terms and then evaluate the closed form of the corresponding trigonometric series as identified in Section 1.14.1 Identity No. 12.

8. With $\omega_o = 2\pi/T$ show that the integral $(2N+1)$ $\int_{-T/2}^{T/2} \frac{\sin((2N+1)\omega_o t/2)}{(2N+1)\omega_o t/2} dt$ is equal to unity as $N \to \infty$.

9. Referring to Figure 1.7 and using $\omega_o = 2\pi/T$, show that the maximum value of (1.52) is $(2N + 1)/T$ and that the closest zero or null removed from a maximum occurs at $t = nT \pm T/(2N + 1)$: $|n| = 0,1,\ldots$.

10. Consider a radix-2, N-point, pipeline FFT with the output sampled at intervals of $T = N_s T_s$ seconds, where N_s is the number of samples per symbol. If the sequential input samples are simply passed through the FFT delay elements with the complex multiplications and additions only performed at the output sampling instants: (A) determine the percentage of complex multiplies relative to the pipeline FFT sampled every T_s seconds. Examine the result as a function of increasing N_s with $1 \leq N_s \leq 32$ and $N \geq N_s$; (B) determine the minimum number of complex multiplications when 100 % zero padding is used for frequency estimation and tracking and discuss the pipeline FFT sampling requirements.

11. Compute the second moment, $E[X^2]$, of the Gaussian random variable X with mean m and variance σ^2.

12. Referring to (1.165) compute $E\left[g_2^2(X_2)E\left[g_1^2(X_1)|X_2 = x_2\right]\right]$ for the conditional Gaussian *pdf*, expressed by the second equality of (1.168), with $g_2^2(X_2) = X_2^2$ and $g_1^2(X_1) = X_1^2$. Express the result in terms of the expectations as $E\left[X_2^2 X_1^2\right] = C_1 E\left[X_2^2\right] + C_2 E\left[X_2^3\right] + C_3 E\left[X_2^4\right]$ and express C_1, C_2, and C_3 in terms of the parameters ρ, σ_1^2, σ_2^2, m_1, and m_2.

    Using $E\left[X_2^2\right] = \sigma_2^2 + m_2^2$, $E\left[X_2^3\right] = 3\sigma_2^2 m_2 + m_2^3$, and $E\left[X_2^4\right] = 3\sigma_2^4 + 6\sigma_2^2 m_2^2 + m_2^4$ evaluate $E\left[X_2^2 X_1^2\right]$ with $m_1 = m_2 = 0$.

13. Repeat Problem 12 using (1.172) and show that

$$E\left[x_1^2 x_2^2\right] = E\left[x_1^2\right]E\left[x_2^2\right] + 2E^2[x_1 x_2]$$

   when x_1 and x_2 are zero-mean Gaussian random variables.

14. In the transformation from $f_X(x)$ to $f_Z(z)$, discussed in Section 1.5.4.1, show that the inverse relationship in (1.188) applies for the function $z = ax^2$.
    Part B: Express $f_Z(z)$ using (1.186) or (1.187).

Part C: Express $f_Z(z)$ when the *pdf* of $f_X(x)$ is Gaussian with mean value m and variance σ^2. Plot or sketch your expression $f_Z(z)$ as a function of z.

Note: $e^\lambda + e^{-\lambda} = 2\cosh(\lambda)$.

Part D: Express $f_Z(z)$ when $m = 0$ in Part C and plot or sketch as a function of z.

15. Given the statistically independent ordered random variables $\{X_1, X_2, ..., X_n\}$ such that $a \leq X_1 < X_2 < \cdots < X_n \leq b$ and characterized by the uniformly distributed *pdf* $f_X(x_i) = 1/(b-a)$: $\forall i$, $i = 1, 2, ..., i', ..., n$ with the corresponding *cdf* expressed as $F_X(x) = \int_a^x f_X(x_i) dx_i$. Show that

$$\frac{1}{(i'-2)!} \int_a^{x_{i'}} F_X^{i'-2}(x_{i'-1}) f_X(x_{i'-1}) dx_{i'-1} = \frac{1}{(i'-1)!} F_X^{i'-1}(x_{i'})$$

with $x_n \leq b$.

Hint: Start with $F_X^1(x_2) = \int_a^{x_2} F_X^0(x_1) f_{X_1}(x_1) dx_1$ with $F_X^0(x_1) \triangleq 1$ and note that $F_X^1(x_2) = (x_2-a)/(b-a)$.

16. For the transformation in Section 1.5.5, evaluate the Jacobian in (1.211) using the phase angle expressed as $\theta = \tan^{-1}(x_s/x_c)$.

Hint: use $g_{11}(x_c, x_s) = g_{12}(x_c, x_s) = \sqrt{x_c^2 + x_s^2}$ and $g_{21}(x_c, x_s) = g_{22}(x_c, x_s) = \tan^{-1}(x_s/x_c)$.

17. Given the joint *pdf* $f_{X,Y}(x,y)$, expressed in (1.166), compute the marginal *pdf* $M_X(x)$.

Hint: Complete the square using: $a^2 + ba + c^2 = (a + b/2)^2 - b^2/4 + c^2$.

18. Given the *pdf* $f_X(x)$, perform the following:

A. Compute the *pdf* $f_Y(y)$ under the condition $y = |x|$. Note that $f_Y(y) = 0$ for $y < 0$.

B. Determine and sketch $f_Y(y)$ when $f_X(x)$ is described by the normal distribution $N(m_x, \sigma_x)$

C. Repeat Part B with $m_x = 0$

19. Show that the limiting form of the Ricean distribution, expressed by (1.222), corresponds to the Rayleigh distribution as $A \to 0$. Refer to Table 1.8.

Hint: Use the ascending series expression

$$I_o(z) = 1 + (z^2/4)/(1!)^2 + (z^2/4)^2/(2!)^2$$
$$+ (z^2/4)^3/(3!)^2 + \cdots \text{ with } z = Ar/\sigma^2.$$

20. Show that the limiting form of the Ricean distribution, expressed by (1.222), corresponds to the Gaussian distribution as $A \to \infty$. Refer to Table 1.8.

Hint: Use the asymptotic expansion of $I_o(z)$ for large arguments expressed as

$$I_o(z) \sim \frac{e^z}{\sqrt{2\pi z}}\left(1 + 1/8z + 9/2!(8z)^2 + \cdots\right) : z \to \infty$$

with $z = Ar/\sigma^2$.

Recognize that as $r \to A$ the condition $r = A$ results in the Gaussian distribution.

21. Determine the marginal *pdf of* $Y_1 = \min\{X_1, X_2, ..., X_n\}$ given the joint *pdf* $g_Y(y_1, y_2, ..., y_n)$ of the uniformly distributed ordered samples $a \leq y_1 < y_2 < \cdots < y_n \leq b$ corresponding to $f_{Y_j}(y_j) = 1/(b-a)$: $\forall j$.

Hint: Show that the *cdfs* in the descending order $y_n, y_{n-1}, ..., y_{j'}, ...y_2$ are expressed as

$$\frac{1}{(n-j'+1)!}\bar{F}_Y^{n-j'+1}(y_{j'-1}) = \frac{1}{(n-j')!}\int_{y_{j'-1}}^{b} \bar{F}_Y^{n-j'}(y_{j'})f(y_{j'})dy_{j'}$$

with $\bar{F}_Y^{n-j'}(y_{j'}) = \left[\frac{(b-y_{j'})}{(b-a)}\right]^{n-j'}$ and $\bar{F}_Y^0(y_n) \triangleq 1$.

Also show that $\bar{F}_Y^{n-j'}(y_{j'}) = \left[1 - F_Y(y_{j'})\right]^{n-j'}$ where $F_Y(y_{j'}) = \frac{(y_{j'}-a)}{(b-a)}$.

22. Show that the Nakagami-m distribution is the same as the Rayleigh power distribution.

Hint: Use the transformation $y = x/\sqrt{2}$ in the Rayleigh distribution.

23. Derive the expression for the characteristic function $C_X(v)$ for the Gaussian distribution $f_X(x)$ with mean value x_o and variance σ^2.

24. Set up the integrations identifying the integration limits and ranges of the variable z for the evaluation of $f_Z(z)$ where the random variable Z is the summation of three (3) zero-mean uniformly distributed random variables X between $-a$ and a.

Hint: There are three unique ranges on z. The evaluation of the integrations is optional; however, the application of Mathsoft's Mathcad® symbolic formula evaluation is an error-free time saver.

25. Using $f_Z(z)$ evaluated in Problem 24 for $N = 3$, compute the first and second moments of the random variable Z using (1.254) and compare the results with those in Table 1.6.

Hint: It is much easier and less prone to mistakes to use Mathsoft's Mathcad symbolic formula evaluation.

26. Show that the moments of the random variable X are determined from the characteristic function as expressed in (1.240).

Hint: Take the first derivative of $C_X(v)$ with respect to v and evaluate the result for $v = 0$; and observe that the resulting integral is $E[x]$. Repeat this procedure for additional derivatives of $C_X(v)$ and show that (1.240) follows.

27. Plot the *cdf* of a zero-mean Gaussian distribution with variances corresponding to the second moments in

Table 1.6 for $N = 3$ and 4 and compare the results with the corresponding *cdf's* in Figure 1.23; comment on the quality of the match in light of the central limit theorem. Repeat this exercise using the theoretical second moments from Table 1.7 for $N = 3$ and 4 and compare with the corresponding *cdf's* in Figure 1.26.

28. Show that equations (1.261) and (1.262) apply for $\lambda v \ll 1$ as N increases in the respective summation of N *iid* distributions in Examples 1 and 2 of Section 1.5.6.1.

29. The narrowband noise process $n(t)$, given by (1.307), is expressed in terms of the baseband analytic noise $\tilde{n}(t)$ as

$$n(t) = \frac{1}{2}\left(\tilde{n}(t)e^{j\omega_c t} + \tilde{n}^*(t)e^{-j\omega_c t}\right)$$

Using this relationship, express the correlation function $R_{nn}(\tau) = E[n(t)n(t-\tau)]$ in terms of the individual correlation functions $R_{\tilde{n}\tilde{n}^*}(\tau)$, $R_{\tilde{n}\tilde{n}}(\tau)$, $R_{\tilde{n}^*\tilde{n}^*}(\tau)$ and $R_{\tilde{n}^*\tilde{n}}(\tau)$. What are the required conditions on these correlation functions to satisfy the stationarity property of the narrowband process $n(t)$?

30. Express the individual correlation functions in Problem 29 in terms of the correlation functions $R_{cc}(\tau)$, $R_{cs}(\tau)$, $R_{sc}(\tau)$, and $R_{ss}(\tau)$, where the baseband analytic noise is given by $\tilde{n}(t) = n_c(t) + jn_s(t)$. Use these results and the conditions for stationarity found in Problem 29 to express $R_{nn}(\tau)$ in terms of the $R_{cc}(\tau)$ and $R_{sc}(\tau)$.

31. Referring to (1.315), that applies to the noise power out of a bandpass filter centered at the positive frequency f_c. When the bandpass filter output is mixed to baseband, express the noise power out the baseband filter in terms of the bandwidth B and the one-sided noise spectral density N_o.

32. Given the noise input, expressed by (1.307), to a linear filter with impulse response $h(t)$, show that the respective input and output of the correlation responses $R_{nn}(\tau)$ and $R_{n'n'}(\tau)$ are related by the convolutions $R_{n'n'}(\tau) = h^*(-\tau)*h(\tau)*R_{nn}(\tau)$. Using this result with Fourier transform pairs $h(\tau) \leftrightarrow H(f)$ and $h^*(-\tau) \leftrightarrow H^*(f)$, show the relationship between the input and output noise spectrums.

Hint: Using the convolution integral $n'(t) = \int_{-\infty}^{\infty} n(t-\lambda)h(\lambda)d\lambda$ show that $n'(t)$ has zero-mean. Then from the correlation

$$R_{n'n}(\tau) = E[n'(t)n^*(t-\tau)] = E\left[\int n(t-\lambda)h(\lambda)n^*(t-\tau)d\lambda\right]$$

and show that $R_{n'n}(\tau) = R_{nn}(\tau)*h(\tau)$ and, as the final step, form the correlation

$$R_{n'n'}(\tau) = E\left[n'(t+\lambda)n'^*(t-\tau)\right] = E\left[\int n'(t+\tau)n^*(t-\lambda)h^*(\lambda)d\lambda\right]$$

and show that $R_{n'n'}(\tau) = R_{n'n}(\tau)*h^*(-\tau)$.

33. Derive the expression for the matched filter output signal-to-noise ratio when the additive noise is not white noise, that is, the noise power spectral density into the matched filter is $N_i(f) \neq N_o$.

34. Under the condition stated in Section 1.7.1 show that (1.332) is a wide-sense stationary random process.

35. Given the random process $x(t_i) = a$ where t_i is a discrete-time sample and a is a discrete random variable such that $a = 1$ with probability p and $= -1$ with probability $q = 1 - p$. Using (1.303) and (1.304) determine if $x(t_i)$ is ergodic.

36. Show that the random process $y(t) = x(t)\cos(\omega_c t + \varphi)$ is wss if f_c is constant and $x(t)$ is a wss random process independent of the random variable φ uniformly distributed over the interval 0 to 2π. Also, express the PSD $S_y(\omega)$ in terms of the autocorrelation $R_x(\tau)$ and the PSD $S_x(\omega)$.

37. The risk for the mean-square estimate is defined as

$$\Re_{ms} \triangleq \int_{-\infty}^{\infty} \left\{\int_{-\infty}^{\infty} [a-\hat{a}(s_r)]^2 p_{a|s_r(a|s_r)da}\right\} p_{s_r}(s_r)ds_r$$

Show that $\partial\Re_{ms}/\partial\hat{a}(r_s) = 0$ and results in the optimum estimate given by (1.356).

38. Determine if the MS and MAP estimates in the example of Section 1.9.1 are unbiased estimates. If not, what is the bias of the estimate? Also, evaluate the Cramér–Rao bound for the estimates and, using (1.366), determine if the estimates are efficient.

39. Given that the received baseband signal amplitude is A volts, using the ML estimate, determine the following: Part 1, the variance σ_a^2 of the estimation error of A given the baseband samples $r_i = A + n_i$: $i = 1, \ldots, N$ where n_i are *iid* Gaussian random variables characterized as $N(0,\sigma_n)$, Part 2, show that the estimate $\hat{a}_{ml}(r)$ is efficient, Part 3 show the condition for which the estimate $\hat{a}_{ml}(r)$ is unbiased.

40. Repeat Problem 39 under the following condition: the baseband signal amplitude is Gaussian distributed with a priori *pdf* $p_a(A)$ characterized by $N(A,\sigma_a)$.

41. Using (1.384) determine the effective bandwidth (β) for the isosceles triangle shaped pulse with base equal to 2τ and peak amplitude of AN volts.

Hints: The solution to the integral $\int_0^{\infty} \frac{\sin^{2m}(ax)}{x^2}dx = \frac{(2m-3)!!}{(2m-2)!!}\left(\frac{a\pi}{2}\right)$ is encountered with $m = 2$ and the double

factorial [96] is defined as $(2m+1)!! = 1 \times 3 \times 5 \dots$ $(2m+1)$. The denominator in the expression for α^2 is the signal energy E.

42. Determine the normalized effective bandwidth (βT) and the corresponding standard deviation (σ_{Td}) for the SRC and SRRC waveforms with 100% excess bandwidth, that is, $\alpha = 1$.

43. Determine the normalized effective bandwidth (βT) and the corresponding standard deviation (σ_{Td}) of the delay estimate for the SRC and SRRC waveforms with zero excess bandwidth, that is, $\alpha = 0$.

44. Determine the noise bandwidth for the SRRC and SRC frequency functions.

Note: the noise bandwidth is defined by (1.46).

45. Using (1.387) determine the normalized effective time duration $(\bar{\alpha}T)$ for the rectangular pulse $Arect(t/T - 0.5)$.

REFERENCES

1. C.E. Shannon, "Communication in the Presence of Noise," Proceedings of the IEEE, Vol. 86, Issue 2, pp. 447–457, February, 1998.
2. M. Abramowitz, I.A. Stegun, *Handbook of Mathematical Functions with Formula, Graphs and Mathematical Tables*, National Bureau of Standards, Applied Mathematical Series 55, Washington, DC, U.S. Government Printing Office, p. 361, June 1964.
3. R.A. Manske, "Computer Simulation of Narrowband Systems," IEEE Transactions on Computers, Vol. C-17, No. 4, pp. 301–308, April 1968.
4. E.C. Titchmarsh, *The Theory of Functions*, 2 ed., Oxford University Press, New York, 1939.
5. E.C. Titchmarsh, *Introduction to the Theory of Fourier Integrals*, 2 ed., Oxford University Press, New York, 1948.
6. W.B. Davenport, Jr., W.L. Root, *An Introduction to the Theory of Random Signals and Noise*, McGraw Hill Book Company, New York, 1958.
7. A. Papoulis, *The Fourier Integral and Its Applications*, pp. 9, 42–47, McGraw-Hill Book Company, New York, 1987.
8. A. Papoulis, *Probability, Random Variables and Stochastic Processes*, McGraw-Hill Book Company, New York, 1965.
9. A.V. Oppenheim, R.W. Schafer, *Digital Signal Processing*, Chapter 11, "Power Spectrum Estimation", Prentice-Hall, Inc., Englewood Cliffs, NJ, 1975.
10. M.S. Bartlett, *An Introduction to Stochastic Processes with Special Reference to Methods and Applications*, Cambridge University Press, New York, 1953.
11. B.P. Bogert, Guest Editor, "The Fast Fourier Transform and Its Application to Digital Filtering and Spectral Analysis," Special Issue of the IEEE Transactions on Audio and Electroacoustics, Vol. AU-15, No. 2, June 1967.
12. J.W. Cooley, P.A.W. Lewis, P.D. Welch, "The Finite Fourier Transform," IEEE Transactions on Audio and Electroacoustics, Vol. AU-17, No. 2, pp. 77–85, June 1969.
13. R.C. Singleton, "A Short Bibliography on the Fast Fourier Transform," IEEE Transactions on Audio and Electroacoustics, Vol. AU-17, No. 2, pp. 166–169, June 1969.
14. G.D. Bergland, "A Guided Tour of the Fast Fourier Transform," IEEE Spectrum, Vol. 6, pp. 41–52, July 1969.
15. T.H. Glisson, C.I. Black, A.P. Sage, "The Digital Computation of Discrete Spectra Using the Fast Fourier Transform," IEEE Transactions on Audio and Electroacoustics, Vol. AU-18, No. 3, pp. 271–287, September 1970.
16. J.D. Merkel, "FFT Pruning," IEEE Transactions on Audio and Electroacoustics, Vol. AU-19, No. 4, pp. 305–311, September 1971.
17. P.D. Welch, "The Use of the Fast Fourier Transform for the Estimation of Power Spectra: A Method Based on Time Averaging over Short, Modified Periodograms," IEEE Transactions on Audio and Electroacoustics, Vol. AU-15, pp. 70–73, June 1967.
18. J.W. Cooley, J.W. Tukey, "An Algorithm for Machine Calculation of Complex Fourier Series," Mathematical Computation, Vol. 9, No. 5, pp. 297–301, April 1965.
19. E.O. Brigham, R.E. Morrow, "The Fast Fourier Transform," IEEE Spectrum, Vol. 4, No. 2, pp. 63–70, December 1967.
20. E.O. Brigham, *The Fast Fourier Transform and Its Applications*, Prentice-Hall, Inc., Englewood Cliffs, NJ, 1988.
21. H.L. Groginsky, G.A. Works, "A Pipeline Fast Fourier Transform," IEEE Transactions on Computers, Vol. C-19, No. 11, pp. 1015–1019, November 1970.
22. A.V. Oppenheim, R.W. Schafer, *Digital Signal Processing*, pp. 542–554, Prentice-Hall, Inc., Englewood Cliffs, NJ, 1975.
23. A.V. Oppenheim, R.W. Schafer, *Digital Signal Processing*, pp. 548–549, Prentice-Hall, Inc., Englewood Cliffs, NJ, 1975.
24. P.M. Woodward, *Probability and Information Theory, with Applications to Radar*, Pergamon Press, London, 1960.
25. M. Abramowitz, I.A. Stegun, *Handbook of Mathematical Functions with Formula, Graphs and Mathematical Tables*, National Bureau of Standards, Applied Mathematical Series 55, Washington, DC, U.S. Government Printing Office, p. 231, June 1964.
26. P.F. Panter, *Modulation, Noise, and Spectral Analysis Applied to Information Transmission*, McGraw-Hill Book Company, New York, 1965.
27. S. Goldman, *Transformation calculus and Electrical Transients*, Chapter 9, "Bessel Functions," Prentice-Hall, Inc., Englewood Cliffs, NJ, 1950.
28. H. Cramér, *Mathematical Methods of Statistics*, Princeton University Press, Princeton, NJ, 1974.
29. A. Leon-Garcia, *Probability and Random Processes for Electrical Engineering*, Second Addition, Addison-Wesley Publishing Company, Inc., New York, May 1994.
30. J.M. Wozencraft, I.M. Jacobs, *Principles of Communication Engineering*, John Wiley & Sons, Inc., New York, 1967.
31. H.D. Brunk, *An Introduction to Mathematical Statistics*, Blaisdell Publishing Company, Waltham, MA, 1965.
32. W. Feller, *An Introduction to Probability Theory and Its Applications*, John Wiley & Sons, Inc., New York, 1957.

33. A. Papoulis, *Probability, Random Variables, and Stochastic Processes*, p. 236, McGraw-Hill Book Co., New York, 1965.

34. A. Papoulis, *Probability, Random Variables, and Stochastic Processes*, p. 176, McGraw-Hill Book Co., New York, 1965.

35. A. Papoulis, *Probability, Random Variables, and Stochastic Processes*, pp. 207–209, McGraw-Hill Book Co., New York, 1965.

36. W.B. Davenport, Jr., W.L. Root, *An Introduction to the Theory of Random Signals and Noise*, p. 149, McGraw Hill Book Co., New York, 1958.

37. A. Papoulis, *Probability, Random Variables, and Stochastic Processes*, p. 221, McGraw-Hill Book Co., New York, 1965.

38. W.B. Davenport, Jr., W.L. Root, *An Introduction to the Theory of Random Signals and Noise*, pp. 33–35, McGraw Hill Book Co., New York, 1958.

39. A. Papoulis, *Probability, Random Variables, and Stochastic Processes*, pp. 126–127, McGraw-Hill Book Co., New York, 1965.

40. N.A.J. Hastings, J.B. Peacock, *Statistical Distributions: A Handbook for Students and Practitioners*, A Halsted Press Book, John Wiley & Sons, Inc., New York, 1975.

41. W.B. Davenport, Jr., W.L. Root, *An Introduction to the Theory of Random Signals and Noise*, p. 165, McGraw Hill, New York, 1958.

42. W.B. Davenport, Jr., W.L. Root, *An Introduction to the Theory of Random Signals and Noise*, p. 166, McGraw Hill, New York, 1958.

43. M. Abramowitz, I.A. Stegun, *Handbook of Mathematical Functions with Formulas, Graphs, and Mathematical Tables*, National Bureau of Standards, Applied Mathematics Series No. 55, U.S. Government Printing Office, Washington, DC, p. 376, Integral 9.6.16, June 1964.

44. W.B. Davenport, Jr., W.L. Root, *An Introduction to the Theory of Random Signals and Noise*, pp. 165–167, McGraw Hill Book Co., New York, 1958.

45. J.C. Hancock, *An Introduction to the Principles of Communication Theory*, McGraw-Hill Book Co., New York, 1961.

46. I.S. Gradshteyn, I.M. Ryzhik, *Table of Integrals, Series, and Products*, Corrected and Enlarged Edition, Academic Press, Inc., New York, 1980.

47. G.A. Campbell, R.M. Foster, *Fourier Integrals for Practical Applications*, Fourth Printing, D. Van Norstrand Company, Inc., New York, 1948.

48. H. Urkowitz, "Energy Detection of Unknown Deterministic Signals," Proceeding of the IEEE, Vol. 55, No. 4, pp. 523–531, April 1967.

49. M. Nakagami, "The *m*-distribution—A general formula for Intensity Distribution of Rapid Fading," W.C. Hoffman, Editor, *Statistical Methods in Radio Wave Propagation*, pp. 3–36, Pergamon Press, New York, 1960.

50. M.G. Kendall, A. Stuart, *The Advanced Theory of Statistics*, Vol. I, II, Hafner Publishing Company, New York, 1958, 1961 and *Advanced Theory of Statistics*, Vol. III, Hafner Press, New York, 1982.

51. H.A. David, H.N. Nagaraja, *Order Statistics*, 3rd Addition, John Wiley & Sons, Hoboken, NJ, 2003.

52. B.W. Lindgren, *Statistical Theory*, The Macmillan Company, New York, 1962.

53. R.C. Borgioli, "Fast Fourier Transform Correlation versus Direct Discrete Time Correlation," Proceeding of the IEEE, Vol. 56, No. 9, pp. 1602–1604, September, 1968.

54. E.O. Brigham, Editor, *The Fast Fourier Transform and its Applications*, Chapter 10, "FFT Convolution and Correlation," Prentice-Hall, Englewood Cliffs, NJ, 1988.

55. A. Papoulis, Editor, *Probability, Random Variables, and Stochastic Processes*, Chapter 9, "Stochastic Processes: General Concepts," McGraw-Hill Book Co., New York, 1965.

56. W.B. Davenport, Jr., W.L. Root, *An Introduction to the Theory of Random Signals and Noise*, pp. 38–42, 66–71, McGraw Hill Book Co., New York, 1958.

57. A. Papoulis, *Probability, Random Variables, and Stochastic Processes*, pp. 323–332, McGraw-Hill Book Co., New York, 1965.

58. A. Papoulis, Editor, *Probability, Random Variables, and Stochastic Processes*, Chapter 10, "Stochastic Processes: Correlation and Power Spectrum of Stationary Processes," McGraw-Hill Book Co., New York, 1965.

59. D.O. North, "Analysis of the Factors Which Determine Signal/Noise Discrimination in Radar," Radio Corporation of America (RCA), Technical Report PTR-6-C, June, 1943; reprinted in Proceeding of the IRE, Vol. 51, pp. 1016–1028, July 1963.

60. G.L. Turin, "An Introduction to the Matched Filter," IRE Transactions on Information Theory, Vol. 6, No. 3, pp. 311–329, June 1960.

61. M.L. Skolnik, *Introduction to Radar Systems*, McGraw-Hill Book Company, Inc., New York, 1962.

62. D. Slepian, "Estimation of Signal Parameters in the Presence of Noise," IRE Transactions on Information Theory, Vol. PGIT-3, No. 4, pp. 68–89, March 1954.

63. P.M. Woodward, I.L. Davies, "Information Theory and Inverse Probability in Telecommunication," Proceedings of the IEE, Vol. 99, Part III, pp. 37–44, March 1952.

64. H. Cramér, *Mathematical Methods of Statistics*, Chapter 32, "Classification of Estimates," Princeton University Press, Princeton, NJ, 1974.

65. C.R. Rao, "Information and Accuracy Attainable in the Estimation of Statistical Parameters," Bulletin Calcutta Mathematical Society, Vol. 37, pp. 81–91, 1945.

66. H.L. Van Trees, *Detection, Estimation, and Modulation Theory: Part I*, John Wiley & Sons, New York, 1968.

67. C.E. Cook, M. Bernfeld, *Radar Signals: An Introduction to Theory and Application*, Academic Press, New York, 1967.

68. L. Kleinrock, *Queueing Systems, Volume I: Theory*, John Wiley & Sons, New York, 1975.

69. D. Gabor, "The Theory of Communication," Journal of the IEE, Vol. 93, Part III, pp. 429–441, 1946.

70. R. Manasse, "Range and Velocity Accuracy from Radar Measurements," MIT Lincoln Laboratory, Lexington, MA, February, 1955. (This unpublished internal report is not generally available.)

71. M.L. Skolnik, *Introduction to Radar Systems*, pp. 467–469, McGraw-Hill Book Co., Inc., New York, 1962.

72. F. Halsall, *Data Communications, Computer, Networks and Open Systems*, Fourth Edition, Addison-Wesley Publishing Company, Harlow, UK, 1996.

73. C. Fujiwara, K. Yamashita, M. Kasahara, T. Namekawa, "General Analyses Go-Back-N ARQ System," Electronics and Communications in Japan, Vol. J59-A, No. 4, pp. 24–31, 1975.

74. A.V. Oppenheim, R.W. Schafer, *Digital Signal Processing*, Chapter 5, "Digital Filter Design Techniques," Prentice-Hall, Inc., Englewood Cliffs, NJ, 1975.

75. F.J. Harris, "On the Use of Windows for Harmonic Analysis with the Discrete Fourier Transform," Proceeding of the IEEE, Vol. 66, No. 1, pp. 51–83, January 1978.

76. L.S. Metzger, D.M. Boroson, J.J. Uhran, Jr., I. Kalet, "Receiver Windows for FDM MFSK Signals," IEEE Transactions on Communications, Vol. 27, No. 10, pp. 1519–1527, October 1979.

77. P.M. Derusso, R.J. Roy, C.M. Close, *State Variables for Engineers*, John Wiley & Sons, Inc., New York, 1965.

78. S. Haykin, *Adaptive Filter Theory*, Prentice-Hall, Englewood Cliffs, NJ, 1986.

79. A.P. Sage, C.C. White, III, *Optimum System Control*, 2nd Edition, Prentice-Hall, Inc., Englewood Cliffs, NJ, 1977.

80. A. Gelb, Editor, *Applied Optimum Estimation*, The M.I.T. Press, Massachusetts Institute of Technology, Cambridge, MA, 1974.

81. C.R. Wylie, Jr., *Advanced Engineering Mathematics*, McGraw-Hill Book Company, Inc., New York, 1960.

82. S. Haykin, *Adaptive Filter Theory*, Chapter 2, "Stationary Discrete-Time Stochastic Processes," Prentice-Hall, Englewood Cliffs, NJ, 1986.

83. S. Haykin, *Adaptive Filter Theory*, pp. 54–56, Prentice-Hall, Englewood Cliffs, NJ, 1986.

84. G.W. Stewart, *Introduction to Matrix Computations*, Academic Press, New York, 1973.

85. J.S. Frame, "Matrix Functions and Applications, Part I – Matrix Operations and Generalized Inverses," IEEE Spectrum, Vol. 1, No. 3, pp. 209–220, March 1964.

86. J.S. Frame, "Matrix Functions and Applications, Part II – Functions of a Matrix," IEEE Spectrum, Vol. 1, No. 4, pp. 102–110, April 1964.

87. J.S. Frame, H.E. Koenig, "Matrix Functions and Applications, Part III – Applications of Matrices to Systems Analysis, a Matrix," IEEE Spectrum, Vol. 1, No. 5, pp. 100–109, May 1964.

88. J.S. Frame, "Matrix Functions and Applications, Part IV – Matrix Functions and Constituent Matrices," IEEE Spectrum, Vol. 1, No. 6, pp. 123–131, June 1964.

89. J.S. Frame, "Matrix Functions and Applications, Part V – Similarity Reductions by Rational or Orthogonal Matrices," IEEE Spectrum, Vol. 1, No. 7, pp. 103–109, June 1964.

90. L.L. Smail, *Calculus*, Appleton-Century-Crofts, Inc., New York, 1949.

91. O.W. Eshbach, *Handbook of Engineering Fundamentals*, John Wiley & Sons, Inc., New York, 1952.

92. R.S. Burington, *Handbook of Mathematical Tables and Formulas*, 3rd Addition, Handbook Publishers, Inc., Sandusky, OH, 1957.

93. G.A. Korn, T.M. Korn, *Mathematical Handbook for Scientists and Engineers*, 2nd Addition, McGraw-Hill Book Co., New York, 1961.

94. M. Milton, I.A. Stegun, Editors, *Handbook of Mathematical Functions with Formulas, Graphs, and Mathematical Tables*, National Bureau of Standard Applied Mathematical Series 55, U.S. Government Printing Office, Washington, DC, 1964.

95. I.S. Gradshteyn, I.M. Ryzhik, *Table of Integrals, Series, and Products*, Corrected and Enlarged Edition, p. xliii, Academic Press, Inc., New York, 1980.

96. I.S. Gradshteyn, I.M. Ryzhik, *Table of Integrals, Series, and Products*, Corrected and Enlarged Edition, p. 446, Integral No. 10, Academic Press, Inc., New York, 1980.